This is to certify that the

dissertation entitled

Characteristics of the Methylmercury-Induced Decrease of Whole Cell Barium Current in Cerebellar Granule Neurons

presented by

Jay Edward Sirois

has been accepted towards fulfillment
of the requirements for

Ph.D. degree in **Pharm/Tox**

William D. Atchison
Major professor

Date **2-4-97**

CHARACTERISTICS OF THE METHYLMERCURY-INDUCED DECREASE OF WHOLE CELL BARIUM CURRENT IN CEREBELLAR GRANULE NEURONS

By

Jay Edward Sirois

A DISSERTATION

Submitted to Michigan State University in partial fulfillment of the requirements for the degree of

DOCTOR OF PHILOSOPHY

Department of Pharmacology and Toxicology
and
Institute for Environmental Toxicology

1997

ABSTRACT

CHARACTERISTICS OF THE METHYLMERCURY-INDUCED DECREASE OF WHOLE CELL BARIUM CURRENT IN CEREBELLAR GRANULE NEURONS

By

Jay Edward Sirois

Methylmercury (MeHg) is an organomercurial compound which preferentially disrupts granule cells of the cerebellum. To examine a possible mechanism which may contribute to the sensitivity of granule cells to MeHg, whole cell barium (Ba^{2+}) currents were measured in primary cultures of cerebellar granule cells in the presence and absence of MeHg. 0.25 - 1 μM MeHg decreased Ba^{2+} currents irreversibly, in a concentration- and time-dependent fashion. Following exposure to 0.25, and in some cases 0.5, μM MeHg in the absence of depolarizing stimuli, current at the end of the voltage step was decreased to a greater degree than peak current. At 1 μM MeHg, peak and end currents were reduced an equal amount in the absence of depolarizing stimuli. Increasing the stimulation frequency from 0.1 to 0.2 Hz facilitated the reduction in current by 0.25 and 0.5 μM MeHg, but not 1 μM MeHg.

Several peptide toxins and a dihydropyridine compound were used to examine the role of Ca^{2+} channel subtypes in the MeHg-induced decrease of whole cell Ba^{2+} current. Perfusion of these compounds prior to MeHg exposure did not prevent MeHg from decreasing whole cell Ba^{2+} current. When nimodipine or calcicludine were added prior to MeHg, the subsequent

decrease in peak Ba^{2+} current produced by MeHg was greater than that seen with MeHg alone. Perfusion of GVIA or MVIIC following removal of a portion of the whole cell Ba^{2+} current by MeHg resulted in an initial apparent rate of decline of the remaining current that was similar to the rate observed in the absence of MeHg. Addition of nimodipine in the presence of MeHg did not alter the apparent MeHg-induced rate of current reduction, suggesting that reductions in Ba^{2+} current produced these two agents was not additive. Thus, cerebellar granule cell Ca^{2+} channels are sensitive to micromolar concentrations of MeHg. The results are consistent with an ability of MeHg to decrease current through all Ca^{2+} channel subtypes.

DEDICATION

This dissertation is dedicated to my Mom and Dad, who I could never thank enough for all they have done.

ACKNOWLEDGEMENTS

I would like to thank my guidance committee: Drs. Atchison, Fischer, Moore, Pax and especially Dr. Cobbett, for their efforts.

TABLE OF CONTENTS

LIST OF TABLES

LIST OF FIGURES

Ac

ACh

Aga-

AME

ATP

Ara-

[Ca²

[Ca²

cAM

CME

DME

DRG

EGT

EPF

FBS

FIT

g

GAB

GFA

GVT

HEP

LIST OF ABBREVIATIONS

Ac	Acetate
ACh	acetylcholine
Aga-IVA	ϖ-agatoxin IVA
AMPA	α-amino-3-hydroxy-5-methylisoxazole-4-propionic acid
ATP	adenosine 5'-triphosphate
Ara-C	cytosine arabinoside
$[Ca^{2+}]_e$	extracellular calcium concentration
$[Ca^{2+}]_i$	intracellular calcium concentration
cAMP	adenosine 3', 5'-cyclic monophosphate
CMF-HBSS	calcium and magnesium-free HEPES buffered salt solution
DMEM	Dulbeco's modified eagle medium
DRG	dorsal root ganglion
EGTA	ethylene glycol bis(ß-aminoethyl ether) N,N,N',N',-tetraacetic acid
EPP	end-plate potential
FBS	fetal bovine serum
FITC	fluorescein isothiocyanate
g	force of gravity
GABA	γ-aminobutyric acid
GFAP	glial fibrillary acidic protein
GVIA	ϖ-conotoxin GVIA
HEPES	(N-[2-Hydroxyethyl] piperazine-N'-[2-ethanesulfonic acid])

HVA

IgG F_c

LVA

MeHg

MEPP

min

MVHC

NEM

NMDA

PC12

pS

QNB

sec

TEA

TTX

HVA	high voltage-activated
IgG F_c	immunoglobulin G constant region
LVA	low voltage-activated
MeHg	methylmercury
MEPP	miniature end-plate potential
min	minutes
MVIIC	ϖ-conotoxin MVIIC
NIM	nimodipine
NMDA	N-methyl *d*-aspartate
PC12	pheochromocytoma cell
pS	picosiemen
QNB	quinuclidinyl benzilate
sec	seconds
TEA	tetraethylammonium chloride
TTX	tetrodotoxin

CHAPTER ONE

INTRODUCTION

A Me

Me

primar

industr

mercur

imparte

environ

particul

fish Ha

The

revealed

impairm

Hunte

histolo

cerebe

appea

insidi

findin

of peo

seafood

decades

A. Methylmercury

Methylmercury (MeHg) is an environmental contaminant found primarily in aquatic ecosystems. Produced as a by-product of various industrial processes, as well as by bacterial methylation of inorganic mercury (Heintze *et al.*, 1983), the lipophilic character of this compound, imparted by the methyl group, allows the bioaccumulation of MeHg in the environment. It thus poses a significant risk to aquatic life, and in particular humans who consume a large quantity of MeHg-contaminated fish (Hansen, 1990).

The first description of the effects of chronic low level MeHg exposure revealed various disturbances in sensory function such as ataxia, impairments in speech, hearing and vision and numbing in the extremities (Hunter *et al.*, 1940). Upon the death of an individual exposed to MeHg, a histological examination of the brain revealed that the granule cells of the cerebellum were particularly sensitive, while other cerebellar cell types appeared less affected (Hunter and Russell, 1954).

Two larger scale outbreaks of poisoning with MeHg exhibited the insidious neurotoxic potential of this compound and confirmed the initial findings by Hunter and his colleagues. In Minimata Bay, Japan, thousands of people were exposed to MeHg through the consumption of contaminated seafood over the course of several years (Takeuchi *et al.*, 1967). Two decades later in Iraq, 462 people died, and countless others were affected, as

a result

MeHg-co

disruptio

present

MeHg on

numerou

the offsp

Th

unknown

<10 μm

MeHg, to

such as

inactive

complex

1972 o

acting

answe

one.

ensue

startin

by MeI

insult is

the intrac

a result of ingesting bread made from seed grain contaminated with a MeHg-containing fungicide (Bakir *et al.*, 1973). A pattern of cerebellar disruption, with especially prominent effects on granule cells, was again present among those who died as a result of these incidents. The effects of MeHg on the developing fetus were also shown to be quite conspicuous, as numerous cases of a cerebral palsy-like syndrome were observed to occur in the offspring of women chronically exposed to MeHg.

The reason for the heightened sensitivity of granule cells to MeHg is unknown. Speculations have ranged from the small size of the granule cell (<10 μm) which may in turn lead to a greater intracellular concentration of MeHg, to the lack of potential protective MeHg-sequestering mechanisms, such as sulfhydryl groups, some of which may sequester MeHg in an inactive form. Because of the ability of MeHg to react with a number of complexation sites such as carbonyl, amino and hydroxyl groups (Dales, 1972) on the plasma membrane or within the cell, the likelihood of MeHg acting at a single site to produce neurotoxicity is extremely low. Thus, the answer to the question 'How does MeHg cause neurotoxicity' is not a simple one. Accordingly, it is important to understand the sequence of events that ensues subsequent to MeHg exposure. In trying to determine this, a logical starting point would be to examine a cellular process that would be affected by MeHg at an early time point. The first line of defense against any toxic insult is the plasma membrane, which forms an effective barrier between the intracellular and extracellular environments.

V

commu

family

functio

allowir

which

expres

et al.,

to the

[Ca^{2+}]

can po

determ

sensiti

examir

portion

subtyp

curren

Ca^{2+} c

based

the un

possibi

could c

Within the plasma membrane are numerous proteins which act to communicate messages from the outside of the cell to the inside. One family of these proteins, the voltage-gated Ca^{2+} channels, perform a critical function in cellular communication. Ca^{2+} channels are responsible for allowing the influx of extracellular Ca^{2+}, an important second messenger, which activates a number of processes such as growth cone extension, gene expression, synapse development and exocytic release of transmitter (Scott *et al.*, 1991). Along with a host of other proteins, Ca^{2+} channels contribute to the maintenance of intracellular Ca^{2+} levels ($[Ca^{2+}]_i$) at ~100 nM. Since $[Ca^{2+}]_i$ is so tightly controlled, altered regulation of Ca^{2+} channel function can potentially affect a number of events. This study was undertaken to determine **1)** if cerebellar granule cell Ca^{2+} channel currents were more sensitive to MeHg-induced decreases than Ca^{2+} channels in other previously examined cell types; and **2)** to examine the ability of agents which block a portion of the whole cell Ba^{2+} current through one or more Ca^{2+} channel subtypes to alter the MeHg-induced reduction of whole cell Ca^{2+} channel current. Cerebellar granule cells have been shown to possess a multitude of Ca^{2+} channel subtypes, with a recent study describing 5 different types based on pharmacological characterization (Randall and Tsien, 1995). Thus, the unique complement of granule cell Ca^{2+} channels may increase the possibility of MeHg disruption of Ca^{2+}-mediated events, an effect which could contribute to cell death.

B. Structure and function of voltage-gated Ca^{2+} channels

Neuronal voltage-gated Ca^{2+} channels are comprised of 4 subunits (α_1, ß, α_2 and δ). The α_1 subunit forms the pore region of the channel and, when expressed in a system such as *Xenopus* oocytes, can form a functional channel by itself. α_1 is a transmembrane protein comprised of 4 homologous repeats (I-IV), each of which contains 6 transmembrane segments (Fig. 1.1; for review see Catterall, 1993; 1995). Expression studies with clones of the α_1 subunit have also shown that this is the region of the Ca^{2+} channel which determines its voltage- and pharmacological-sensitivity. The other subunits play various modulatory roles in shaping the activation and inactivation profiles of the channel. Numerous genes for each of the subunits have been identified (see Table 1). The genes responsible for encoding the α_1 subunits of the L-, N- and P-type Ca^{2+} channels have been well characterized. Two genes (α_{1C}, α_{1D}), encode for the α_1 subunit of the L-type channel, while N-type (α_{1B}) and P-type (α_{1A}) are encoded by only one gene. Interestingly, when expressed in *Xenopus* oocytes, α_{1A} shows characteristics distinct from that of a typical P-type channel (Zhang *et al.*, 1993). This has led to the speculation that perhaps α_{1A} encodes for a separate channel, termed Q-type. Originally described in cerebellar granule cells, Q-type channels are sensitive to block by low concentrations of ϖ-conotoxin MVIIC and are relatively resistant to block by the P-type Ca^{2+} channel antagonist ϖ-agatoxin IVA (Zhang *et al.*, 1993; Randall and Tsien, 1995). The product of the α_{1E} gene has been found to be resistant to pharmacological modulation.

FIG. 1.1. The proposed structure of a voltage-gated Ca^{2+} channel (from Catterall, 1993; 1995). **(A)** Diagram of the proposed arrangement of a skeletal muscle Ca^{2+} channel containing α_1, α_2-δ, ß and δ subunits (δ is only present in skeletal muscle Ca^{2+} channels). **(B)** Detail of the α_1 subunit domain showing the 4 transmembrane regions (I-IV) and the presence of phosphorylation and glycosylation sites. **(C)** Detail of the 6 membrane spanning regions (S1-S6) within each of the four motifs. Changes in transmembrane voltage are thought to be detected by the S4 region, which is highly charged (represented by +). The movement of this region results in the opening of the channel pore and the subsequent flux of ions. The SS1/SS2 region separates the 5^{th} and 6^{th} membrane spanning segments and is thought to contain the binding site(s) for dihydropyridine compounds (Tang *et al.*, 1993).

Fig. 1.1

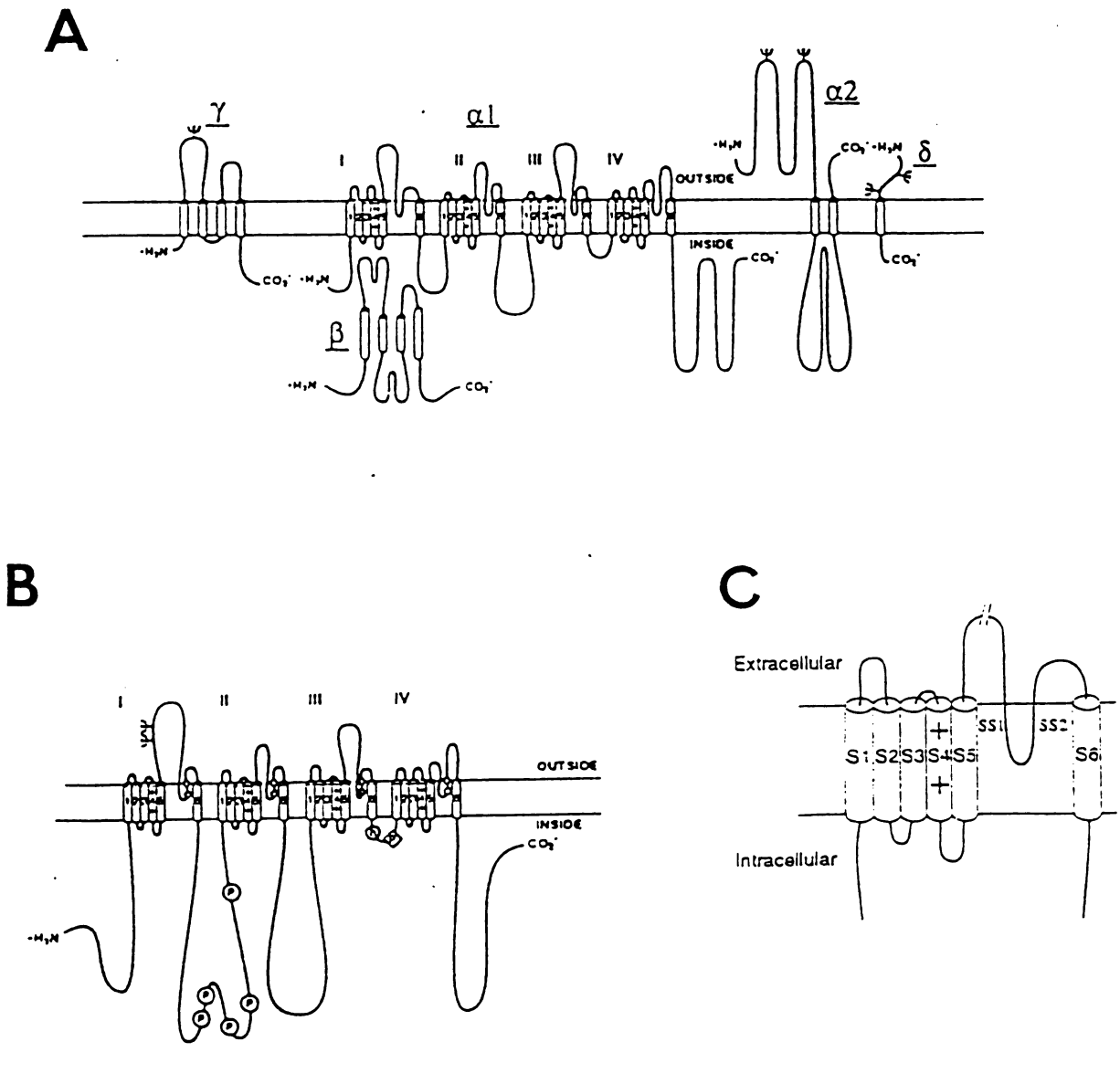
A
γ
α1
α2
δ
β
I
II
III
IV
OUTSIDE
INSIDE
B
C
Extracellular
Intracellular
S1
S2
S3
S4
S5
S6

Table 1. Characteristics of voltage-gated Ca^{2+} channels.

[1] Approximate voltages at which current is activated.

[2] Not available

[3] Approximate rate (fast, medium or slow) of current inactivation.

[4] Single channel conductance

[5] Based partly upon results obtained by expression of α_{1A} in *Xenopus*.

[6] Based upon similarity of granule cell R-type current to α_{1E} current in *Xenopus*.

[7] Sensitive refers to the relative ability of the antagonist to decrease current through the respective channel types.

[8] Calcicludine

[9] In rat cerebellar Purkinje neurons and chicken DRG neurons.

Ca^{2+} channel	T	L	N	P	Q	R
Activation Range[1]	+ to -70mV	+ to -10mV	+ to -20mV	+ to -50mV	NA[2]	NA
Decay Rate[3]	Med-Fast	Slow	Med	Slow	Med-Fast	Slow
g[4]	8pS	25pS	13pS	~15pS	NA	NA
α_1 subunit	rbe-II	α_{1C}/α_{1D}	α_{1B}	α_{1A}	α_{1A}[5]	α_{1E}[6]
GVIA sensitive[7]	No	No	Yes	No	No	No
MVIIC sensitive	No	No	Yes	Yes	No	Yes
DHP sensitive	No	Yes	No	No	No	No
Calcicl.[8] sensitive	No	Yes	Yes[9]	Yes[9]	No	No
Aga-IVA sensitive	No	No	No	Yes	Yes	No

Current

pharma

granule

subunit

characte

produce

1993).

and inv

the futu

Tl

exist; op

the tran

pore reg

permitte

Inactivat

current

At the s

openings

by less

Inactivati

voltage-

facilitates

injection

Current carried by expressed α_{1E} subunits shares kinetic and pharmacological characteristics of a portion of current seen in cerebellar granule cells that has been termed R-type (Zhang *et al.*, 1993). The α_1 subunit possessed by the T-type Ca^{2+} channel has not been definitively characterized, although this current does share similarity to current produced by expression of the rbe-II gene in *Xenopus* oocytes (Soong *et al.*, 1993). Ongoing studies of Ca^{2+} channel types in a number of mammalian and invertebrate cell types will likely yield new classes of Ca^{2+} channels in the future as well.

Three main states of a voltage-gated Ca^{2+} channel are proposed to exist; open, closed and inactivated. In the open state, the channel permits the transmembrane flux of ions following a conformational change in the pore region of the channel. When the channel is closed, ion flux is not permitted. In some cases, multiple closed states of a Ca^{2+} channel exist. Inactivation of whole cell HVA Ca^{2+} current entails a relaxation of the current back to a non-zero value in the presence of a maintained stimulus. At the single channel level, this is manifest as more frequent or longer openings of the Ca^{2+} channel at the beginning of the depolarization followed by less frequent and/or shorter openings at the end of the pulse. Inactivation of voltage-dependent Ca^{2+} channels occurs through either voltage- or Ca^{2+}-dependent means. Evidence which suggests that Ca^{2+} facilitates channel inactivation include the findings that intracellular injection of Ca^{2+} (Standen, 1981) and EGTA (Eckert and Tillotsen, 1981) can

enhance and reduce inactivation, respectively. The ability of Ca^{2+} to cause inactivation can involve changes in the activity of enzymes which are activated by Ca^{2+}, including calmodulin and calcineurin which acts by enhancing the rate of dephosphorylation of the Ca^{2+} channel (Chad and Eckert, 1986). Voltage-dependent inactivation of is the predominant form of inactivation of T-type channels (Lux and Brown, 1984; Bossu and Feltz, 1986; Lux and Gutnick, 1986; Gutnick *et al.*, 1989). In cerebellar granule cells, Q-, R-, and N-type Ca^{2+} channels inactivate (to a somewhat similar degree), while L- and P-type Ca^{2+} channels are non-inactivating.

The Ca^{2+} channel is postulated to be a multi-ion pore through which Ca^{2+} passes in single file fashion as it enters the cell (Hess and Tsien, 1984). Ca^{2+} channels exhibit a high affinity for Ca^{2+} over other metal ions present in higher concentrations such as Na^{+}, K^{+} and Mg^{2+}. The basis of this selectivity is thought to reside in two negatively charged glutamate residues, aligned in single file fashion along the pore of the Ca^{2+} channel. These residues, termed the inner site and the outer site, interact very briefly with the Ca^{2+} ion as it traverses the channel. The importance of these residues in Ca^{2+} channel function has been shown in amino acid substitution experiments where replacing these glutamate residues with lysine at the SS2 segment of the S5-S6 linker region alters the selectivity of the Ca^{2+} channel (Tang *et al.*, 1993). Following a depolarizing stimulus and the opening of the pore, Ca^{2+} enters the channel and binds to the inner site. Subsequent binding of another Ca^{2+} at the outer site facilitates the entry of

the inner Ca^{2+} into the cell (Hess and Tsien, 1984).

Calcium channels are classified as either low voltage-activated (LVA) or high voltage-activated (HVA). From a constant holding potential (*i.e.*, -90 mV), LVA Ca^{2+} channels are activated by weakly depolarizing pulses (*i.e.*, to -60 mV). Activation of HVA Ca^{2+} channels requires stronger depolarizing steps (*i.e.*, to -20 mV). To date only one LVA channel has been characterized, termed T-type (Llinas and Yarom, 1981). T-type Ca^{2+} channels, which carry a very small single channel current compared to HVA channels (Carbone and Lux, 1984; Fox *et al.*, 1987), inactivate following a large depolarization step (*i.e.*, to -20 mV). For all HVA channels, when the membrane is at its resting potential, the pore is closed, preventing ion flux. This is not necessarily the case with T-type channels, due to their relatively low activation threshold (~-60 mV), which allows them to potentially be open at the resting potential. In order to accomplish the process of opening, the change in membrane voltage must be converted to physical movement of a portion of the Ca^{2+} channel. Transmembrane changes in voltage are thought to be detected by a proposed voltage-sensing region within the channel protein termed the S4 segment (Catterall, 1986; Sigworth, 1993). Following depolarization, this highly charged region apparently moves outward, creating the gating current and facilitating channel opening (Armstrong and Bezanilla, 1977; Yang *et al.*, 1996).

The pharmacology of T-type Ca^{2+} channels is also unique compared to HVA channels. While HVA Ca^{2+} channels are more sensitive to block by

Cd^{2+} than Ni^{2+}, the reverse is true of T-type channels. T-type Ca^{2+} channels are also sensitive to block by amiloride (Tang *et al.*, 1988) and 1-octanol (Llinás, 1988).

The relatively recent discovery of a number of peptide toxins from fish-hunting snails of the *Conus* species as well as from venomous spiders such as *Agelenopsis aperta*, (Olivera, 1991; 1994) has allowed the pharmacological characterization of a number of different types of voltage-gated Ca^{2+} channels. Table 1 provides the relative sensitivity of each of the known voltage-gated Ca^{2+} channel types to the peptide toxins, as well as a class of L-type Ca^{2+} channel antagonists termed dihydropyridines, used in this study.

In cerebellar granule cells, all of the Ca^{2+} current is considered to be HVA (L-, N-, P-, Q- and R-type). L-type Ca^{2+} channels, which are activated by voltage commands positive to -10 mV, have a conductance of 25 picosiemens (pS) and are sensitive to block by micromolar concentrations of dihydropyridines (Fox *et al.*, 1987). The N-type Ca^{2+} channel has a single channel conductance of 13 pS and activates following depolarizations greater than -30 mV (Fox *et al.*, 1987). N-type channels are sensitive to ω-conotoxin GVIA, a peptide toxin isolated from the piscivorous cone snail *Conus geographus* (Olivera *et al.*, 1984). P-type Ca^{2+} channels (10-15 pS), so called because they were originally observed in Purkinje cells (Llinas *et al.*, 1989), are sensitive to ϖ-agatoxin IVA, a peptide isolated from the funnel web spider *Agelenopsis aperta* (Llinás *et al.*, 1989). Depolarizations more

positive than -50 mV are required to activate P-type Ca^{2+} channels. The Q-type Ca^{2+} channel is similar to the P-type channel in its activation kinetics and is sensitive to low concentrations of ϖ-conotoxin MVIIC (Zhang *et al.*, 1993; Randall and Tsien, 1995), a peptide isolated from the cone snail *Conus magnus*. Current that is resistant to a pharmacological cocktail of all the aforementioned blockers, is termed R-type (Zhang *et al.*, 1993; Randall and Tsien, 1995). Because of the relative paucity of studies examining the proposed Q- and R-type Ca^{2+} channels, the voltage at which the current activates and the single channel conductance are as yet unknown. An overview of many of the characteristics of the various types of Ca^{2+} channels presented in the previous paragraphs is given in Table 1.

C. MeHg-induced disruption of Ca^{2+}-mediated events

A prominent finding in patients exposed to MeHg was a loss of fine motor control. In these severely affected patients, injection of neostigmine, a cholinesterase inhibitor, was shown to alleviate partially the effects of MeHg (Rustam *et al.*, 1975). This finding suggested that some type of alteration in synaptic transmission was occurring. This study led to the examination of MeHg on patterns of neurotransmitter release using isolated nerve-muscle preparations, which display the normal physiology of an intact synapse.

In several preparations including frog sartorius muscle (Manalis and Cooper, 1975; Juang, 1976; Cooper and Manalis, 1983), rat diaphragm

(Atchison and Narahashi, 1982; Atchison *et al.*, 1984) and mouse diaphragm (Atchison *et al.*, 1984), MeHg was shown to block the nerve-evoked release of acetylcholine (ACh). This effect appears to be both time- and concentration-dependent, as low concentrations of MeHg will abolish glutaminergic synaptic transmission if the preparation can be maintained for a long enough period of time (Yuan and Atchison, 1995). A predominantly presynaptic effect of MeHg was demonstrated by the finding that iontophoretic perfusion of acetylcholine onto the endplate region (postsynaptic) produced results that were similar to control experiments (Atchison *et al.*, 1984).

Similar findings are seen following *in vivo* exposure to MeHg. In the rat gastrocnemius muscle, subcutaneously injected MeHg decreased contractility following either acute (10 mg Hg^{2+}/kg body weight/day for 7 days) or subchronic (2 mg Hg^{2+}/kg body weight/day, 5 days/wk for 3-4 wks) exposure (Somjen *et al.*, 1973). Following a single exposure to MeHg (20 or 40 mg/kg body weight) similar results were produced in the rat tail motor nerve (Fehling *et al.*, 1975). A time-dependent block of nerve-evoked twitches was seen following MeHg exposure in the rat diaphragm (Von Burg and Landry, 1976) and frog sartorius (Juang, 1976) isolated nerve-skeletal muscle preparations. Following wash with MeHg-free solution, twitch height of rat diaphragm recovered from complete block to 10-30 percent of control (Von Burg and Landry, 1976). Juang (1976) reported that following MeHg exposure, twitch height of frog sartorius continued to decrease even

following wash with MeHg-free solution. Thus, although reports differ as to the reversibility of MeHg effects at the neuromuscular junction, *in vitro* results are consistent with the clinical signs of neuromuscular weakness seen following MeHg exposure at both Minamata Bay and Iraq.

Whereas nerve-evoked transmitter release is highly dependent on extracellular calcium concentration ($[Ca^{2+}]_e$), block of the nerve-evoked end-plate potential (EPP) by MeHg is apparently independent of $[Ca^{2+}]_e$. Increasing $[Ca^{2+}]_e$ from 2 mM to 4 or 8 mM does not prolong the time to block or decrease the magnitude of block of the EPP (Atchison *et al.*, 1986; Traxinger and Atchison, 1987). Similar effects are seen centrally, where the time to MeHg-induced block of action potentials elicited from CA1 hippocampal neurons is not changed by elevating $[Ca^{2+}]_e$ from 2 mM to 6 mM (Yuan and Atchison, 1995). However, the situation is complex and multiple actions may be involved. Increasing the stimulation intensity following MeHg-induced block restores the EPP or synaptically-evoked action potentials to control values (Traxinger and Atchison, 1987; Yuan and Atchison, 1993). MeHg may block synaptic transmission by causing membrane depolarization or by increasing the charge required to activate Na^+ channels through some type of sulfhydryl interaction (Traxinger and Athcison, 1987). The increased stimulus intensity may restore synaptic transmission by the activation of another pathway(s) not affected initially by MeHg. Alternatively, MeHg could be removed from its binding sites by a strong stimulus, thus causing a restoration of transmission. After

overcoming the MeHg-induced block of synaptic transmission by increasing the stimulation intensity, continued exposure to MeHg results in a subsequent block of the EPP or action potential. Increasing $[Ca^{2+}]_e$ at this time reversed the MeHg-induced effects on synaptic transmission (Traxinger and Atchison, 1987). Thus, under certain conditions, it is possible to overcome the MeHg-induced block of synaptic transmission. That the initial block is not reversed by elevations in $[Ca^{2+}]_e$ is consistent with either a non-competitive block of Ca^{2+} influx by MeHg or alternatively, that the block occurs by $[Ca^{2+}]_e$- independent mechanisms. The ability of raising $[Ca^{2+}]_e$ to restore transmission following block by MeHg in the presence of an increased stimulation intensity suggests that the block of synaptic transmission by MeHg is not solely due to alterations in conductance (Traxinger and Atchison, 1987).

D. Effects of MeHg on Ca^{2+} channels.

In synaptosomes isolated from rat brain, MeHg (2.5-1000 µM) decreases Ca^{2+} channel-mediated $^{45}Ca^{2+}$ uptake and also that portion of uptake due to a reversed Na^+/Ca^{2+} exchanger (Shafer *et al.*, 1990; Hewett and Atchison, 1992). Relatively high concentrations of MeHg (5-200 µM), coupled with extremely brief exposure periods (1 sec), were used to examine channel function in isolation. This type of situation minimizes the potential of MeHg interaction with other intracellular processes which may confound interpretation of channel-mediated effects.

Increasing the extracellular K^+ concentration in the presence of 100 μM MeHg caused a greater percentage reduction in synaptosomal $^{45}Ca^{2+}$ influx, demonstrating the effect to be voltage-dependent. Thus, MeHg may somehow associate with the channel, perhaps in a manner similar to Ca^{2+}, as the reduction was facilitated by stronger depolarizations. The MeHg-induced reduction in $^{45}Ca^{2+}$ uptake was not dependent on whether the channel was in the closed, activated or inactivated state at the time of MeHg exposure (Shafer *et al.*, 1990). Thus, these results suggest an interaction of MeHg with Ca^{2+} channels and possibly that the ability of MeHg to reduce $^{45}Ca^{2+}$ uptake may be dependent on the strength of the interaction between MeHg and the channel. MeHg (100 μM) also altered the ionic selectivity of synaptosomal Ca^{2+} channels by decreasing $^{85}Sr^{2+}$ influx to a greater extent than $^{45}Ca^{2+}$ or $^{133}Ba^{2+}$ (Shafer and Atchison, 1990).

MeHg has also been shown to interact with Ca^{2+} channels in synaptosomes isolated from rat cerebellum (Yan and Atchison, 1996). Pretreatment of synaptosomes with omega-conotoxin (ω-CgTx) GVIA (1 or 5 μM) or ω-CgTx MVIIC (0.1 or 0.5 μM), but not omega-agatoxin (ω-Aga) IVA (10 or 100 nM) or nifedipine (10 μM), partially attenuated the ability of MeHg to inhibit $^{45}Ca^{2+}$ uptake, suggesting that in the cerebellum, MeHg interacts with channels sensitive to these toxins.

MeHg (1-20 μM) rapidly and completely decreases whole cell currents carried by Ba^{2+}, a Ca^{2+} surrogate, through both N- and L-type Ca^{2+} channels in PC12 cells without altering leak or capacitive currents (Shafer and

Atchison, 1991). Following 2 min of exposure, a similar degree of current reduction is obtained both when the channel is activated repeatedly and following a period of channel inactivity, indicating that MeHg has access to the channel by a means other than entry through the open pore. As with synaptosomes, the effect is not dependent on the state of the channel. Washing the preparation with MeHg-free bath solution does not reverse the MeHg-induced reduction in Ba^{2+} current, a finding which differs from that of other heavy metals such as Cd^{2+} and Pb^{2+}, whose blocking effect is reversed by washing with metal-free solution (Nachsen, 1984; Suszkiw *et al.*, 1985; Shafer and Atchison, 1991). At 10 µM MeHg also altered the apparent ionic selectivity of PC12 cell Ca^{2+} channels for Ca^{2+} and Sr^{2+} over Ba^{2+} (Shafer and Atchison, 1991).

In rat DRG cells, MeHg (0.25 - 20 µM) reduces Ba^{2+} currents with an IC_{50} of 2.6 µM (Leonhardt *et al.*, 1996). Higher concentrations (>10 µM) of MeHg produced a biphasic current which exhibited both inward and outward components. The effect of MeHg occurred at all potentials which elicited inward current. In addition, a slight positive shift of the current-voltage (I-V) relationship was noted.

MeHg has been found to decrease the specific binding of ^{3}[H]-nitrendipine, an L-type Ca^{2+} channel agonist, in synaptosomes. This occurred at a concentration (100 µM) which also inhibited $^{45}Ca^{2+}$ influx. However, as dihydropyridines will specifically bind to synaptosomes at much lower concentrations than those which block Ca^{2+} influx (Dunn, 1988),

the exact significance of this result is difficult to determine. MeHg also inhibited the binding of ^{125}I-ω-CgTx GVIA in rat clonal pheochromocytoma (PC12) cells. These findings suggest that MeHg may interact with L-and N-type Ca^{2+} channels (Shafer *et al.*, 1990).

Other indirect evidence suggests that MeHg can alter Ca^{2+} channel function. In NG108-15 cells (Hare *et al.*, 1993), as well as cerebellar granule cells (Marty and Atchison, *submitted*), MeHg causes a biphasic elevation in $[Ca^{2+}]_i$. Part of this $[Ca^{2+}]_i$ rise appears to occur through Ca^{2+} channels. In NG108-15 cells, nifedipine, an L-type Ca^{2+} channel antagonist, can delay the onset of the $[Ca^{2+}]_i$ elevation, while ϖ-conotoxin MVIIC causes a similar effect in cerebellar granule cells.

Thus, the ability of MeHg to alter Ca^{2+} channel function and possibly associate with the Ca^{2+} channel has been demonstrated in a number of experimental paradigms including synaptosomal $^{45}Ca^{2+}$ flux experiments, whole cell Ba^{2+} current measurements and antagonist binding studies. While evidence to date suggests that Ca^{2+} channels are susceptible to MeHg-induced alteration, it has yet to be determined conclusively whether Ca^{2+} channels are inherently more sensitive than other voltage-gated channels.

E. Effects of MeHg on other voltage-dependent ion channels

MeHg also disrupts both Na^+ and K^+ channel function as measured using patch clamp techniques. In N1E-115 mouse neuroblastoma cells, 20 to 60 µM MeHg blocked both Na^+ and K^+ currents (Quandt *et al.*, 1982). A

steady increase in the threshold for action potential generation and eventual block of conduction was attributed to block of Na^+ and K^+ channels by MeHg (25-100 μM) in the squid giant axon (Shrivastav *et al.*, 1976). Na^+ channel function was also disrupted by MeHg (50-100 μM) in mouse *triangularis sterni* motor nerves (Shafer and Atchison, 1992). Interestingly, in cerebellar granule cells, higher concentrations of MeHg (2-40 μM) are required to block K^+-currents (Sirois and Atchison, 1995) compared to Ba^{2+} currents. Thus, at least in granule cells, some basis for an increased susceptibility of Ca^{2+} channels to MeHg-induced block over other voltage-gated ion channel types is evident.

In rat DRG cells MeHg, as well as Hg^{2+}, generates a slow inward current which is not blocked by bicuculline, picrotoxin, tetrodotoxin or La^{+3}, suggesting that γ-aminobutyric acid (GABA)-activated Cl^- channels, voltage-dependent Na^+ channels or voltage-dependent Ca^{2+} channels do not mediate the slow inward current (Arakawa *et al.*, 1991). Other heavy metals such as Pb^{2+}, Cd^{2+}, Cu^{2+}, Co^{2+} and Al^{+3} have been shown to elicit similar slow inward currents in mouse neuroblastoma cells (Oortgiesen *et al.*, 1990) and in molluscan neurons (Weinreich and Wonderlin, 1987). This current is thought to arise from activation of a non-specific cation channel, which permits the passage of more than one cation (*i.e.*, Ca^{2+}, Na^+, K^+). However, in brown fat cells both organic and inorganic mercury block a non-selective cation channel (Koivisto *et al.*, 1993). Thus, MeHg can decrease current carried by the major classes of voltage-gated ion channels (Ca^{2+}, Na^+, and

K^+). However, channels from different mammalian and invertebrate species display differential susceptibility to block.

F. Cerebellar granule cells

Because of its relatively ordered structure and the presence of a limited number of neuronal cell types, the cerebellar cortex has been studied in great detail. It consists of three layers (granular, molecular and Purkinje cell) and five neuronal cell types (granule, basket, stellate, Golgi and Purkinje; Eccles *et al.*, 1967). The most numerous cell type in the cerebellum is the granule cell (rat cerebellum contains ~1.1 x 10^8 granule cells, Palay and Chan-Palay, 1974). Granule cell axons (parallel fibers) are projected upward into the molecular layer of the cerebellar cortex where they form synapses on Purkinje cells. Parallel fibers release glutamate in a Ca^{2+}-dependent fashion (Levi *et al.*, 1982) onto Purkinje cells, thereby partially controlling cerebellar output.

Several toxic agents have been shown to disrupt granule cell function and structure. Methyl chloride can produce lesions in the granule cell layer of both rats and mice (Morgan *et al.*, 1982). Similar findings were observed with styrene oxide and acrylamide following single injections of these compounds (Beiswanger *et al.*, 1993). In addition, chronic alcoholism can cause degeneration of the cerebellum. Differences in the susceptibility of cerebellar cell types to various toxic agents may involve variations in metabolism, neuronal input or blood flow.

G. Patch clamp techniques

Prior to the introduction of the patch clamp technique, studies examining the action of drugs or chemicals on Ca^{2+} channels were limited to uptake studies using radiolabelled $^{45}Ca^{2+}$. The patch clamp technique allowed for the measurement of numerous events ranging from the activity of a single channel to measurement of the whole cell current, with relatively little noise and better time resolution (Hamill *et al.*, 1981). This technique involves positioning a small, heat polished glass pipette against the cell membrane. Application of negative pressure to the pipette creates an electrical seal between the cell and pipette. This configuration is termed a cell-attached patch. This high-resistance seal, termed a gigaseal because the resistance between the cell and pipette is measured in gigaohms, reduces noise and allows the membrane potential at the patch to be "clamped" at a certain voltage. Several configurations of the patch clamp technique exist, but for the purposes of this study, only the whole cell method will be discussed. Following the acquisition of a gigaseal, the whole cell configuration is obtained either by the application of a slight amount of negative pressure to the pipette or by a brief voltage pulse. These procedures create a transient disruption of the membrane in contact with the pipette resulting in a removal of the membrane directly underneath the pipette without the loss of the gigaseal. This allows the contents of the glass pipette to diffuse freely into the cell. Following acquisition of the whole cell configuration, electrical continuity between the cell interior and

the electrode is established, allowing the cell to be held at the desired voltage. The benefits of the whole cell configuration include the fact that the ion compositions on both sides of the membrane are known and to a certain extent can be modified without difficulty and that the activity of a sub-population of voltage-dependent channels can be studied in isolation.

The whole cell technique is not without difficulties however. It is often difficult, particularly with small cells such as granule cells, to acquire and maintain a gigaohm seal. Further, the medium bathing the cells as well as the intracellular pipette solution are often optimized to examine a single channel type, thus creating a situation far removed from anything a cell would see *in vivo*. Measurement of Ca^{2+} channel current also presents an additional problem termed "rundown". This process is observed as a decrease in the Ca^{2+} channel current over time and is believed to result from the washout of factors critical for maintaining the current at a stable level (Scott, 1991). Loss of channel phosphorylation, which is at least partly responsible for Ca^{2+} channel current rundown, can be slowed by the addition of cyclic nucleotides such as adenosine triphosphate (ATP) and cyclic adenosine monophosphate (cAMP) in the intracellular solutions. The action of an intracellular protease has also been shown to facilitate channel rundown (Chad and Eckert, 1986). This likely involves a degradation of the Ca^{2+} channel protein or factors responsible for maintenance of the channel in a conducting state. Protease inhibitors (*i.e.*, leupeptin), although not used in the present study, can be added to the pipette to reduce rundown.

The majority of studies which examine whole cell Ca^{2+} channel activity utilize barium (Ba^{2+}) as the charge carrier instead of Ca^{2+}. The Ca^{2+} channel is more permeant to Ba^{2+} than Ca^{2+}. Thus, Ba^{2+} will typically give a much larger Ca^{2+} channel current than a similar concentration of Ca^{2+} will. Further, Ba^{2+} does not activate intracellular Ca^{2+}-dependent processes. This allows for examination of Ca^{2+} channel current without influence from Ca^{2+}-activated enzymes or Ca^{2+}-induced Ca^{2+} release.

SPECIFIC AIMS

1. Do low micromolar concentrations of MeHg decrease Ca^{2+} channel current in primary cultures of cerebellar granule neurons? What are the characteristics of the reduction in current in terms of frequency- and voltage-dependence?

2. Do Ca^{2+} channel antagonists prevent the ability of MeHg to elicit a decrease in Ca^{2+} channel current? Conversely, does MeHg prevent the ability of Ca^{2+} channel antagonists to elicit a rapid decrease in current?

Specific Aim 1 is addressed in Chapter 2. Time course experiments were performed with three different concentrations of MeHg (0.25, 0.5 and 1 μM) at two different stimulation frequencies (0.1 and 0.2 Hz). In addition, the effect of each concentration of MeHg on the current-voltage relationship was determined. Experiments which examined the ability of a variable magnitude prepulse to facilitate the MeHg-induced reduction of current occurring during a subsequent test pulse were also performed.

The experiments directed to Specific Aim 2 are described in Chapter 3. Only one concentration of MeHg (1 μM) was used for these experiments. The extent of the reduction in current produced by 1 μM MeHg in the control situation (MeHg alone) was compared to experiments where one of the Ca^{2+} channel antagonists (nimodipine, ϖ-conotoxin GVIA, ϖ-conotoxin MVIIC, ϖ-agatoxin IVA or calcicludine) was added prior to MeHg to remove

a portion of the whole cell current. The effect of nimodipine, ω-conotoxin GVIA or ω-conotoxin MVIIC, added after MeHg had decreased a portion of the current, was also determined and compared to the situation where the respective antagonist was added in the absence of MeHg.

CHAPTER TWO

METHYLMERCURY-INDUCED DECREASE OF WHOLE CELL Ba^{2+} CURRENT IN CEREBELLAR GRANULE NEURONS

ABSTRACT

In this study I show that low concentrations of MeHg (0.25 - 1 μM) decrease both peak and end Ba^{2+} currents in a concentration-dependent fashion in primary cultures of cerebellar granule cells. The decrease occurs regardless of the test potential used to elicit current. Slight alterations in the current-voltage relationship for current elicited at the end of a depolarizing step were observed; however, this was not the case for the peak (maximal) current. Increasing the stimulation frequency from 0.1 to 0.2 Hz did not affect the apparent rate or total amount of reduction produced by a 5 min exposure to 1 μM MeHg, but did hasten the onset and increase the magnitude of the effect at both 0.25 and 0.5 μM MeHg. When cells were held at -90 mV and not depolarized, exposure to MeHg was able to elicit decreases in both peak and end currents. Both 0.25 and 0.5 μM, but not 1 μM, MeHg decreased a greater proportion of the end current relative to the peak current in this situation. Application of a variable magnitude prepulse prior to a depolarizing test pulse resulted in a similar degree of current reduction at all prepulse potentials, suggesting that the effect was not voltage-dependent. Longer exposures to MeHg, especially at 1μM, often abolished the inactivating portion of the current. These results show that acute exposure to submicromolar concentrations of MeHg can decrease whole cell Ba^{2+} currents in cerebellar granule cells. In some cases, the pattern of Ba^{2+} current reduction seems to depend on the stimulation frequency. Based on the low concentration of MeHg needed to reduce Ba^{2+}

currents and the rapidity of the action compared to other events mediated by MeHg in granule cells, these results suggest that reduction of Ca^{2+} channel current may play a role in the sensitivity of cerebellar granule cells to MeHg.

INTRODUCTION

The neurotoxic organomercurial MeHg was the causative agent of two catastrophic outbreaks of poisoning in the past half century (Takeuchi *et al.*, 1968; Bakir *et al.*, 1968). Coincident with exposure, a marked degeneration of cerebellar architecture occurred, especially in the cerebellar granule cell layer, while other cell types in the cerebellum were typically spared (Chang, 1977). Mechanisms to explain this selective disruption have been postulated, including small size of granule cells (<10 μm) and selective uptake of MeHg, but none has been shown to contribute directly to the enhanced sensitivity. One family of proteins which seems to possess a sensitivity to the disruptive effects of MeHg is the voltage-dependent Ca^{2+} channel. Ca^{2+} channels participate in intracellular events such as neurotransmitter release, axonal growth and gene expression by allowing influx of extracellular Ca^{2+}, resulting in the subsequent activation of proteins. Brief exposures to relatively high concentrations of MeHg have been shown to alter Ca^{2+} channel function in several preparations, including $^{45}Ca^{2+}$ uptake in synaptosomes (Shafer *et al.*, 1990; Hewett and Atchison, 1992), whole cell Ba^{2+} currents in pheochromocytoma (PC12) cells (Shafer and Atchison, 1991) and dorsal root ganglion neurons (Büsselberg, 1995; Büsselberg *et al.*, 1995) and miniature end-plate potential frequency at the neuromuscular junction (Atchison *et al.*, 1984). Cerebellar granule cells possess a large diversity of Ca^{2+} channels, with 5 postulated types (L, N, P, Q and R) being described to date (Randall and Tsien, 1995). Because of

their location on the plasma membrane and strict regulation by various processes, such as elevations in $[Ca^{2+}]_i$, enzyme activity and membrane voltage, all of which have been shown to be affected by MeHg, Ca^{2+} channels are a likely target of this compound. MeHg also possesses several characteristics which increase its likelihood for interaction with Ca^{2+} channels, as well as other channel types. These include such factors as the monovalent charge of MeHg, its high lipophilicity and its affinity for sulfhydryl groups. Thus, the presence of a unique type of Ca^{2+} channel or perhaps a differential expression of Ca^{2+} channels, may confer upon granule cells a heightened sensitivity to MeHg. To begin to examine potential mechanisms contributing to the sensitivity of cerebellar granule cells to MeHg, whole cell Ba^{2+} currents in primary cultures of rat cerebellar granule cells were examined using conventional patch clamp methodology.

MATERIALS AND METHODS

Chemicals and Solutions: Stock solutions (5 mM) of methylmercuric chloride (ICN Biomedicals, Aurora, OH) were prepared weekly in deionized water. Extracellular recording solution contained the following (mM): HEPES (10), TEACl (117), $BaCl_2$ (5), $MgCl_2$ (1), d-glucose (25) and tetrodotoxin (TTX) (0.001), pH 7.2 at room temperature. Internal (pipette) solution contained (mM): CsAc (130), $MgCl_2$ (2), $CaCl_2$ (1), EGTA (5) and HEPES (10), pH 7.2. Adenosine 5'-triphosphate (ATP, 3 mM) and adenosine 3',5'-cyclic monophosphate (cAMP, 1 mM) were added to the pipette solution to minimize rundown of the currents which occurs presumably due to washout of factors responsible for channel activity. Working solutions of MeHg were prepared by diluting stock solutions with the appropriate amount of extracellular solution. TTX, ATP and cAMP were obtained from Sigma Chemical (St. Louis, MO). Sources of compounds used in the isolation, characterization and culture of cerebellar granule cells were as follows: Dulbeco's modified eagle medium (DMEM), fetal bovine serum (FBS) and penicillin-streptomycin - Gibco BRL (Grand Island, NY); deoxyribonuclease I (DNAse I) and type III trypsin - Worthington Biochemicals (Freehold, NJ); Neurotag Red - Boehringer-Mannheim (Indianapolis, IN); anti-glial fibrillary acidic protein (GFAP) monoclonal antibody from mouse ascites fluid (1° antibody), anti-mouse IgG F_c (directed against the constant tail region of mouse IgG) fluorescein isothiocyanate (FITC) conjugate raised in goat (2° antibody), cytosine arabinofuranoside

(Ara-C), kainic acid, insulin and GABA - Sigma Chemical (St. Louis, MO).

Isolation and Culture of Cerebellar Granule Cells: Granule cells were isolated according to a procedure adapted from Conn (1990). 7 day old Sprague-Dawley rat pups were anesthetized with CO_2, decapitated and the cerebella were removed surgically. Excess tissue and meninges were then removed following addition of cerebellar tissue to an ice-cold Ca^{2+}-Mg^{2+}-free HEPES buffered saline solution (CMF-HBSS) which contained the following (mM): 5.4 KCl, 0.4 KH_2PO_4, 136.9 NaCl, 0.3 Na_2HPO_4, 20.0 HEPES, 0.6 EDTA, 5.6 *d*-glucose, and 4.2 $NaHCO_3$ (pH 7.3). Cerebellar tissue was minced using 2 scalpel blades and placed in CMF-HBSS containing 0.025% type III trypsin (w/v) and incubated in a shaking water bath at 37°C for 15 min. Following transfer of the cell suspension to a 50 ml centrifuge tube, trypsin was inactivated by addition of 10 ml of ice-cold DMEM containing 0.04% DNAse I (w/v) and 5% fetal bovine serum (v/v). This crude cell/tissue suspension was centrifuged at 134 x *g* for 3 min at 4°C. The supernatant was discarded and the cell pellet resuspended in 3 ml of DMEM containing 5% fetal bovine serum and 0.04% DNAse I. The cell suspension was then triturated with a wide bore pasteur pipette (~15 times) and allowed to stand for 4 min on ice. Supernatant containing dissociated cells was transferred to a sterile tissue culture tube and kept on ice. The cell pellet was redigested in 3 ml of 0.04% DNAse I solution, triturated and allowed to stand on ice for 4 min. Following collection of dissociated cells in

the supernatant, and transfer to the sterile tissue culture tube, the cell pellet was again redigested in 0.04% DNAse I, triturated and allowed to stand for 4 min on ice. A final collection of dissociated cells contained in the resulting supernatant was then performed. The total fraction of dissociated cells was then separated into 2 50 ml sterile tissue culture tubes. Using a 20 ml syringe, cell suspensions were underlayed with 10 ml CMF-HBSS containing 4% bovine serum albumin (w/v) and 0.03% $MgSO_4$ solution. Cells were centrifuged at 134 x *g* for 3 min at 4°C and the supernatant was discarded. The cell pellet was rinsed in 10 ml CMF-HBSS and centrifuged again. The resulting supernatant was discarded and the cell pellet resuspended in 10 ml CMF-HBSS and an aliquot removed for cell counting and trypan blue exclusion assay. After centrifugation, the cells were resuspended in DMEM growth medium which contained the following: 10% v/v fetal bovine serum, 25 mM KCl, 50 µM GABA, 50 µM kainic acid, 5 µg/ml insulin and 100 U/ml penicillin- 100µg/ml streptomycin. Cells (approximately 37 µl of a suspension containing 100,000 cells/ml) were plated onto poly-lysine coated glass coverslips in 35 mm plastic dishes containing 2 ml of DMEM growth medium. Cells were maintained at 37°C in a humidified, 5% CO_2 atmosphere.

To limit glial cell contamination of cultures, 20-22 h after plating cells, 1 ml of growth medium was removed and replaced with 1 ml medium containing 20 µM cytosine arabinoside (Ara-C, final concentration 10 µM). Antibiotics were omitted from this medium change as streptomycin has

been shown to alter Ca^{2+} channel function (Atchison *et al.*, 1988; Redman and Silinsky, 1994).

For labelling experiments, cells were plated onto poly-lysine coated glass coverslips at approximately the same density as that used for electrophysiology experiments. On day 7 *in vitro*, cells were incubated with 5 µg/ml Neurotag Red, a fluorochrome-conjugated, recombinant C fragment of tetanus toxin, which specifically labels neuronal cells (Helting and Zwisler, 1977), for 1 hr at room temperature. Cells were then fixed by addition of cold acetone (-20°C). To determine the extent of glial contamination of cultures, cells were first incubated for 1 hr with fetal bovine serum at room temperature to block non-specific binding sites. Following this, cells were incubated with a 1:400 dilution of anti-glial fibrillary acidic protein (GFAP) from mouse ascites fluid for 1 hr. A 1:2000 dilution of anti-mouse IgG (Fc specific) fluorescein isothiocyanate conjugate raised in goat was then added and this was allowed to incubate at room temperature for 30 min. Cells were examined with a Nikon Diaphot (Garden City, NY) epifluorescence microscope equipped with a G2A filter (510 to 560 nm excitation band and 590 nm barrier filter) for determination of cells labelled with Neurotag Red and a B2A filter (450 to 490 nm excitation band and 520 nm barrier filter) to determine the extent of glial cell contamination. Cell cultures were determined to be composed of >90% neurons, nearly all of which were likely to be granule cells based upon their similar size and morphology.

Electrophysiology: Cells were cultured for 2-5 days prior to use in experiments. Current density, as well as cell capacitance, increased with the number of days in culture, but no attempt was made to describe contributions of various current types to the whole cell current as a function of days in culture. Prior to recording, a coverslip shard containing granule cells was washed with extracellular solution, placed into the recording chamber and covered with approximately 1 ml of extracellular recording solution. The remaining shards were kept in culture medium at room temperature for periods of up to 40 min, during which time no alteration in current size or waveform could be detected. Voltage-activated Ba^{2+} currents were recorded using the whole cell patch voltage-clamp method (Hamill *et al.*, 1981). Resistance of patch electrodes (World Precision Instruments, Sarasota, FL) was typically 4-8 MΩ. Solutions containing MeHg and other chemicals were gravity perfused into the chamber through a series of tubes positioned immediately adjacent to the cell. The patch clamp circuit consisted of an Axon Instruments (Foster City, CA) CV-4 head stage and Axopatch 1BN patch clamp amplifier. Pulse protocols were generated and current responses were recorded on-line using a microcomputer and the Axon Instruments pClamp^R program interfaced to the Axopatch 1B *via* an Axon Instruments TL-1 interface board. Following acquisition of a cell-attached patch and cancellation of pipette capacitance, the whole cell configuration was obtained either by applying negative pressure to the pipette or by application of a brief (<1 ms) voltage pulse. All currents

shown were elicited from a holding potential (V_h) of -90 mV. An estimate of the non-specific (leak) current was obtained by applying hyperpolarizing pulses which were of equal duration but one-quarter the magnitude of the test pulse. In some cases, a small (+10 mV) depolarizing pulse applied prior to the test pulse was used to measure leak current. Current responses were filtered at 1-2 kHz using a four-pole low-pass Bessel filter. Recorded currents were the same regardless of whether or not series resistance was compensated. As such, series resistances were not compensated. Following scaling, leak currents were subtracted from gross current using the Clampfit^R analysis program. Peak current is defined as the maximum current elicited during the first several ms of the voltage step while end current represents the average current during the final 10 ms of the voltage step. All recordings were made at room temperature. A minimum of three replications were performed for each experiment. Statistical analysis consisted either of a repeated measures analysis of variance and Dunnett's multiple comparison test or a Student's t-test.

Correction for Rundown of Ba^{2+} current: In control experiments, peak and end Ba^{2+} currents exhibited a rundown from a normalized value of 1.0 to 0.87 and 0.85, respectively, over a 5 min period. Figure 2.1A shows a representative example of the decline in peak and end currents over a 5 min period. No observed alteration in current inactivation was evident during the course of rundown (Fig. 2.1B). This was determined by measurement of

the percentage of current which inactivated during the test pulse using the formula,

$$x = I_p - I_e / I_p \times 100$$

where x is the percent inactivation, I_p is the peak current and I_e is the end current. To correct data points at various times for MeHg- and drug-sensitive currents, values obtained from averaged control experiments were used. Thus, if a 5 min exposure to MeHg resulted in a 50% reduction of the peak current, the corrected MeHg-sensitive current would be 37% (50% - 13% (rundown) = 37%). All of the current traces depicted in the figures have been corrected for leak current.

FIG. 2.1. Rundown of control peak and end whole cell Ba^{2+} currents in cerebellar granule neurons. **(A)** From H_p = -90 mV, cells were depolarized to 0 mV (0.1 Hz). Extracellular bath solution was continually perfused onto the cell starting at time 0. Rundown of pak (filled circls) and end (open circles) current typically occurred in a gradual fashion ovre a 5 min period. **(B)** Current traces from the experiment depicted in **(A)** showing the control current (bottom trace) taken at time 0, and the current remaining after 5 min of exposure to extracellular bath solution (top trace). Note that no apparent change in the current waveform was evident after 5 min.

Fig. 2.1

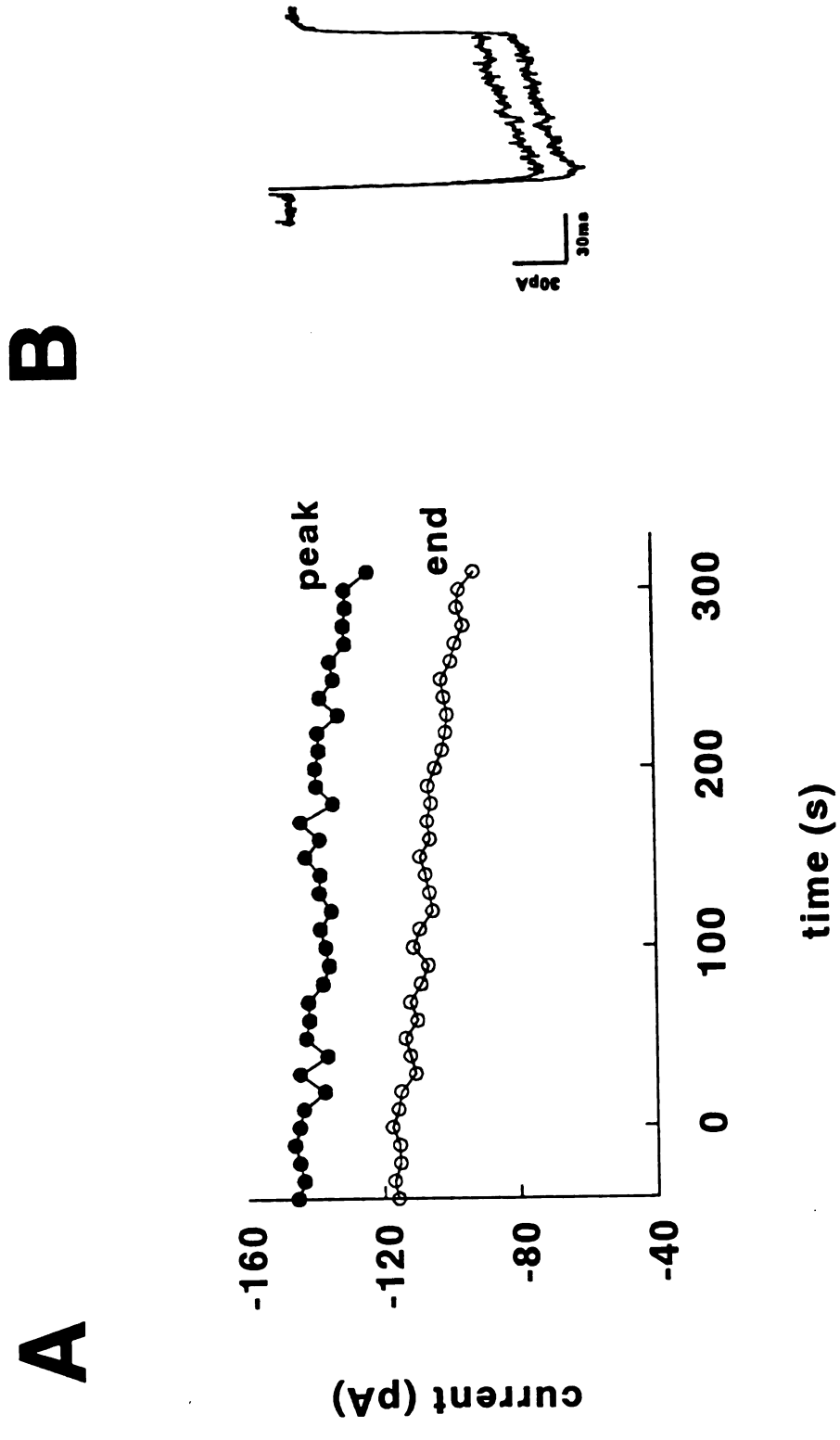
A
B
peak
end
-160
-120
-80
-40
0
100
200
300
current (pA)
time (s)
30pA
30ms

RESULTS

Short depolarizing test pulses from -90 mV elicited Ba^{2+} current which displayed both sustained and inactivating components (Fig. 2.2A). Ba^{2+} current was entirely high voltage-activated, typically activated at -30 mV and the maximum current was usually elicited by a depolarization to -10 or 0 mV (Fig. 2.2B). Mean peak and end control currents averaged -105 ± 6 and -81 ± 8 pA, respectively. To verify that Ba^{2+} currents arose from Ca^{2+} channel activity, sensitivity of the currents to 1 µM $CdCl_2$ was tested. Cd^{2+} rapidly and completely blocked Ba^{2+} currents in a reversible fashion (Fig. 2.2C).

The effect of MeHg on whole cell Ba^{2+} currents was determined following stabilization of control current. Experiments which examined the effect of a higher concentration of MeHg (10 µM, n=6) revealed a sharp decline in both peak (56 ± 6%) and end (48 ± 6%) current in less than 1 min of exposure (Fig 2.3A). Longer exposures resulted in large increases in the leak current (Fig. 2.3B) and the loss of the gigaohm seal. Thus, to facilitate examination of the effect of MeHg over a longer period, 3 lower concentrations (0.25, 0.5 and 1 µM) were used in subsequent experiments.

Concentration-dependent effect of MeHg

At 0.1 Hz, MeHg (0.25 - 1 µM) decreased both peak and end Ba^{2+} currents in a concentration- and time-dependent fashion. The onset of the decrease in current was slow and progressed in a gradual fashion following

FIG. 2.2. Properties of whole cell Ba^{2+} current in cerebellar granule neurons. **(A)** Current evoked by depolarizing voltage steps (shown -30 to +10) from a holding potential (V_h) of -90 mV. **(B)** Plot of peak Ba^{2+} current versus step potential for a representative experiment. Maximum peak current was typically elicited by depolarizations to -10 or 0 mV. **(C)** Block of whole cell Ba^{2+} current by 1 μM $CdCl_2$ and subsequent reversal following wash with Cd^{2+}-free extracellular recording solution.

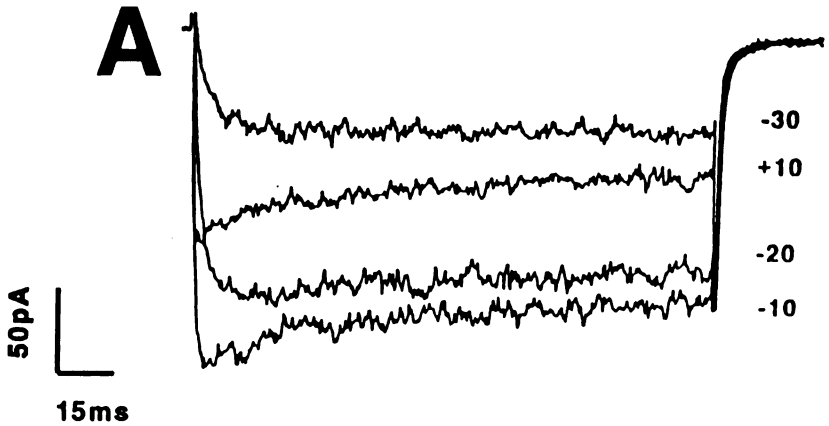
A
-30
+10
-20
-10
50pA
15ms

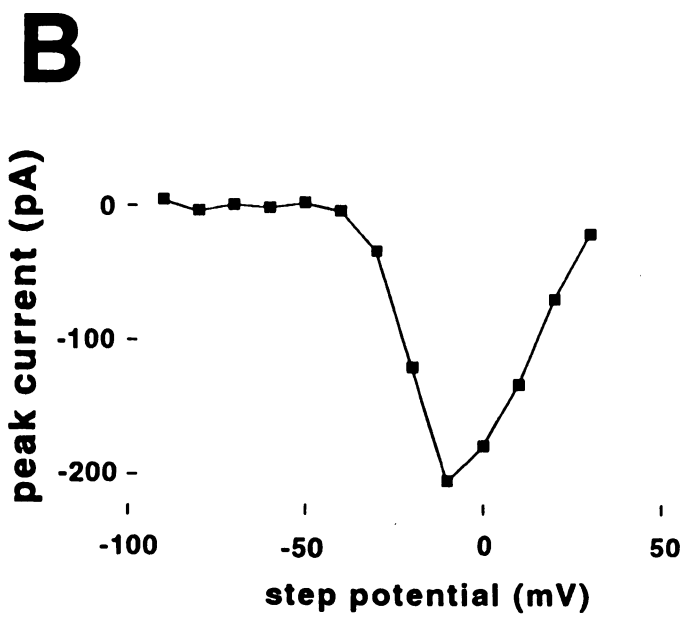
B
peak current (pA)
0
-100
-200
-100
-50
0
50
step potential (mV)

Fig. 2.2

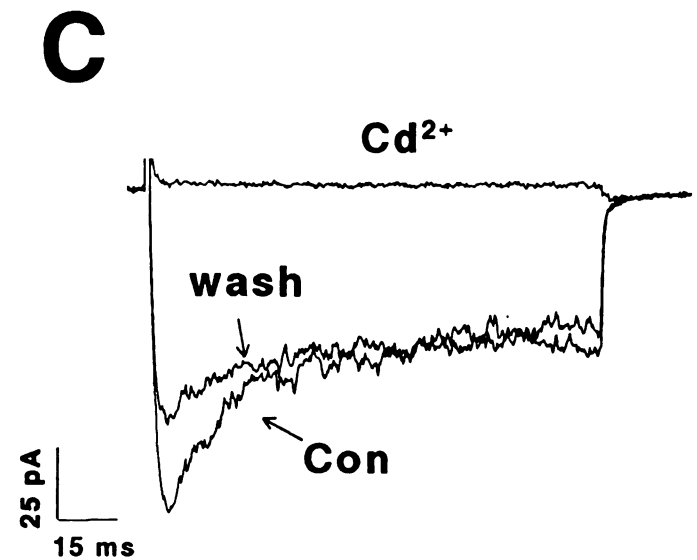
C
Cd2+
wash
Con
25 pA
15 ms

FIG. 2.3. 10 μM MeHg decreases Ba^{2+} current and increases leak current. **(A)** Control Ba^{2+} current **(a)** was decreased >50% following a 30 second exposure **(b,c)**. **(B)** Hyperpolarizing pulses (-10 mV) given after the depolarizing step elicited small non-specific (leak) currents in the control situation **(a)** and following 30 seconds of exposure to MeHg **(b)**. At 70 seconds, leak current was increased **(c)** relative to the two earlier time points.

Fig. 2.3

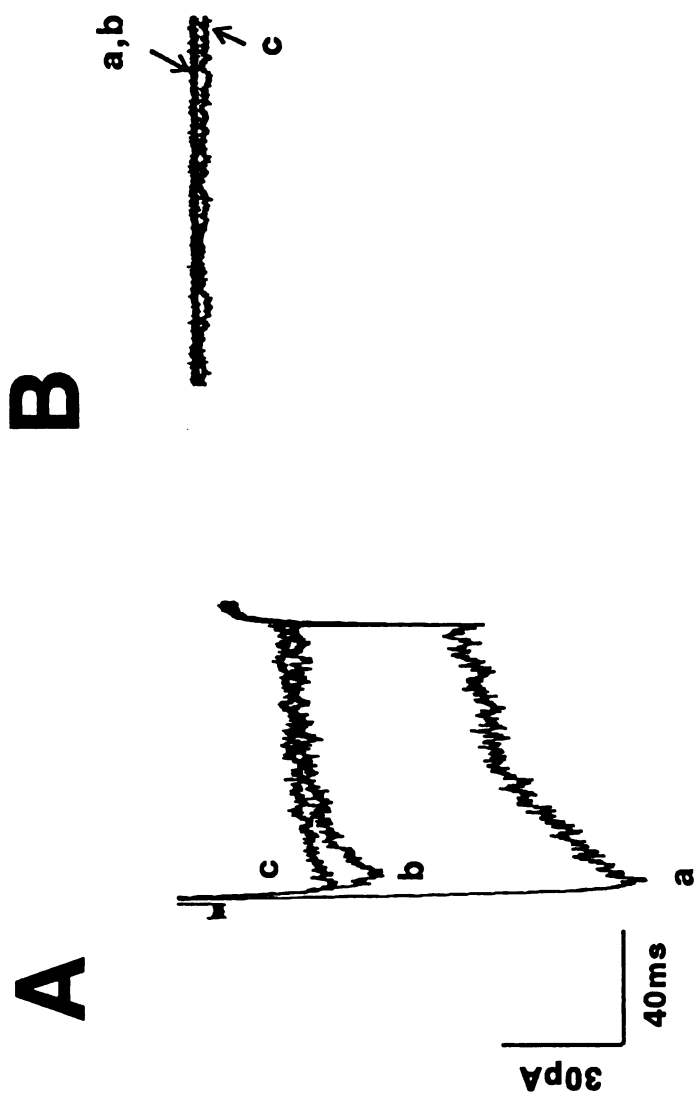

addition of 0.25 µM MeHg. At this concentration, the effect of MeHg on Ba^{2+} current amplitude was somewhat more variable than at the higher concentrations. Indeed, in one experiment, 0.25 µM MeHg was without effect on either peak or end current amplitude. When a decrease in current amplitude was evident, it appeared that this effect leveled off after a variable exposure time. However, it cannot be stated with certainty that longer exposures to lower concentrations of MeHg do not produce a similar magnitude reduction of Ba^{2+} current as a short term exposure to a higher concentration. The mean decrease in Ba^{2+} current amplitude produced by 0.25 µM MeHg was 13 ± 6% of the peak current and 14 ± 9% of the end current (n=7). Even at 0.25 µM, the decrease in Ba^{2+} current elicited by MeHg was irreversible (Fig. 2.4), a finding which was repeated at the higher concentrations (0.5, 1 µM) and is consistent with previous reports of the irreversibility of MeHg effects.

0.5 µM MeHg also caused a time-dependent decrease in both peak and end currents (Fig. 2.5A). Current traces from a representative experiment with 0.5 µM MeHg obtained prior to MeHg addition **(a)** and after 1 **(b)** and 4 **(c)** min of exposure to MeHg show a sizable reduction in current amplitude accompanied by an apparent decrease in the percentage of current which inactivates (Fig. 2.5B). As with 0.25 µM MeHg, the decrease in current amplitude did tend to level off as the time of exposure increased. Pooled data from seven experiments revealed that 0.5 µM MeHg removed 32 ± 9% and 24 ± 8% of the original peak and end control Ba^{2+}

FIG. 2.4. Irreversible reduction of peak Ba^{2+} current by 0.25 μM MeHg. **(A)** 0.25 μM MeHg caused a small, steady decline in the amplitude of peak and end (not shown) Ba^{2+} currents. **(B)** Wash with MeHg-free extracellular solution did not reverse the decrease or prevent a further decrease presumably due to MeHg. Similar effects were observed at the higher concentrations of MeHg. Shown are traces obtained in the control situation **(a)**, following ~3 min of MeHg exposure **(b)** and following a 4 min wash with MeHg-free bath solution.

Fig. 2.4

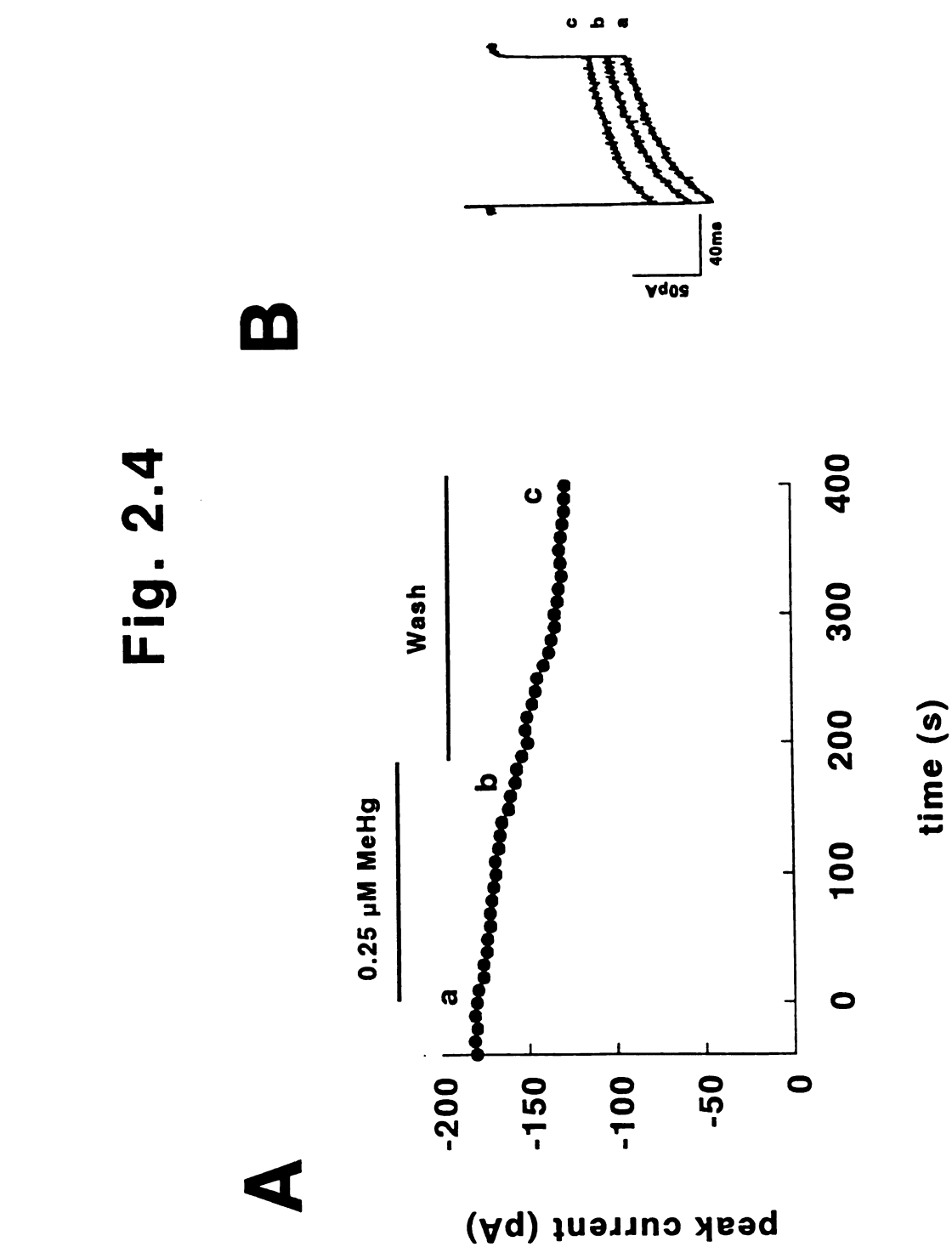
A
B
0.25 µM MeHg
Wash
a
b
c
-200
-150
-100
-50
0
0
100
200
300
400
peak current (pA)
time (s)
50pA
40ms

FIG. 2.5. Reduction of peak and end Ba^{2+} current by 0.5 μM MeHg at a stimulation frequency of 0.1 Hz. **(A)** 0.5 μM MeHg decreased both peak (filled circles) and end (open circles) currents while leaving the leak current (triangles) relatively unaffected. **(B)** Traces from the experiment in **(A)** depicting control **(a)**, 1 **(b)** and 4 **(c)** min of exposure to 1 μM MeHg.

currents (n=7).

When cells were exposed to 1 μM MeHg, the onset of the decrease in current was rapid. Typically, the decrease in current proceeded in a gradual fashion, albeit at an apparently faster rate than that observed at the two lower concentrations. Complete removal of the current was never observed, even in one case where the cell was held for >8 minutes. Current traces from a representative experiment with 1 μM MeHg show that current was decreased relative to control following 1 min **(b)** of exposure but the inactivation profile was little affected. Following 4 min **(c)** of exposure, inactivation was noticeably reduced (Fig. 2.6). Overall, 1 μM MeHg decreased peak and end Ba^{2+} currents by 44 ± 3% and 54 ± 7% (n=8), respectively. Values for 1 μM MeHg-induced decreases in end current were significantly greater ($p<0.05$, unpaired *t*-test) than those obtained at 0.25 and 0.5 μM MeHg. 1 μM MeHg also decreased peak current to a significantly greater degree compared to the value obtained at 0.25 μM MeHg. A comparison of the reduction in peak and end Ba^{2+} currents elicited by 0.25 - 1 μM MeHg at a stimulation frequency of 0.1 Hz is given in Figure 2.7.

The ability of 1 μM $HgCl_2$ (Hg^{2+}) to decrease whole cell Ba^{2+} currents was also tested. Like other inorganic heavy metals, $Hg^{2+}$is a well-known blocker of voltage-gated Ca^{2+} channels (Busselberg *et al.*, 1994; Leonhardt *et al.*, 1996). Hg^{2+} can apparently enter cells through Ca^{2+} channels (Miyamoto, 1983; Hinkle et al., 1987) a process which likely arises due to

FIG. 2.6. Reduction of peak and end Ba^{2+} current by 1 μM MeHg at a stimulation frequency of 0.1 Hz. **(A)** Both peak (filled circles) and end (open circles) current were decreased following a 5 min exposure to MeHg. Leak currents (diamonds) were slightly enhanced in this experiment. **(B)** Current traces from the experiment in **(A)** depicting control **(a)**, and 1 **(b)** and 4 **(c)** min of exposure to 1 μM MeHg. MeHg caused an apparent reduction of the inactivating component of the current (compare **a** and **c**).

Fig. 2.6

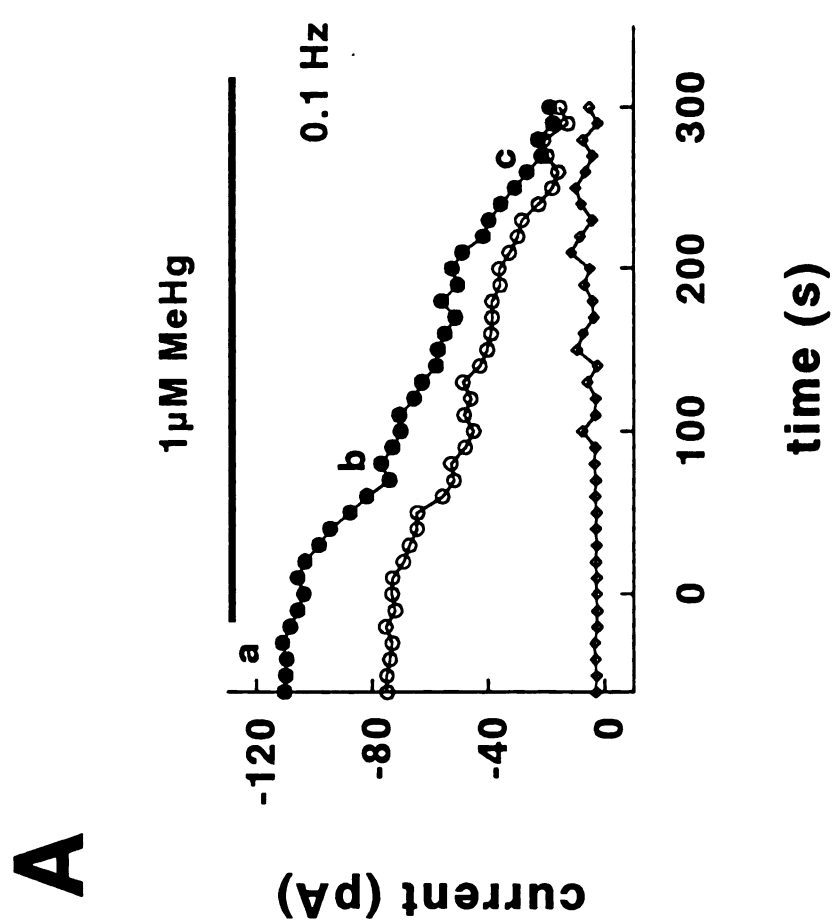
A
1μM MeHg
0.1 Hz
a
b
c
-120
-80
-40
0
current (pA)
0
100
200
300
time (s)
B
c
b
a
25pA
25ms

FIG. 2.7. MeHg (0.25 - 1 μM) decreases peak and end Ba^{2+} currents in a concentration-dependent fashion at 0.1 Hz. Values represent the mean ± SEM MeHg-induced reduction in peak and end Ba^{2+} currents following a 5 min exposure to MeHg. All values have been corrected for rundown as well as leak current. 1 μM MeHg-induced reductions in peak and end Ba^{2+} currents were significantly greater than values obtained at 0.25 μM MeHg. The end current removed by 1 μM MeHg was also significantly greater than the value observed at 0.5 μM MeHg ($p<0.05$; unpaired students *t*-test; n=7-8 experiments).

Fig. 2.7

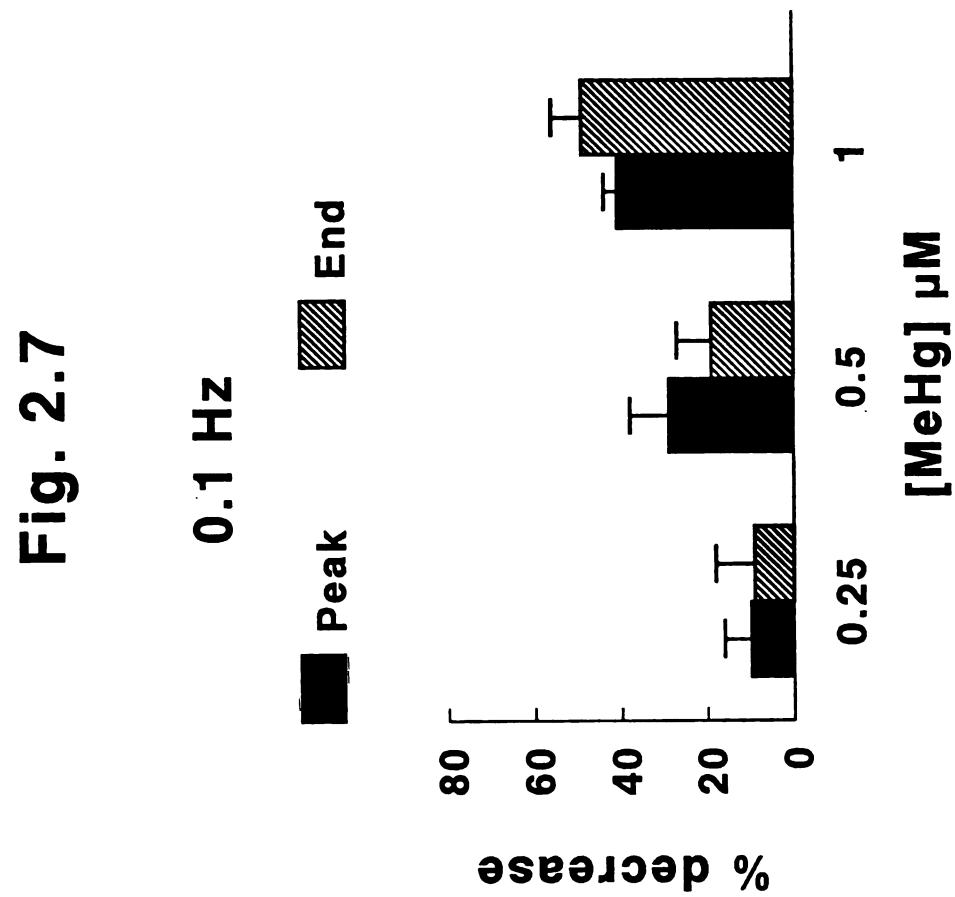

the similar ionic radius and valency of Hg^{2+} to Ca^{2+}. Entry into the Ca^{2+}channel pore is also thought to be the mechanism by which Hg^{2+} reduces Ca^{2+} current. Experiments were performed to determine if the rate and/or extent of Ba^{2+} current reduction by 1 µM Hg^{2+} was similar to that seen with 1 µM MeHg. At 1 µM, Hg^{2+} decreased 55 ± 9% and 52 ± 9% of peak and end currents, respectively (n=6). The time of exposure to Hg^{2+} in all of these experiments was 2 min or less. Large increases in the leakage current precluded the examination of the Hg^{2+}-induced effect for longer periods. Examination of the current-voltage relationship in the presence and absence of Hg^{2+} (Fig. 2.8) revealed that Hg^{2+} decreased peak and end Ba^{2+} currents at all potentials which activated current and shifted the voltage at which the maximum current was reached, consistent with other reports (Büsselberg *et al.*, 1991; Pekel *et al.*, 1993; Weinsberg *et al.*, 1995). Thus, at 1 µM, Hg^{2+} appears to block Ba^{2+} current more effectively than MeHg.

Frequency-dependent effect of MeHg

Facilitation of an antagonist-induced reduction in current by an increase in the stimulation frequency suggests that the antagonist either acts at a site within the channel pore or that the effect is intracellular. I tested the ability of an increased stimulation frequency to enhance the decrease in current produced by each of the three different concentrations of MeHg. At 0.4 Hz, both rate and extent of Ba^{2+} current rundown were too

FIG. 2.8 Effect of 1 μM $HgCl_2$ on the peak Ba^{2+} current-voltage relationship. **(A)** Current-voltage relationship for a single cell in the control situation (filled circles) and following ~1 min of exposure to 1 μM Hg^{2+}. Note that $HgCl_2$ caused a slight depolarizing shift in the potential at which the maximum peak current was elicited. Similar results were obtained in 3 other experiments. **(B,C)** Representative traces from a separate experiment depicting depolarization steps to -10, 0 and +20 mV in the control situation **(B)** and following a brief exposure to 1 μM Hg^{2+} **(C)**. $HgCl_2$ decreased peak and end currents equally well at all potentials which elicited Ba^{2+} currnet.

Fig. 2.8

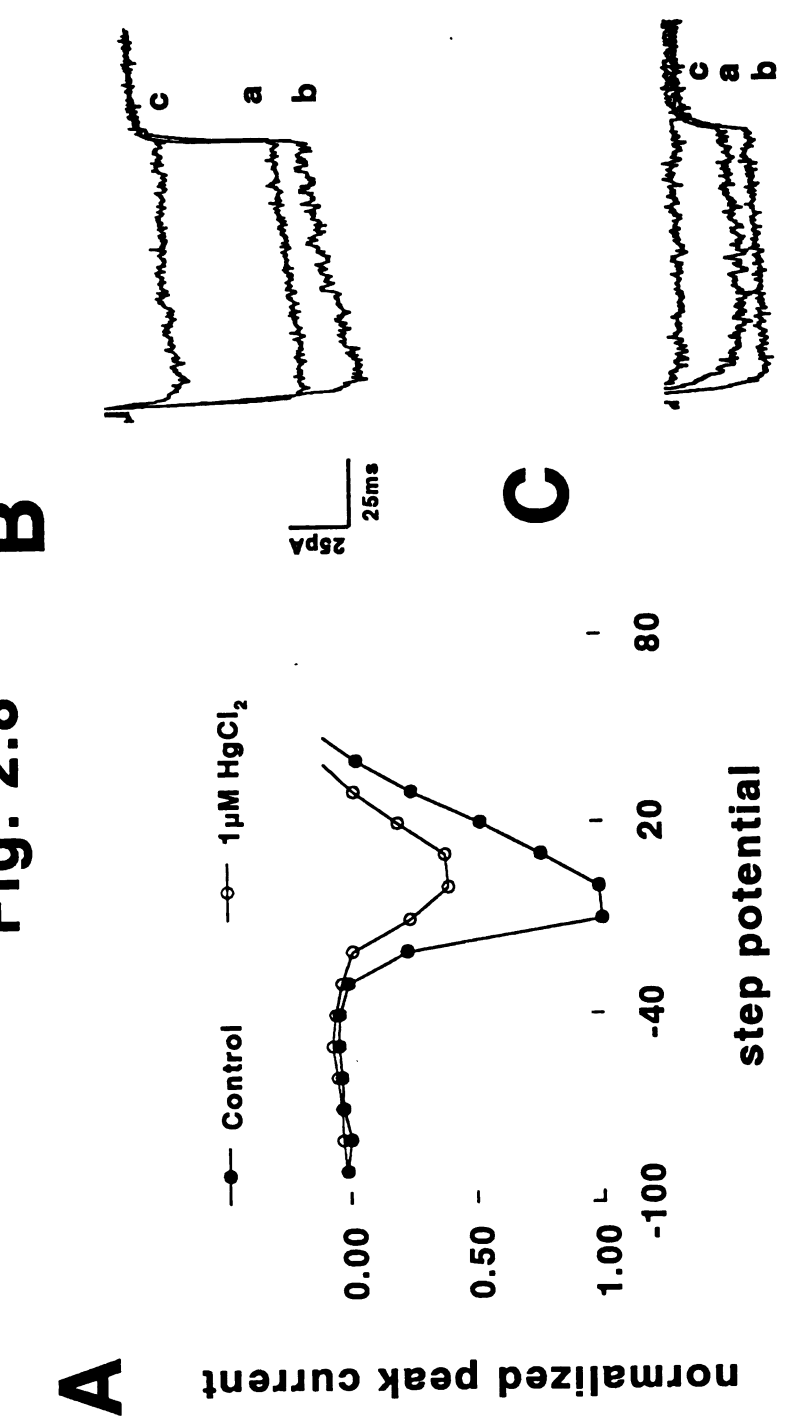
A
normalized peak current
0.00
0.50
1.00
-100
-40
20
80
step potential
Control
1μM HgCl2
B
c
a
b
25pA
25ms
C
c
a
b

significant to allow for an accurate description of the effect of MeHg. At 0.2Hz, control currents ran down slightly faster with peak currents decaying by 23 ± 6% and end current by 20 ± 7% at 5 min (n=6). These values were not statistically different from values obtained at 0.1 Hz. Thus, to examine whether the effect of MeHg is frequency-dependent, as well as use-dependent, experiments were performed at 0.2 Hz.

At the two lower concentrations of MeHg, a facilitation of the MeHg-induced decrease in peak and end currents was apparent. Figure 2.9A shows a representative example of the effect of 0.5 µM MeHg on peak and end currents. A rapid decline in both current fractions was followed by a more gradual reduction. The reduction of both current components eventually progressed to a greater degree than that seen at 0.1 Hz. Current traces from the experiment in **A** taken prior to MeHg addition **(a)** and following 1 **(b)** and 4 **(c)** min of exposure show that MeHg completely abolished the inactivating current (Fig. 2.9B). At 0.5 µM MeHg, peak and end currents were reduced by 68 ± 5% and 73 ± 6 %, respectively (n=3). Following similar exposure periods, 0.25 µM MeHg removed 44 ± 11% and 43 ± 8% of peak and end currents, respectively (n=6). Each of these values was significantly elevated over its respective peak or end value obtained at 0.1 Hz.

A similar enhancement of the decrease in current was not observed when cells were exposed to 1 µM MeHg in the presence of 0.2 Hz stimulation (Fig. 2.10A). Indeed, at this stimulation frequency, the

FIG. 2.9. Increasing the stimulation frequency to 0.2 Hz facilitates the reduction of peak and end Ba^{2+} current induced by 0.5 μM MeHg. **(A)** Following an initial rapid decline in control **(a)** peak and end currents **(b)**, there was a gradual decrease followed in turn by an enhanced reduction of the remaining current **(c)**. **(B)** Current traces from the experiment in **(A)** depicting control **(a)**, and 1 **(b)** and 4 **(c)** min of exposure to 0.5 μM MeHg. The inactivating portion of the Ba^{2+} current in this experiment appeared to be decreased by MeHg.

Fig. 2.9

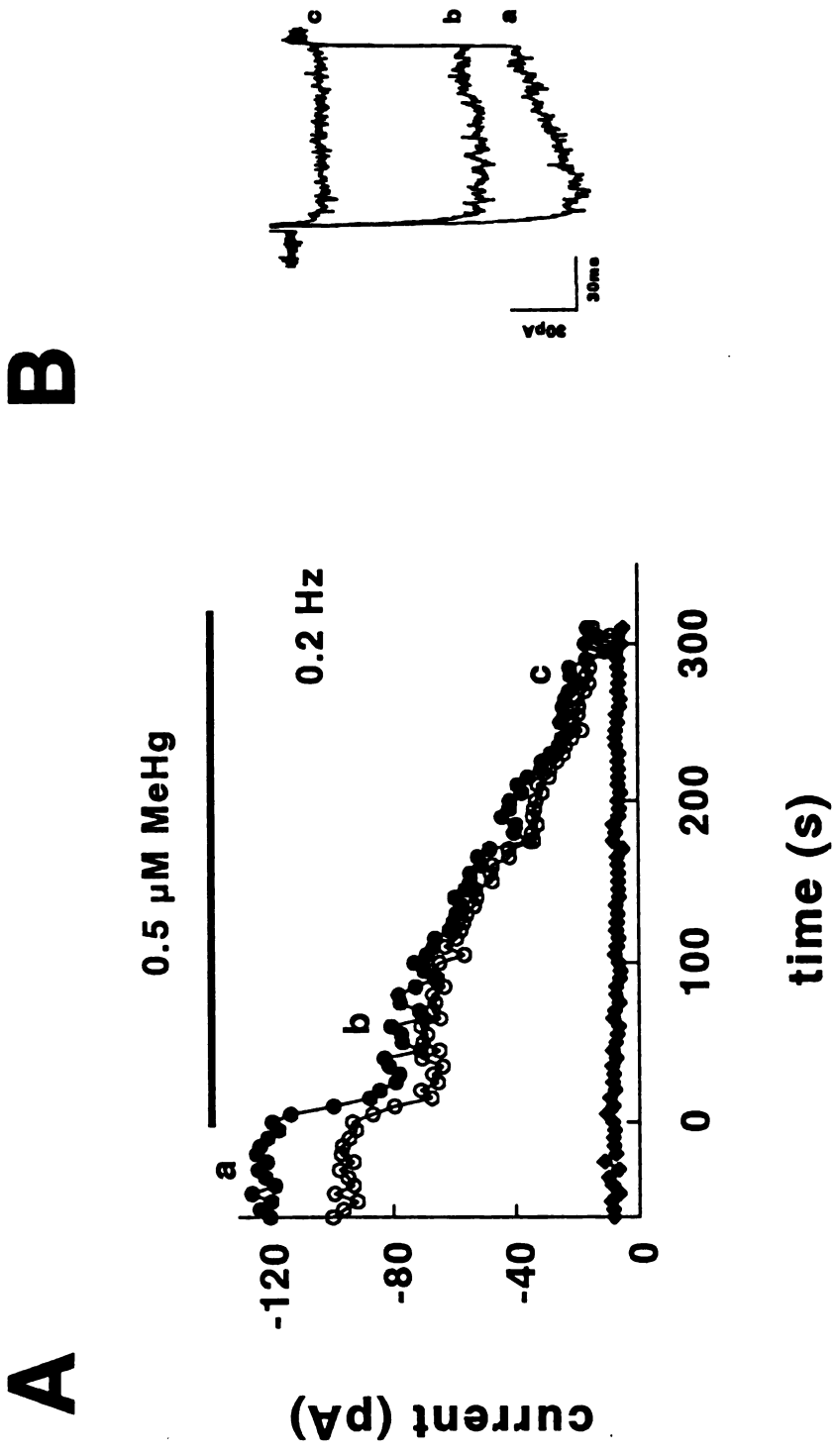
A
B
0.5 µM MeHg
0.2 Hz
a
b
c
-120
-80
-40
0
0
100
200
300
time (s)
current (pA)
30pA
30ms

FIG. 2.10. Increasing the stimulation frequency to 0.2 Hz does not facilitate the reduction of peak and end Ba^{2+} current induced by 1 μM MeHg. **(A)** Peak and end control currents **(a)** were decreased in the presence of 1 μM MeHg at 0.2 Hz **(b,c)**. A 5 min exposure to MeHg at 0.2 Hz produced no greater reduction in either peak or end currents compared to that observed at o0.1 Hz. **(B)** Current traces from the experiment in **(A)** depicting control **(a)**, 1 **(b)** and 4 **(c)** min of exposure to 1 μM MeHg.

Fig. 2.10

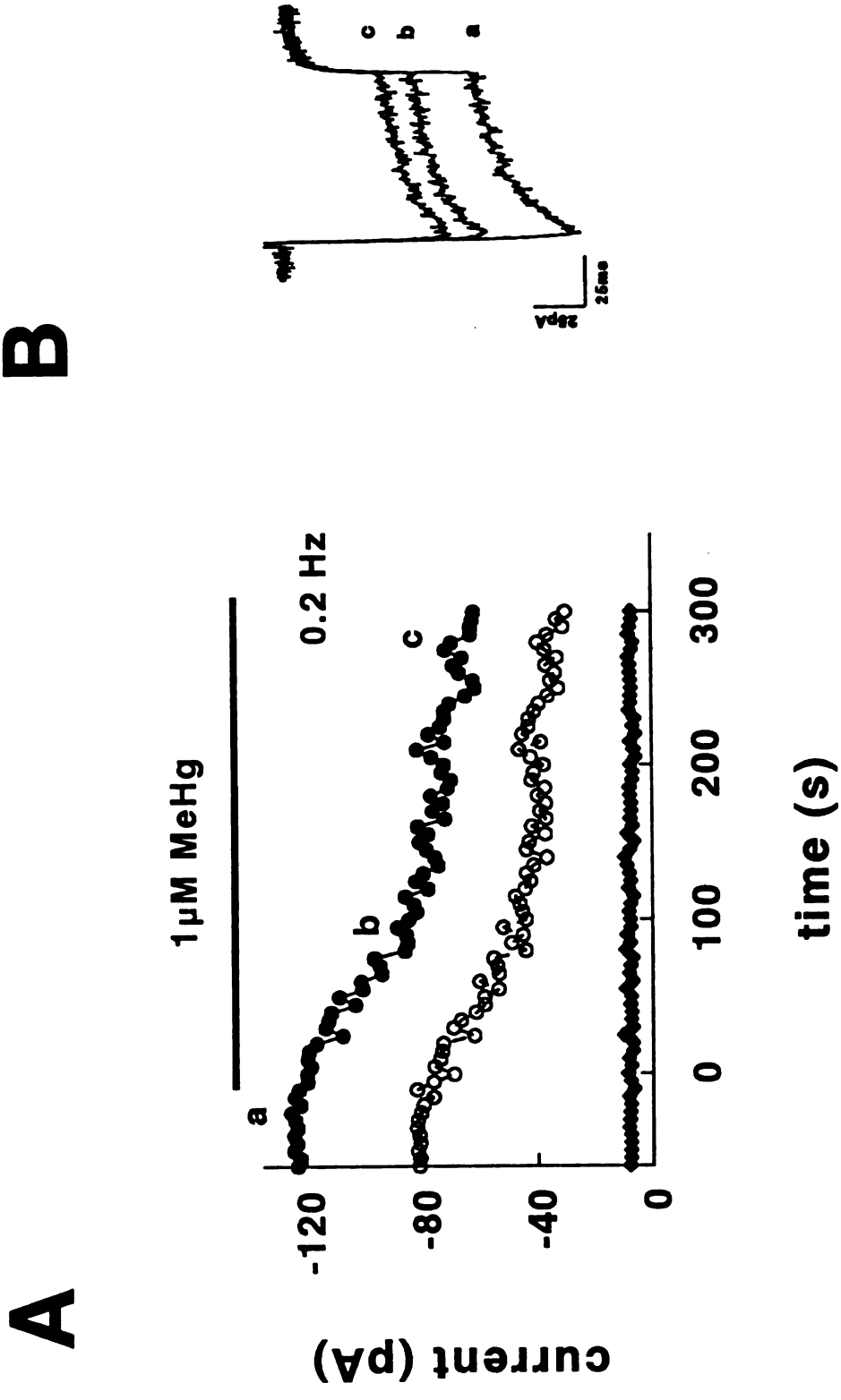
A
B
1μM MeHg
0.2 Hz
a
b
c
-120
-80
-40
0
0
100
200
300
time (s)
current (pA)
22pA
25ms

reduction of peak and end currents by 1 μM MeHg was somewhat less than that observed at 0.1 Hz. Current traces from a representative experiment showing the effect of 1 μM MeHg at 0.2 Hz are shown in Figure 2.10B. Episodes obtained prior to MeHg exposure (a) and following 1 (b) and 4 (c) min of exposure show that in this case the current reduction was diminished relative to the 0.1 Hz situation and the inactivation profile was not altered. The ability of 1 μM MeHg to decrease the inactivating portion of the Ba^{2+} current did not depend on the stimulation rate however, as removal of the inactivating current was also observed in other experiments performed at 0.2 Hz. In five experiments at 0.2 Hz, 1 μM MeHg decreased peak and end currents by 37 ± 4% and 38 ± 4%, respectively. A comparison of the reduction in peak and end Ba^{2+} currents elicited by 0.25 - 1 μM MeHg at both 0.1 and 0.2 Hz is given in Figure 2.11.

MeHg is a relatively lipophilic compound, thus it may access the Ca^{2+} channel and produce a decrease in current by a means other than entry through the open Ca^{2+} channel pore. To examine this possibility, experiments were performed where cells were exposed to MeHg for 3 minutes in the absence of depolarizing stimuli. The extent of reduction in current following a single depolarizing step (0 mV) was then determined.

In control experiments, there was no change in the magnitude of either peak or end currents following the 3 min quiescent period (data not shown), thus no corrections were made for rundown. At 0.25 μM, MeHg consistently decreased a greater amount of the end current compared to the

FIG. 2.11. Comparison of the MeHg-induced decrease in peak **(A)** and end **(B)** Ba^{2+} currents at 0.1 and 0.2 Hz. At 0.1 Hz (filled bars), the effect of MeHg (0.25 - 1 μM) on peak and end currents was concentration-dependent. Increasing the stimulation frequency to 0.2 Hz (striped bars) facilitated the reduction induced by 0.25 and 0.5, but not 1 μM MeHg. (* - significantly different from respective value at 0.1 Hz, $p<0.05$; n=3-8 experiments).

Fig. 2.11


A
peak current
0.1 Hz
0.2 Hz
% decrease
0
20
40
60
80
0.25
0.5
1
*
*
B
end current
0.1 Hz
0.2 Hz
% decrease
0
20
40
60
80
0.25
0.5
1
*
*
[MeHg] µM

peak (Fig. 2.12A). Peak currents were decreased by an average of 19 ± 1%,while end currents were decreased nearly twice as much (35 ± 7%, n=5). The MeHg-sensitive current, obtained by subtracting current following the 3 min exposure to MeHg from control current, is depicted at the bottom of Figure 2.12A. Interestingly, peak and end currents were ultimately decreased to a similar extent following continuation of MeHg exposure (0.1 Hz) for approximately 3 min in this experiment.

A preferential decrease of the end current relative to the peak current was also occasionally observed at 0.5 μM MeHg, although the effect was not consistent. In five pooled experiments, 0.5 μM MeHg removed 36 ± 11% of the peak current and 54 ± 18% of the end current. In 3 of these experiments peak current was decreased an average of 53 ± 6% while end currents were reduced 84 ± 4%. A representative example of the preferential decrease of end current by 0.5 μM MeHg is shown in Figure 2.12B. The MeHg-sensitive current in this example was predominantly non-inactivating, with a slight enhancement of the effect at the end of the pulse relative to the peak.

Following exposure to 1 μM MeHg in the absence of stimulation, the reduction in peak and end current amplitude was typically similar (Fig. 2.12C). In 7 of 9 experiments, 1 μM MeHg decreased peak and end currents by 38 ± 4% and 38 ± 6%. These values are similar to those obtained at 0.2 Hz with 1 μM MeHg. In one experiment, MeHg actually increased peak and end current amplitude by 33% and 46%, while a single experiment

FIG. 2.12. MeHg (0.25 - 1 μM) decreases Ba^{2+} current in the absence of stimulation. Following acquisition of a stable control current (0.1 Hz), cells were held at -90 mV in the absence of depolarizing stimuli and perfused with either control or MeHg-containing solution for 3 min. After 3 min the cell was depolarized to 0 mV and the effect on peak and end currents determined. In control experiments, peak and end current amplitudes were unchanged following 3 min in the absence of stimulation. **(A)** 0.25 μM MeHg removed 19 ± 1% and 35 ± 7% of peak and end currents, respectively (n=4). **(B)** 0.5 μM MeHg decreased 37 ± 7% of the peak and 45 ± 21% of the end current (n=5). **(C)** At 1 μM MeHg, reduction of peak and end currents was 38 ± 4% and 38 ± 6%, respectively (n=5). Shown below each trace is the MeHg-sensitive current obtained by subtracting current in the presence of MeHg from the control current (n=4-9 experiments).

Fig. 2.12

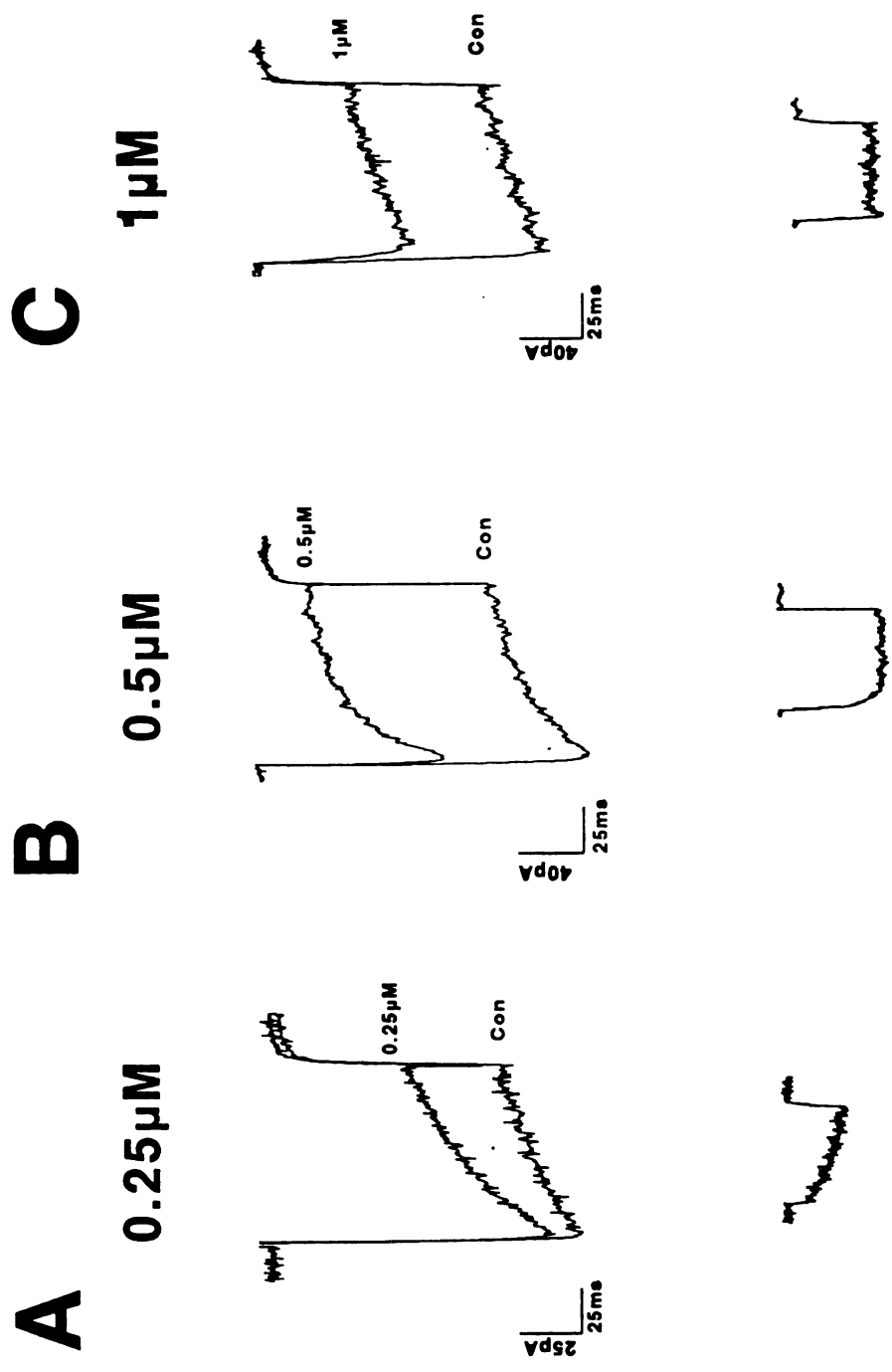
A
0.25µM
0.25µM
Con
25pA
25ms
B
0.5µM
0.5µM
Con
40pA
25ms
C
1µM
1µM
Con
40pA
25ms

exhibited no change in the magnitude of either peak or end current. The MeHg-sensitive current for the experiment shown here was predominantly non-inactivating (Fig. 2.12C, bottom).

Further analysis of the MeHg-induced decrease in peak and end currents was performed by examination of the current-voltage (I-V) relationship in control and MeHg-exposed cells. Averaged results from 4-14 experiments show that all concentrations of MeHg decreased both peak and end currents in a concentration-dependent fashion. The decrease occurred regardless of the potential used to elicit Ba^{2+} current. Although no statistics were performed, 1 μM MeHg did slightly alter the respective potentials at which the current activated and reversed (Fig. 2.13A,B). In addition, 0.5 and 1 μM MeHg caused a slight shift in the potential at which the maximum end current was reached (Fig. 2.13B). Interestingly, the 1 μM MeHg-induced reduction in Ba^{2+} currents which occurred over the course of the I-V relationship experiments was greatly enhanced over that observed following depolarizations to 0 mV at either 0.1 or 0.2 Hz. In control I-V relationship experiments, the rate at which the different step potentials were applied (0.5 Hz) did not cause any additional rundown above that normally observed at 0.1 Hz. Thus, although these results do not concur with those observed following increases in the stimulation frequency from 0.1 to 0.2 Hz, it is possible that the effect of MeHg may be enhanced by an increased stimulation frequency. It is difficult however, to compare these results to those obtained in the MeHg time course experiments, as the

FIG. 2.13. Effect of 1 μM MeHg on the peak **(A)** and end **(B)** Ba^{2+} current-voltage (I-V) relationships. Cells were held at -90 mV and depolarized (250 ms) to the indicated potentials at 2 sec intervals. Averaged currents were normalized to the maximum current elicited in the control situation (0 mV for peak, -10 mV for end) and plotted versus the step potential. **(A)** MeHg blocked peak current in a concentration-dependent fashion, but did not alter the potential at which the current activated, the potential at which the maximum current was reached, or the reversal potential. **(B)** End current was also blocked in a concentration-dependent fashion. At 0.5 and 1 μM MeHg, there was a slight depolarizing shift in the potential at which the maximum current was reached, accompanied by a slight depolarizing shift in the activation potential with 1 μM MeHg only (n = 4-14 experiments).

Fig. 2.13

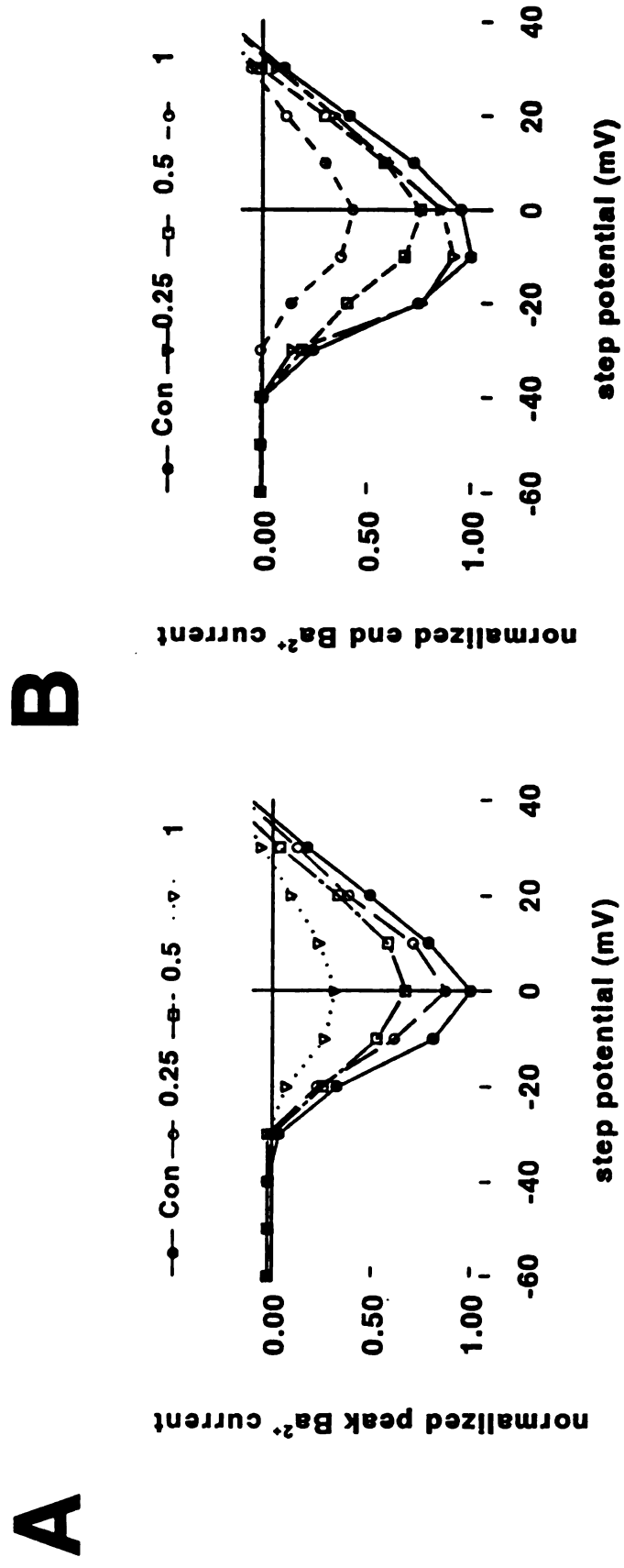
A
B
normalized peak Ba2+ current
normalized end Ba2+ current
Con
0.25
0.5
1
0.00
0.50
1.00
-60
-40
-20
0
20
40
step potential (mV)

duration of the voltage step was greater for the current-voltage relationship experiments (250 ms vs. 105 ms). Representative examples of control currents (Fig. 2.14A) and the effect of 1 μM MeHg (Fig. 2.14B) show that MeHg decreased a similar percentage of the current following step depolarizations to -20 (**a**), -10 (**b**) and +20 (**c**) mV.

To determine if MeHg interacts with Ca^{2+} channels in a voltage-dependent irreversible manner, a variable magnitude prepulse was applied prior to a constant test pulse to determine if the MeHg-induced decrease in peak current during the test pulse could be facilitated. MeHg and Ba^{2+} may compete for a binding site within the channel, or at some other site modulated by a change in voltage. Thus, if the MeHg-induced reduction of peak Ba^{2+} current occurred in a voltage-dependent irreversible manner, altering the prepulse potential should alter the magnitude of the MeHg-induced effect during the test pulse. Figure 2.15A shows normalized peak Ba^{2+} current (elicited during a test pulse to 0 mV) plotted against the prepulse potential for the mean of five pooled experiments with 0.5μM MeHg. All data were normalized within groups (test current elicited following a prepulse to -120 mV was used to normalize all other data for that concentration of MeHg or control). In the control condition,prepulses more positive than -40 mV significantly decreased peak current elicited during the test pulse when compared to the condition in which no prepulse was given. The maximum reduction in peak current (31 ± 4%, n=11) occurred with a prepulse to +10 mV. All concentrations of MeHg decreased

FIG. 2.14. 1 μM MeHg decreases peak and end Ba^{2+} current to a similar extent at all potentials which elicit current. **(A)** Representative traces showing control currents elicited following depolarizations to -20 **(a)**, 0 **(b)** and +20 **(c)** mV. **(B)** The same cell as in **A** following a 4 min exposure to 1 μM MeHg. Percentage values (mean ± SEM) for reduction of peak and end currents were similar at all potentials.

Fig. 2.14

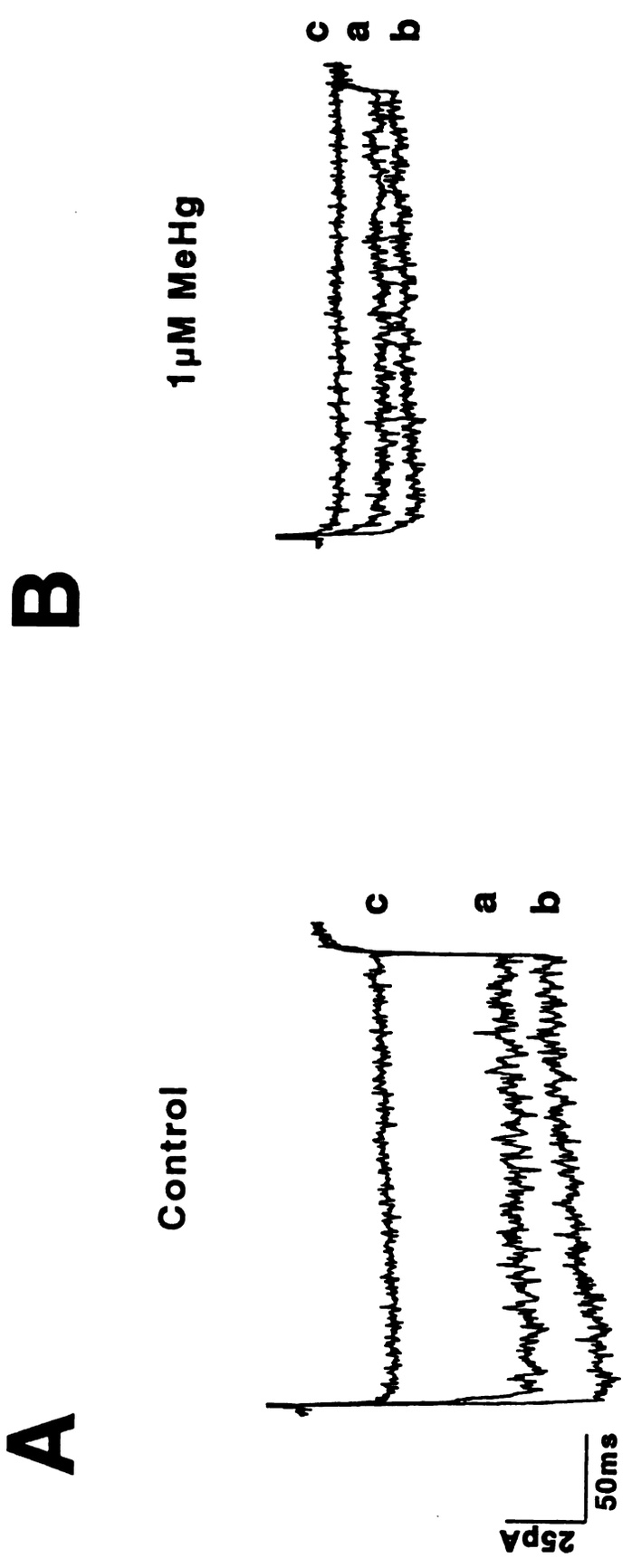

FIG. 2.15. Application of a variable magnitude prepulse does not affect the extent of reduction of peak Ba^{2+} current induced by 0.5 µM MeHg during a subsequent test pulse. **(A)** Plot of normalized peak current elicited during a constant test pulse to 0 mV. The test pulse is preceded by a variable magnitude (-120 to +10 mV), similar duration prepulse. In the control situation, prepulses more positive than -40 mV significantly reduced the peak current elicited during a subsequent test pulse. 0.5 µM MeHg decreased the current at all potentials, but did not appreciably alter the inactivation of the peak current produced by more strongly depolarizing prepulses. Data were normalized within groups to values elicited at a prepulse of -120 mV. **(B)** Representative experiment depicting control and 0.5 µM MeHg-induced reduction of Ba^{2+} current in the presence and absence of a prepulse. Note that the MeHg-induced reduction in Ba^{2+} current is similar in the absence (no prepulse) and presence (prepulse - 0 mV) of a prepulse.

Fig. 2.15

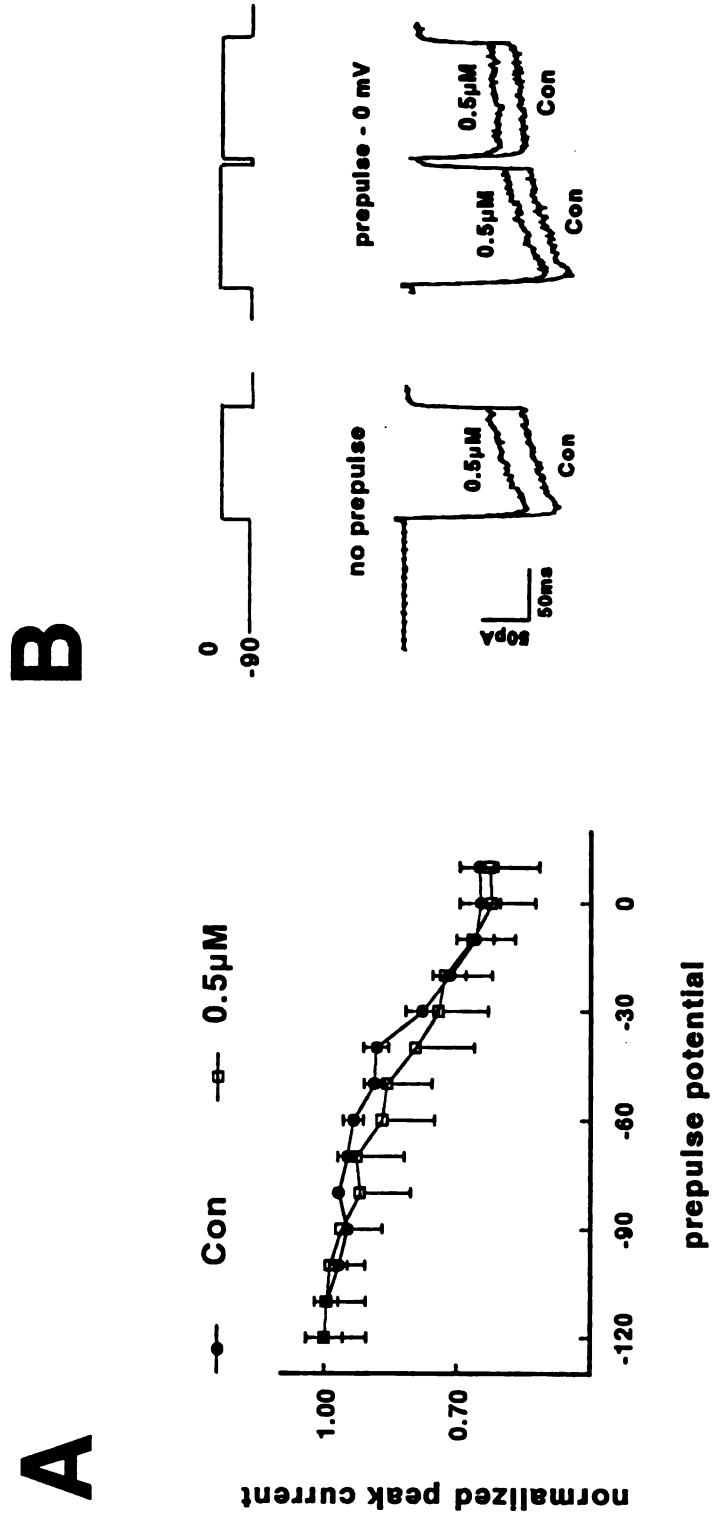
A
Con
0.5μM
normalized peak current
1.00
0.70
-120
-90
-60
-30
0
prepulse potential
B
0
-90
no prepulse
0.5μM
Con
50pA
50ms
prepulse - 0 mV
0.5μM
Con
0.5μM
Con

peak currents elicited during both the prepulse and test pulse. In the presence of 0.5 µM MeHg, prepulses more positive than -20 mV decreased significantly peak current elicited during the test pulse compared to the situation where no prepulse was given (maximum reduction 37 ± 17%, prepulse +10 mV, n=5). Following exposure to 0.5 µM MeHg, peak, as well as end, current was decreased to a similar extent in the presence and absence of a prepulse. Further, the presence of the depolarizing prepulse inactivated a component of the subsequent test pulse current (Fig. 2.15B). 0.25 µM MeHg also decreased peak current to a similar extent in the presence and absence of a prepulse. Significant decreases in peak test pulse current were observed following prepulses to a potential more positive than -50 mV (maximum reduction 43 ± 3%, prepulse +10 mV; n=7).

In the presence of 1 µM MeHg, the pattern of inactivation of peak current in the presence of a prepulse was similar to control (Fig. 2.16A), with more positive prepulses tending to cause a greater inactivation of the peak test pulse current. Under control conditions (Fig. 2.16B), a prepulse to -120 mV followed by a test pulse to 0 mV, elicits a small leak current (**a**) followed by a prominently inactivating Ba^{2+} current (***a***). When a prepulse to 0 mV is given prior to a test pulse to 0 mV, the prepulse current is maximal (**b**) while the test pulse current is reduced and the inactivation is lessened (***b***). When this protocol is repeated in the presence of MeHg (Fig. 2.16C), the prepulse current at -120 mV is basically unchanged (compare **a** from B,C), while the magnitude of the peak current and the rate of

FIG. 2.16. Application of a variable magnitude prepulse does not affect the extent of reduction of peak Ba^{2+} current induced by 1 μM MeHg during a subsequent test pulse. **(A)** Plot of normalized peak current (as in Fig. 2.15). **(B)** Representative experiment depicting control current elicited following a prepulse to -120 mV **(a)** and a test pulse to 0 mV (*a*), and a separate episode depicting currents elicited by a prepulse **(b)** and test pulse (*b*) to 0 mV. **(C)** The same cell as in **B** following a 4 min exposure to MeHg. The magnitude of the test pulse current was decreased to a similar extent in the absence (*a*) or presence (*b*) of a prepulse.

Fig. 2.16

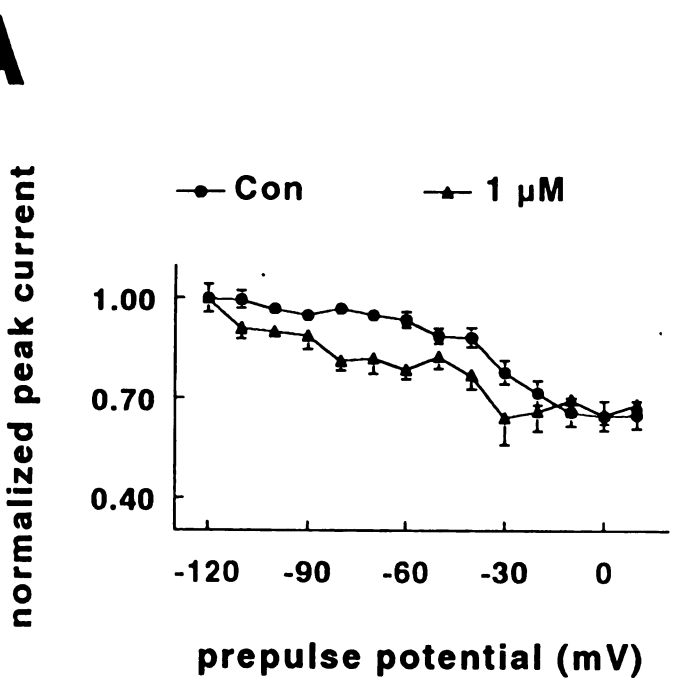
A
Con
1 μM
normalized peak current
1.00
0.70
0.40
-120
-90
-60
-30
0
prepulse potential (mV)

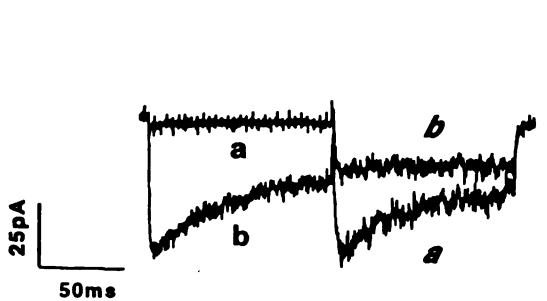
B
a
b
b
a
25pA
50ms


C
a
b
b
a

inactivation observed during the subsequent test pulse are substantially decreased (***a***). Similar decreases in the current magnitude and inactivation are also observed when both the prepulse and test pulse are 0 mV (**b**,***b***).

DISCUSSION

This report is the initial description of the MeHg-induced reduction of whole cell Ba^{2+} current in cerebellar granule neurons, the primary target site of pathological damage in MeHg toxicity. MeHg decreased both peak and end Ba^{2+} currents in a concentration-dependent fashion at concentrations similar to those observed *in vivo* (Skerfving *et al.*, 1970). Several experimental paradigms were employed in an effort to alter the MeHg-induced decrease in Ba^{2+} current. Increasing the stimulation frequency from 0.1 to 0.2 Hz facilitated the reduction in peak and end current produced by 0.5 and 0.25, but not 1, μM MeHg. In the absence of stimulation, the MeHg-induced reduction in peak and end currents was similar to, and in some cases greater than, that observed at either 0.1 or 0.2 Hz. In addition, facilitated reduction of the end current, relative to the peak current, was observed at 0.25, and occasionally 0.5, μM MeHg when cells were exposed in the absence of stimulation. At 1 μM MeHg however, peak and end currents were decreased to a similar extent. Application of a prepulse prior to the test pulse did not facilitate MeHg-induced reduction of the peak current, suggesting that the effect was not voltage-dependent. Taken together, these results suggest that granule cell Ca^{2+} channels represent a sensitive target of MeHg and that they may play a role in the heightened susceptibility of this cell type to MeHg intoxication. Further, alterations in stimulation frequency can apparently modify the pattern(s) of the MeHg-induced reduction in Ba^{2+} current amplitude.

MeHg is capable of altering Ca^{2+} channel activity in a number of experimental paradigms. In synaptosomes, MeHg non-competitively reduces K^+-depolarization induced $^{45}Ca^{2+}$ uptake through both a channel-mediated mechanism as well as by a reversed $Na^+\backslash Ca^{2+}$ exchanger (Atchison *et al.*, 1986; Shafer *et al.*, 1990; Hewett and Atchison, 1992). Whole cell Ba^{2+} currents in PC12 cells (Shafer and Atchison, 1991) and dorsal root ganglion neurons (Büsselberg, 1995) have also been shown to be sensitive to MeHg. In cerebellar granule cells (Sarafian, 1993; Marty and Atchison, *submitted*) and NG108-15 cells (Hare *et al.*, 1993; Hare and Atchison, 1995) concentrations of MeHg similar to those used in this study elevate intracellular Ca^{2+} ($[Ca^{2+}]_i$), as well as the concentration of another intracellular divalent cation and eventually lead to cell death. Paradoxically, a part of the increased $[Ca^{2+}]_i$ may arise from influx through Ca^{2+} channels, as it can be delayed by ω-conotoxin MVIIC (Marty and Atchison, *submitted*), a peptide toxin that blocks N- (Swartz *et al.*, 1993; Grantham *et al.*, 1994) and P-type (Hillyard *et al.*, 1992) Ca^{2+} channels, as well as the putative Q-type channel (Randall and Tsien, 1995). It is also possible that MVIIC may prevent Ca^{2+} entry at a site removed from Ca^{2+} channels. Thus, Ca^{2+} channels represent an important, albeit complex, target of MeHg in a number of neurons and neuron-like cells.

Although Ca^{2+} channels represent a target of MeHg, the mechanism by which MeHg decreases Ca^{2+} channel current are less well understood than for inorganic metals. Pb^{2+} (Simons and Pocock, 1987), Cd^{2+} (Hinkle *et*

al., 1987) and Mn^{2+} (Ogura *et al.*, 1990) all block Ca^{2+} channels, presumably by traversing the channel in a manner similar to that of Ca^{2+}, but at a slower rate (Nachshen, 1984). Factors such as the net charge and size of the metal are important determinants of channel blocking ability. The increased lipophilicity of MeHg, which allows it to diffuse passively through lipid membranes (Lakowicz and Anderson, 1980) suggests that it may have access to the Ca^{2+} channel by means other than entry through the open pore. This hypothesis is supported by results in PC12 cells (Shafer and Atchison, 1991) and the current study showing that MeHg is able to decrease a sizable amount of whole cell current in the absence of prior stimulation. Although the exact site of action is not known, MeHg does have a high affinity for sulfhydryl groups (Hughes, 1957) and can likely interact with several other biological complexation sites as well. While no evidence exists that MeHg can produce changes in protein structure, inorganic mercury is able to produce such an occurrence (Suzuki *et al.*, 1985). Thus, it is possible that the reduction in current involves more than a simple obstruction of the pore.

As shown in PC12 cells (Shafer and Atchison, 1991), MeHg decreased granule cell Ba^{2+} currents in a concentration- and time-dependent fashion. Unlike the situation in PC12 cells, there was no alteration in the apparent reversal potential. Further, only 1 μM MeHg produced a slight depolarizing shift in the potential at which the current activated. This may reflect the lower concentration of Ba^{2+} used here (5 mM versus 10 mM in PC12 cells),

the higher concentration of MeHg (1-20 μM) used in the PC12 cell experiments or that PC12 cell Ca^{2+} channels respond differently to MeHg than do those in granule cells. Alternatively, it may reflect the varied population of Ca^{2+} channels in granule cells compared to PC12 cells. As with experiments in PC12 cells (Shafer and Atchison, 1991), dorsal root ganglion cells in culture (Büsselberg, 1995) and murine neuromuscular junctions (Traxinger and Atchison, 1987), the effect of MeHg was irreversible. This could result from the effectiveness of MeHg binding, or alternatively to initiation of an intracellular (or intramembrane) effect which is not amenable to reversal *via* washout of MeHg.

With longer exposures to MeHg, especially at the highest concentration used (1 μM), removal of the inactivating component of the current was apparent. Ca^{2+} channel inactivation occurs by one (or more) of several means including membrane voltage (Lux and Gutrick, 1986), Ca^{2+} (Brehm and Eckert, 1978) or both (Brown *et al.*, 1981). A conformational change in the protein structure of the channel (Slatin *et al.*, 1994) likely results from the action of one or both of these factors. MeHg has been shown both to increase $[Ca^{2+}]_i$ (Marty and Atchison, *submitted*; Hare *et al.*, 1993; Sarafian, 1993) and to depolarize neuronal membranes (Kauppinen *et al.*, 1989). Thus, these factors may contribute to altered Ca^{2+} channel inactivation *in vivo*; however, the experimental paradigm utilized in these experiments minimizes the contribution from either of these components, as EGTA is contained in the pipette and the membrane voltage is held

constant. Further, concentrations of MeHg similar to those used in this study require 5-20 min of exposure prior to the elevation in granule cell $[Ca^{2+}]_i$ (Marty and Atchison, *submitted*). The possibility of a physical interaction leading to an alteration in inactivation also exists due to the reactive nature of MeHg. Typically, the decrease in the inactivating current occurred in a gradual fashion, thus the site at which it acts may be somewhat inaccessible or the action slow in onset.

I examined both peak and end Ba^{2+} currents in an attempt to determine any differences in the effect of MeHg on the two current fractions. If MeHg decreased current through a certain subset of Ca^{2+} channels, this effect might be manifest as a greater effect on one current component over the other. An examination of each of the five reported Ca^{2+} channel subtypes and their contributions to the peak or end currents was not determined. However, in granule cells, two types of channels have been classified as non-inactivating (L- and P-type), while three types have been classified as inactivating (N-, Q- and R-type) (Randall and Tsien, 1995).

In the absence of stimulation 0.25, and in some cases, 0.5, μM MeHg reduced a greater amount of the end current compared to peak. At these lower concentrations, MeHg may selectively inhibit a channel type which contributes a greater percentage to the end current. Low concentrations of inorganic metals such as Cd^{2+} and Ni^{2+} have been shown to block preferentially slowly inactivating and rapidly inactivating Ba^{2+} currents, respectively (Narahashi *et al.*, 1987; Huang, 1989). At higher

concentrations these metals become less specific and block all current components. A similar effect may be taking place here, as 1 μM MeHg decreased both peak and end currents equally. An alternative explanation is that MeHg may alter channel inactivation by converting channels into a non-conducting state. This could occur *via* an indirect physical interaction of MeHg with a sulfhydryl entity or some other potential complexation site, such as carbonyl, amino or hydroxyl groups (Dales, 1972). MeHg can also alter protein phosphorylation (Sarafian, 1993). As Ca^{2+} channel activity is dependent on both phosphorylation and dephosphorylation, any aberrations in these processes could result in a reduction of Ba^{2+} current. A t a stimulation frequency of 0.1 Hz, MeHg reduced peak and end currents to a similar degree. If the MeHg effect involves entry through the Ca^{2+} channel, as is postulated for other heavy metal ions (Nachsen, 1984; Hinkle *et al.*, 1987; Simons and Pocock, 1987) increasing the stimulation frequency should allow MeHg greater access to the Ca^{2+} channel. In PC12 cells, increases in the stimulation frequency from 0.1 to 0.2 and 0.4 Hz were able to facilitate the reduction in current produced by a higher concentration (5 μM) of MeHg (Shafer and Atchison, 1991). In my experiments, increasing the stimulation rate from 0.1 to 0.2 Hz did cause control currents to run down faster, but did not facilitate the effect of 1 μM MeHg. In contrast, both 0.5 and 0.25 μM MeHg did exhibit an enhanced ability to decrease peak and end currents under this condition. Presumably, if the MeHg-induced effect were due to some type of event mediated at the extracellular side of the plasma

membrane, then all concentrations of MeHg should exhibit a facilitated reduction in current upon increases in the stimulation frequency. The simplest explanation for these results is that 1 μM MeHg produces an additional effect (or effects) which counteracts the facilitated reduction in current produced by increasing the stimulation frequency.

In PC12 cells, MeHg-induced decreases in Ba^{2+} current were voltage-dependent at a holding potential of -40 mV, but not at -90 mV. Thus, non-inactivating Ca^{2+} channels may exhibit voltage-sensitive reductions in current (Shafer and Atchison, 1991). To test whether MeHg decreased granule cell Ba^{2+} currents in a voltage-dependent irreversible fashion, a variable magnitude prepulse was given prior to a constant test pulse. Increasing the strength of the depolarizing pulse (in the range of ~-30 to +20 mV) facilitates Ba^{2+} entry into the cell through the Ca^{2+} channel. MeHg possesses a monovalent charge, thus if the interaction of MeHg with the Ca^{2+} channel occurred in a voltage-dependent irreversible manner, then increasing the driving force during the prepulse should facilitate the decrease in current during the test pulse. In my experiments, a depolarizing prepulse given in the presence of MeHg caused no further reduction of peak and end currents during the subsequent test pulse compared to the situation in which no prepulse was given. This suggests that sites other than the proposed Ca^{2+} binding region within the channel pore are important in determining the extent of MeHg-induced reductions in Ba^{2+} current. Following longer exposures, the decrease in current

inactivation caused by MeHg was typically maximal, such that depolarizing prepulses caused no further removal of inactivation during the test pulse. This is consistent with the time course experiments, in which 1 μM MeHg typically decreased the percentage of the current which inactivated.

In summary, MeHg decreases cerebellar granule cell Ca^{2+} channel current at concentrations similar to those observed during episodes of MeHg intoxication. Moreover, these effects occur at concentrations much lower than those needed to decrease Ca^{2+} channel current in other preparations, or K^+ channels in granule cells (Sirois and Atchison, 1995). The role that the MeHg-induced decrease of Ca^{2+} channel current plays in MeHg neurotoxicity remains to be determined, as does the interaction of MeHg with other ligand- and voltage-gated channel types on these cells. Because of the reactive nature of MeHg, it is difficult to ascribe the ability of MeHg to decrease Ba^{2+} current to a single mechanism. However, the results presented here suggest that this effect of MeHg on Ca^{2+} channels is among the most sensitive endpoints tested to date. Decreases in Ca^{2+} channel current by MeHg could lead to disruption of neurotransmitter release, depolarization of plasma and mitochondrial membranes and altered regulation of $[Ca^{2+}]_i$ and could ultimately contribute to MeHg-induced cell death in the cerebellum.

CHAPTER THREE

EFFECTS OF CALCIUM CHANNEL ANTAGONISTS ON THE METHYLMERCURY-INDUCED DECREASE OF BARIUM CURRENT IN CEREBELLAR GRANULE NEURONS

ABSTRACT

Granule cells of the cerebellum exhibit a unique sensitivity to the neurotoxic effects of methylmercury (MeHg). I have previously shown that MeHg decreases Ca^{2+} channel current amplitude, an action which could contribute to MeHg-induced cell death. In this study, the effect of several pharmacological agents which decrease current through Ca^{2+} channels was examined in an effort to determine if MeHg acted preferentially on distinct components of the whole cell Ba^{2+} current. When given alone, 1 μM MeHg reduced peak and end currents by 35 ± 3% and 34 ± 4%, respectively, following exposure times ranging from 2 to 6 min. In an attempt to isolate possible channel types at which MeHg may act, a portion of the whole cell current was first removed by addition of either ω-conotoxin GVIA, ω-conotoxin MVIIC, ω-agatoxin IVA, calcicludine or the dihydropyridine nimodipine. Examination of the extent and apparent rate of subsequent reductions in current induced by the combination of MeHg and the antagonist was then determined and compared to the situation where MeHg alone was added. When given alone, all of the pharmacological agents tested decreased whole cell Ba^{2+} current to varying degrees; some overlap in specificity was apparent between the toxins. Of the total peak Ba^{2+} (5 mM) current, ω-conotoxin GVIA-sensitive current (N-type) contributed approximately 55%, ω-conotoxin MVIIC-sensitive (P- and Q-type) 40%, ω-agatoxin IVA-sensitive (P-type) 10%, and nimodipine-sensitive (L-type) 25%. Calcicludine, reported to block L-type channels in cerebellar granule cells,

blocked on average, about 25% of the peak current, but exhibited 2 differing degrees of efficacy, blocking only ~10% of the current in some cells, but ~40% in others. None of the agents tested, including GVIA or MVIIC, were able to attenuate significantly the MeHg-induced reduction of whole cell Ba^{2+} current. In the presence of calcicludine or nimodipine, the MeHg-induced decrease following a 5 min exposure was increased relative to the situation where MeHg alone was added. When MeHg was perfused onto cells prior to MVIIC or GVIA such that 25 to 50% of the control whole cell current was removed, the apparent rate of current decline induced by the combination of MeHg and the Ca^{2+} channel antagonist did not differ from that observed with the Ca^{2+} channel antagonist alone. These results suggest that MeHg is able to decrease whole cell Ba^{2+} current by mechanisms distinct from those utilized by Ca^{2+} channel antagonists. Prior removal of L-type Ca^{2+} channels can apparently facilitate the extent of MeHg-induced reductions in Ba^{2+} current, but it is unlikely that MeHg decreases preferentially the current through any particular channel type.

INTRODUCTION

Human *in vivo* exposures and experimental *in vitro* studies have shown that cerebellar granule cells are sensitive to the neurotoxic effects of the environmental contaminant methylmercury (MeHg) (Hunter and Russell, 1954; Leyshon-Sorland *et al.*, 1994). One of the possible reasons for the enhanced susceptibility of these cells compared to other cerebellar cell types is the presence of a uniquely diverse voltage-gated Ca^{2+} channel population. In addition to the commonly encountered L-, N- and P-type channels, cerebellar granule cells also possess 2 relatively novel Ca^{2+} channels termed Q- and R-type (Randall and Tsien, 1995). MeHg has been shown to decrease $^{45}Ca^{2+}$ uptake in synaptosomes (Atchison *et al.*, 1986; Shafer and Atchison, 1989; Shafer *et al.*, 1990; Hewett and Atchison, 1992), decrease whole cell Ba^{2+} current in pheochromocytoma (PC12) cells (Shafer and Atchison, 1991) and displace dihydropyridines from high affinity binding sites on PC12 cells (Shafer and Atchison, 1990). Experiments performed at the murine neuromuscular junction (Atchison, 1986; 1987), in NG108-15 cells (Hare and Atchison, 1995) and in cerebellar granule cells (Marty and Atchison, *submitted*) suggest that MeHg may also utilize Ca^{2+} channels to traverse the plasma membrane. Entry of MeHg through Ca^{2+} channels may contribute to the MeHg-induced rise in intracellular Ca^{2+} (Hare *et al.*, 1993; Hare and Atchison, 1995; Marty and Atchison, submitted) and may participate in altered patterns of spontaneous and nerve-evoked release of neurotransmitter at the neuromuscular junction (Atchison, 1986;

1987).

Much of what is known about the taxonomy of Ca^{2+} channels has been deduced through pharmacological means. Both peptide toxins and dihydropyridine compounds have been instrumental in the isolation and characterization of specific Ca^{2+} channel types. By pharmacologically removing a particular subtype of channel, it is possible to determine its contribution to a particular event. In an effort to isolate possible sites of MeHg action, various Ca^{2+} channel antagonists were added prior to MeHg to determine if they could alter the pattern of MeHg-induced reductions in Ba^{2+} current. In a similar fashion, experiments were performed where MeHg was added prior to ϖ-conotoxin GVIA or ϖ-conotoxin MVIIC to determine if any alterations in the apparent rate and/or extent of toxin block occurred.

MATERIALS AND METHODS

Chemicals: Nimodipine was obtained from Research Biochemicals International (Natick, MA). ω-conotoxin GVIA, ω-conotoxin MVIIC and ω-agatoxin IVA were all obtained from Bachem (Torrance, CA). Nimodipine was dissolved as a 100 mM stock solution (ethanol). Toxins were dissolved in deionized water and frozen as stock solutions.

Application of toxins, nimodipine or MeHg: To determine the effect of MeHg in the presence of toxin or nimodipine (collectively referred to as antagonists) the following protocol was employed. After acquisition of a stable control current, a single antagonist was perfused onto the cell and the resultant decrease in Ba^{2+} current was allowed to reach a steady state. In the continued presence of antagonist, the decrease in Ba^{2+} current induced by perfusion of MeHg was determined. Unless otherwise noted, experiments examining the effect of MeHg in the presence of antagonist, involved a 5 min exposure to MeHg. Exposure of the cell to antagonist was therefore approximately 6-7 min. Thus, although antagonist block had leveled off prior to MeHg addition, it cannot be stated with absolute certainty that the subsequent reduction of current amplitude (following MeHg addition) was due entirely to an action of MeHg. To avoid confusion however, the decrease elicited following MeHg addition in the presence of antagonist is described as a MeHg-induced decrease.

The percentage inhibition (x) of Ba^{2+} current by pharmacologic agents

was determined using the following equation

$$x = (\blacktriangle I/I_C) \text{ X } 100$$

where $\blacktriangle I$ is the difference between the control current and the current remaining in the presence of the pharmacologic agent and I_C is the control current. In experiments conducted to determine the percentage inhibition (y) of Ba^{2+} current by MeHg in the presence of pharmacologic agent, a slightly modified version of the above equation was used,

$$y = (\blacktriangle I_i/I_C) \text{ X } 100$$

where $\blacktriangle I_i$ is the difference between current remaining in the presence of antagonist (without MeHg) and that remaining with antagonist in the presence of MeHg. Statistical comparisons were made using students *t* test (unpaired) or the Mann Whitney test if the difference between standard deviations was significant. A minimum of three replications was performed for each experiment.

RESULTS

Effect of MeHg on peak and end Ba^{2+} currents: Following acquisition of a stable control current (mean peak and end currents were -106 ± 7 and -88 ± 6 pA, respectively; n=77), perfusion of 1 µM MeHg resulted in a gradual decline in peak and end currents (Fig 3.1 A,B). The waveform of the MeHg-sensitive current (obtained by subtracting trace **c** from trace **a**, Fig. 3.1B) was predominantly non-inactivating (Fig. 3.1C). After correcting for current rundown, 1 µM MeHg-induced decreases in peak and end current reached 35 ± 5% and 34 ± 4 %, respectively (0.1 Hz, n=12, Fig. 3.2) following exposure times which ranged from 2 - 6 min. No assumptions were made regarding the extent of 1 µM MeHg-induced decreases following exposures > 6 min as leakage current tended to increase with longer exposures to this concentration of MeHg. In some instances MeHg was able to alter the apparent rate of current activation (compare **a** and **c**, Fig. 3.1B), as well as inactivation. However, no mathematical calculations were performed on either activation or inactivation rates.

Nimodipine experiments: The dihydropyridine antagonist nimodipine, which blocks specifically current through L-type Ca^{2+} channels (Cohen and McCarthy, 1987), was used to determine if removal of L-type Ca^{2+} channel current could alter the MeHg-induced reduction of Ba^{2+} current. In control experiments, 0.1 µM nimodipine removed 20 ± 2% of the peak current and 31 ± 3% of the end current (n=6). Invariably, the waveform of the

FIG. 3.1. **(A)** 1 μM MeHg-induced reduction of whole cell peak Ba^{2+} current. Following stabilization of control current **(a)**, perfusion of 1 μM MeHg (time 0) resulted in a time-dependent decrease in both peak and end (not shown) currents following exposure times which ranged from 2-6 min. **(B)** Current traces from the experiment in **(A)** depicting control current **(a)** and current remaining after 3 **(b)** and 5 **(c)** min of exposure to 1 μM MeHg. **(C)** The waveform of current sensitive to MeHg in the presence of nimodipine (obtained by subtracting trace **c** from trace **a**).

Fig. 3.1

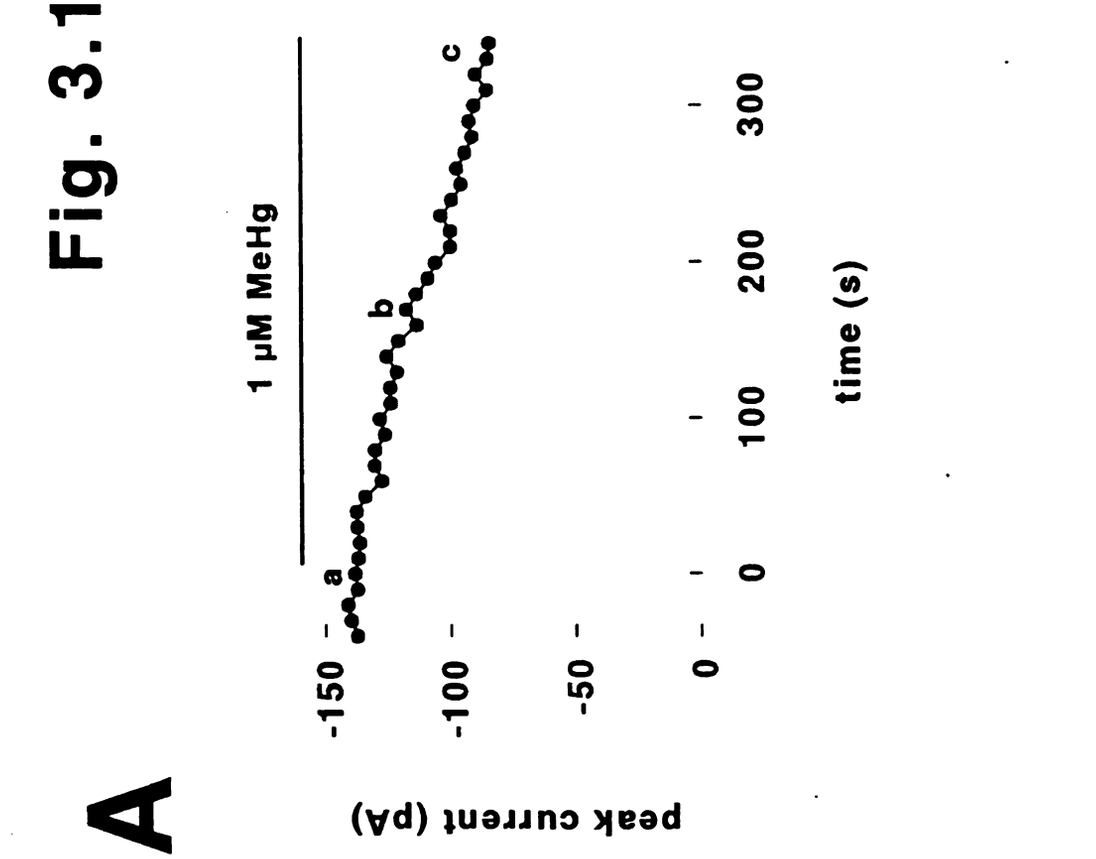
A
peak current (pA)
-150
-100
-50
0
1 µM MeHg
a
b
c
0
100
200
300
time (s)
B
c
b
a
30pA
40ms
C
(a-c)

FIG. 3.2. Reduction of peak Ba^{2+} current (mean ± SEM for n=12 experiments) by 1 μM MeHg over the course of a 5 min exposure. 1 μM MeHg was added at time 0. Average decrease (leak subtracted, rundown corrected) after a 5 min exposure to 1 μM MeHg was 35 ± 3% for peak current and 34 ± 4% for end current.

Fig. 3.2

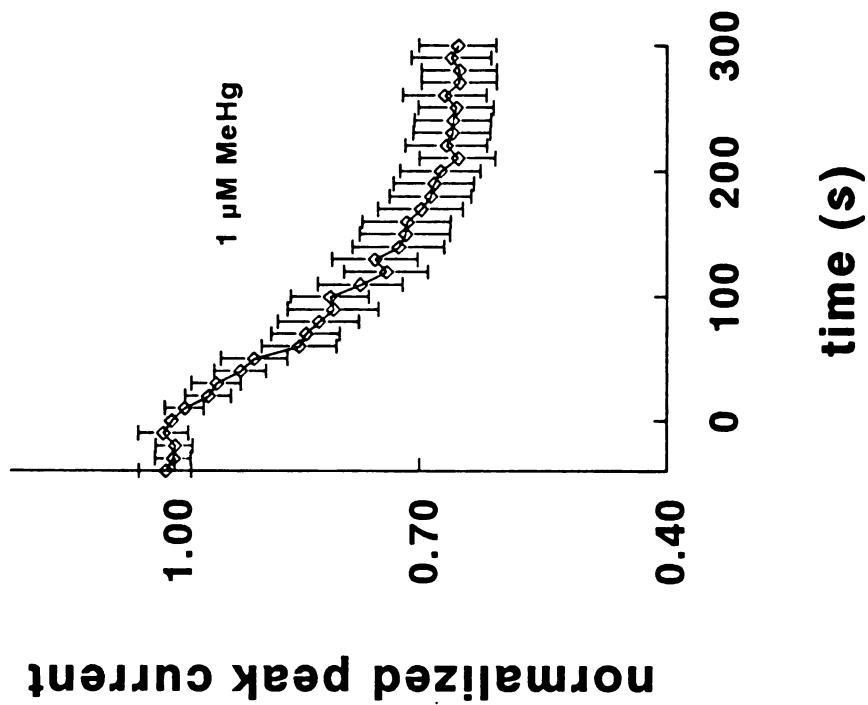
1 µM MeHg
1.00
0.70
0.40
0
100
200
300
time (s)
normalized peak current

nimodipine-sensitive current was non-inactivating. Following stabilization of the nimodipine-induced reduction in current, addition of MeHg resulted in further decreases in peak and end currents. A comparison of the decrease in normalized peak Ba^{2+} current elicited by nimodipine alone, 1 μM MeHg alone and 1 μM MeHg in the presence of nimodipine is given in Figure 3.3A. The steady-state decrease in Ba^{2+} current amplitude induced by nimodipine alone was fairly stable over several minutes. When MeHg was added after nimodipine, the extent of the decrease in current induced by MeHg was enhanced over that observed with MeHg alone. Current traces from the experiment in which nimodipine was added prior to MeHg are shown in Figure 3.3B. Following nimodipine-induced reduction of the control current **(a,b)**, a 5 min exposure to MeHg **(c)** resulted in a further reduction of the current. A subtractive determination of the MeHg-sensitive current in the presence of nimodipine reveals that both inactivating and non-inactivating components were affected (Fig. 3.3C). Pooled results from 6 experiments revealed that 1 μM MeHg decreased 51 ± 8% and 42 ± 10% of peak and end currents, respectively, in the presence of nimodipine. The reduction in peak current amplitude was significantly greater than that obtained with 1 μM MeHg alone. Overall, the combination of 0.1 μM nimodipine and 1 μM MeHg removed 71 ± 8% of peak and 73 ± 8% of end currents.

Experiments were also performed where MeHg was added prior to nimodipine. In these experiments, I sought to determine if MeHg affected

FIG. 3.3. 1 μM MeHg-induced reductions in peak Ba^{2+} current are enhanced in the presence of nimodipine. **(A)** Representative traces depicting the effect of 0.1 μM nimodipine alone (triangles), 1 μM MeHg alone (open circles) and 1 μM MeHg added following nimodipine-induced block (filled circles). To simplify the comparison, data in the presence of nimodipine alone have been omitted from the experiment in which MeHg was subsequently added (filled circles). The data that are shown for this experiment have been normalized to current in the presence of nimodipine. Addition of MeHg in the presence of nimodipine resulted in an increased extent of peak current reduction compared to the situation where cells were exposed to 1 μM MeHg alone (1 μM MeHg alone 35 ± 3%; 1 μM MeHg after nimodipine 51 ± 8%, n=6; $p<0.05$). **(B)** Current traces from the experiment in **(A)** depicting control current **(a)**, current remaining in the presence of nimodipine **(b)** and current remaining following a 5 min exposure to 1 μM MeHg in the presence of nimodipine **(c)**. **(C)** Current blocked by MeHg in the presence nimodipine possesses both inactivating and non-inactivating components **(b-c)**.

Fig. 3.3

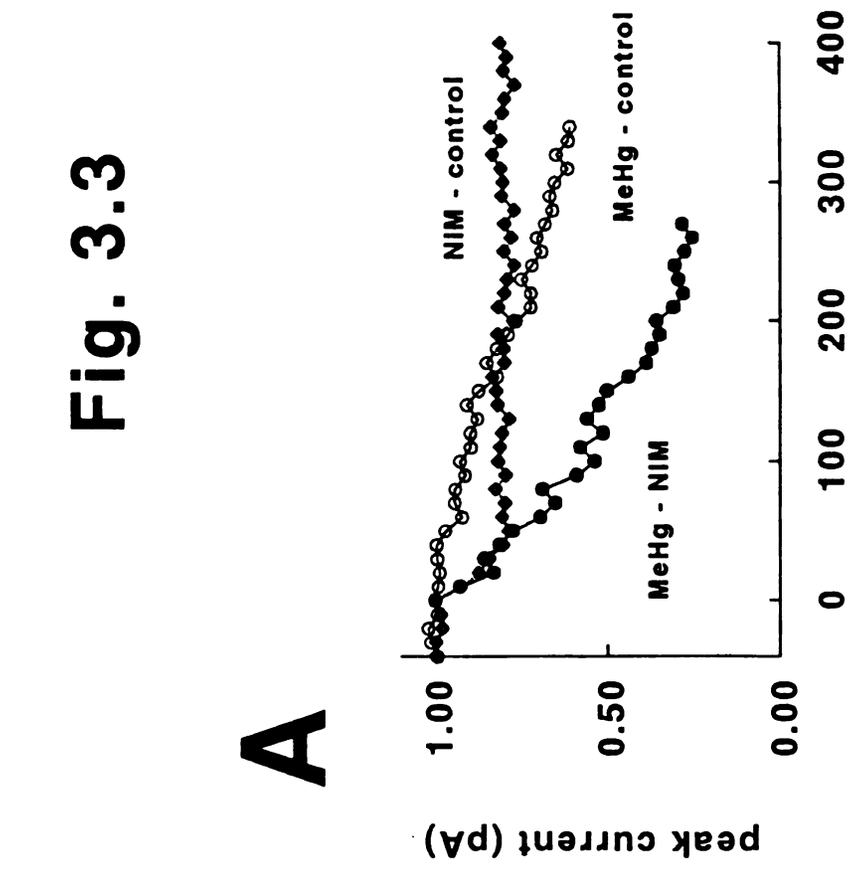
A
peak current (pA)
1.00
0.50
0.00
0
100
200
300
400
time (s)
NIM - control
MeHg - control
MeHg - NIM
B
c
b
a
25pA
40ms
C
b-c

the decrease in current elicited by nimodipine. Following nimodipine addition in the presence of MeHg, the apparent rate of current decline should increase if L-type Ca^{2+} channels have been spared by MeHg. The average 1 μM MeHg-induced decrease in peak current (prior to nimodipine addition) was 26 ± 8% (n=4). A comparison of the decrease elicited by the combination of nimodipine and MeHg to that obtained with MeHg alone reveals that the two apparent rates of current decline are not different (Fig. 3.4). This suggests that MeHg has already removed L-type Ca^{2+} channel current or that MeHg is preventing nimodipine from reaching its binding site.

ω-Conotoxin GVIA experiments: ϖ-conotoxin GVIA (GVIA) is a 27 amino acid peptide toxin isolated from the venom of the marine snail *Conus geographus* (Olivera *et al.*, 1984) which blocks specifically current carried by N-type Ca^{2+} channels (McCleskey *et al.*, 1987). In cerebellar granule cells GVIA has been shown to elicit anywhere from 20 to 90% block of whole cell peak current (Pearson *et al.*, 1993; Haws *et al.*, 1993; Pearson *et al.*, 1995; Randall and Tsien, 1995; Rossi *et al.*, 1995). In my experiments, GVIA rapidly blocked both peak (54 ± 3%) and end (53 ± 4%) currents (n=10). Subsequent perfusion of 1 μM MeHg resulted in further decreases of peak and end currents, which when expressed as a percentage of the original control currents (no GVIA), averaged 38 ± 6% and 30 ± 7% (Fig. 3.5A; n=4). Current traces from the experiment in Figure 3.5A show that GVIA

FIG. 3.4. The apparent rate of peak Ba^{2+} current reduction is similar in the presence of 1 μM MeHg alone and following 0.1 μM nimodipine addition in the presence of MeHg. Shown are normalized peak currents for 1 μM MeHg alone (diamonds) and nimodipine following partial (26 ± 8%, n=4) removal of whole cell current by 1 μM MeHg (circles). For data obtained with nimodipine in the presence of MeHg, the last current value prior to the addition of nimodipine was used to normalize all subsequent values.

Fig. 3.4

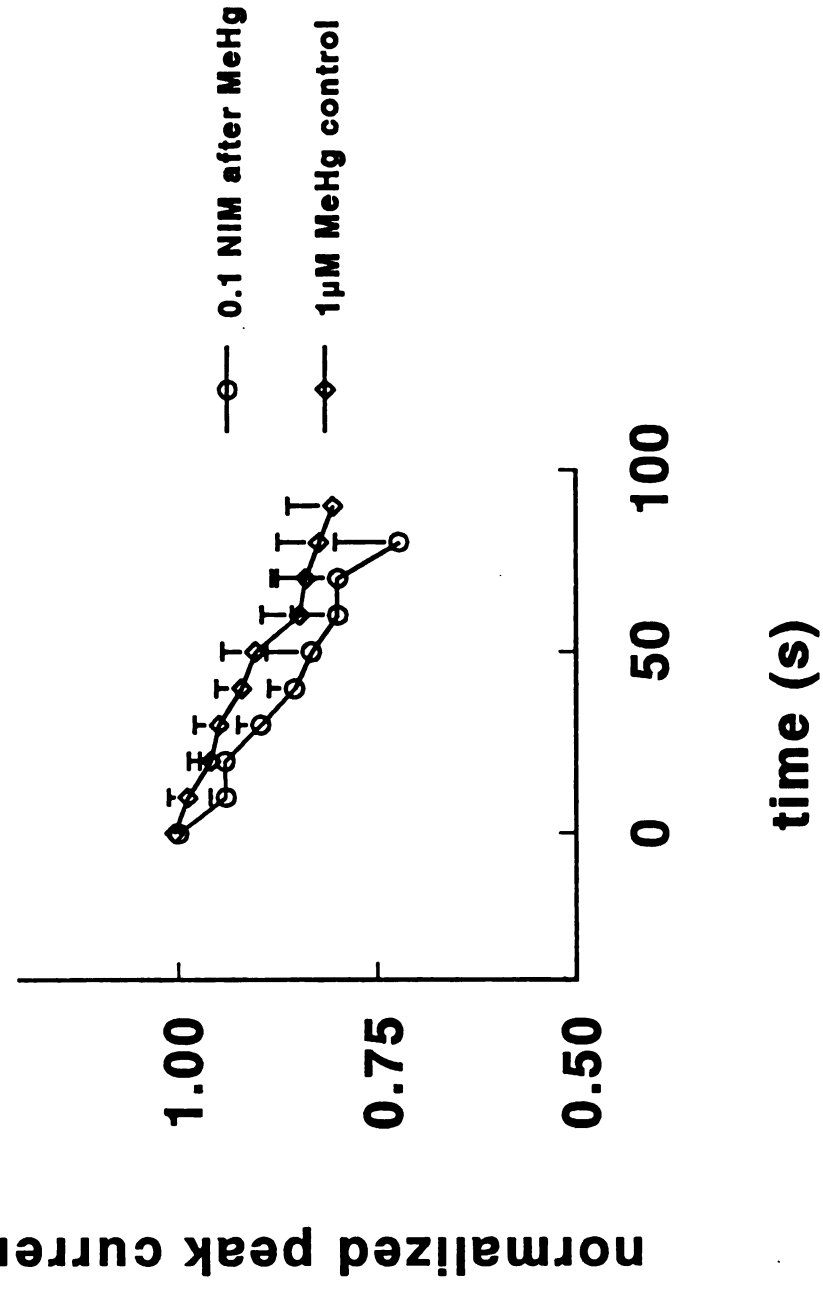
0.1 NIM after MeHg
1μM MeHg control
normalized peak current
1.00
0.75
0.50
0
50
100
time (s)

FIG. 3.5. Prior block of a portion of the peak Ba^{2+} current by 1 μM ϖ-conotoxin GVIA does not prevent the 1 μM MeHg-induced decrease in peak Ba^{2+} current. **(A)** Control peak current **(a)** was rapidly blocked by the addition of 1 μM GVIA **(b)**. MeHg further reduced the peak Ba^{2+} current in the presence of GVIA **(c)**. Similar results were observed for the end current. **(B)** Current traces from the experiment in **(A)** depicting control current **(a)**, current remaining following GVIA-induced block **(b)** and current remaining following a 5 min exposure to 1 μM MeHg in the presence of GVIA **(c)**. While GVIA appeared to affect all current components equally, addition of MeHg resulted decreased the inactivating component of the whole cell current.

Fig. 3.5

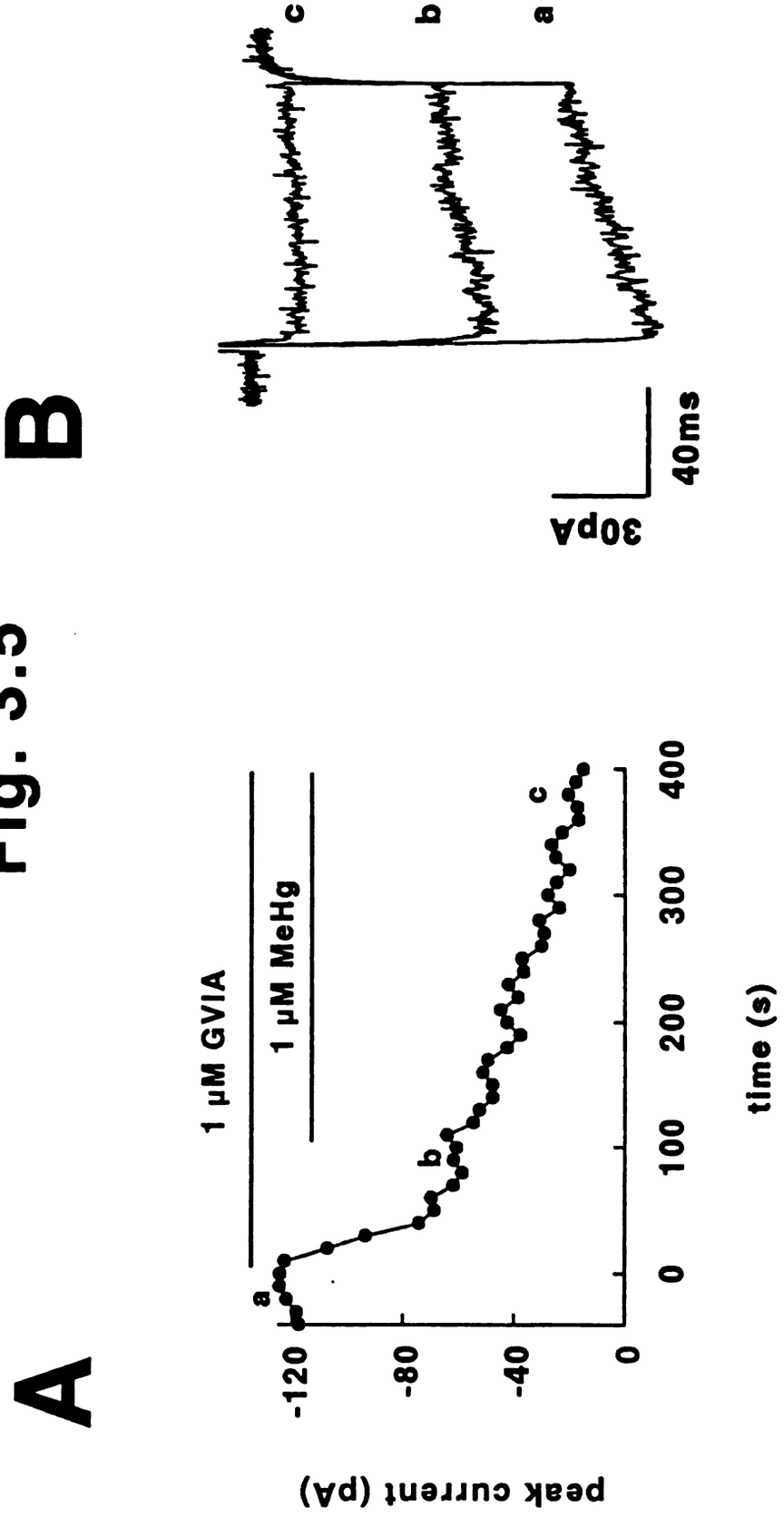
A
1 μM GVIA
1 μM MeHg
a
b
c
-120
-80
-40
0
0
100
200
300
400
time (s)
peak current (pA)
B
c
b
a
30pA
40ms

removed a large percentage of the current after approximately 1 min (Fig. 3.5B, **a,b**). Subsequently, a 5 min exposure to 1 μM MeHg left primarily non-inactivating Ba^{2+} current (Fig. 3.5B, **c**). The combination of GVIA and MeHg decreased peak and end control currents by 92 ± 4% and 83 ± 5%, respectively (n=5) after approximately 4 min of exposure to MeHg in the presence of GVIA.

The effect of a lower concentration of MeHg (0.5 μM) in the presence of GVIA was also determined. Following GVIA-induced block of Ba^{2+} current, a 5 min exposure to 0.5 μM MeHg decreased peak and end GVIA-insensitive Ba^{2+} currents by 16 ± 1% and 26 ± 4%, respectively (n=3, data not shown). Final values for the total reduction in current observed in the presence of 0.5 μM MeHg and GVIA were 69 ± 2% and 75 ± 3% of peak and end currents (n=3), respectively.

To determine whether MeHg would prevent the ability of GVIA to decrease whole cell current Ba^{2+} currents, experiments were performed in which cells were initially exposed to 1 μM MeHg to remove a portion of the whole cell Ba^{2+} current. GVIA was then perfused onto the cell in the continued presence of MeHg. The apparent rate and extent of current reduction were then determined and compared to values observed with GVIA in the absence of MeHg.

Figure 3.6A shows an experiment in which 1 μM MeHg removed ~30% of the control peak current over the course of a 3 min exposure (for n=4 experiments peak and end currents were decreased 50 ± 8% and 51 ±

FIG. 3.6. Removal of a portion of the peak Ba^{2+} current by 1 μM MeHg does not alter the apparent rate of block of peak Ba^{2+} current produced by 1 μM ϖ-conotoxin GVIA. **(A)** The effect of 1 μM GVIA on peak current following partial reduction of whole cell current by 1 μM MeHg. In this experiment, MeHg had decreased the control current **(a)** by approximately 25% **(b)** prior to GVIA addition **(c)**. **(B)** Current traces from the experiment in **(A)** depicting control current **(a)**, current remaining following a 3 min exposure to MeHg **(b)** and current remaining after addition of GVIA **(c)**. In this example, MeHg appeared to decrease all current components to a similar extent over the 3 min prior to GVIA addition. Subsequent perfusion of GVIA resulted in a complete removal of the inactivating portion of the current.

Fig. 3.6

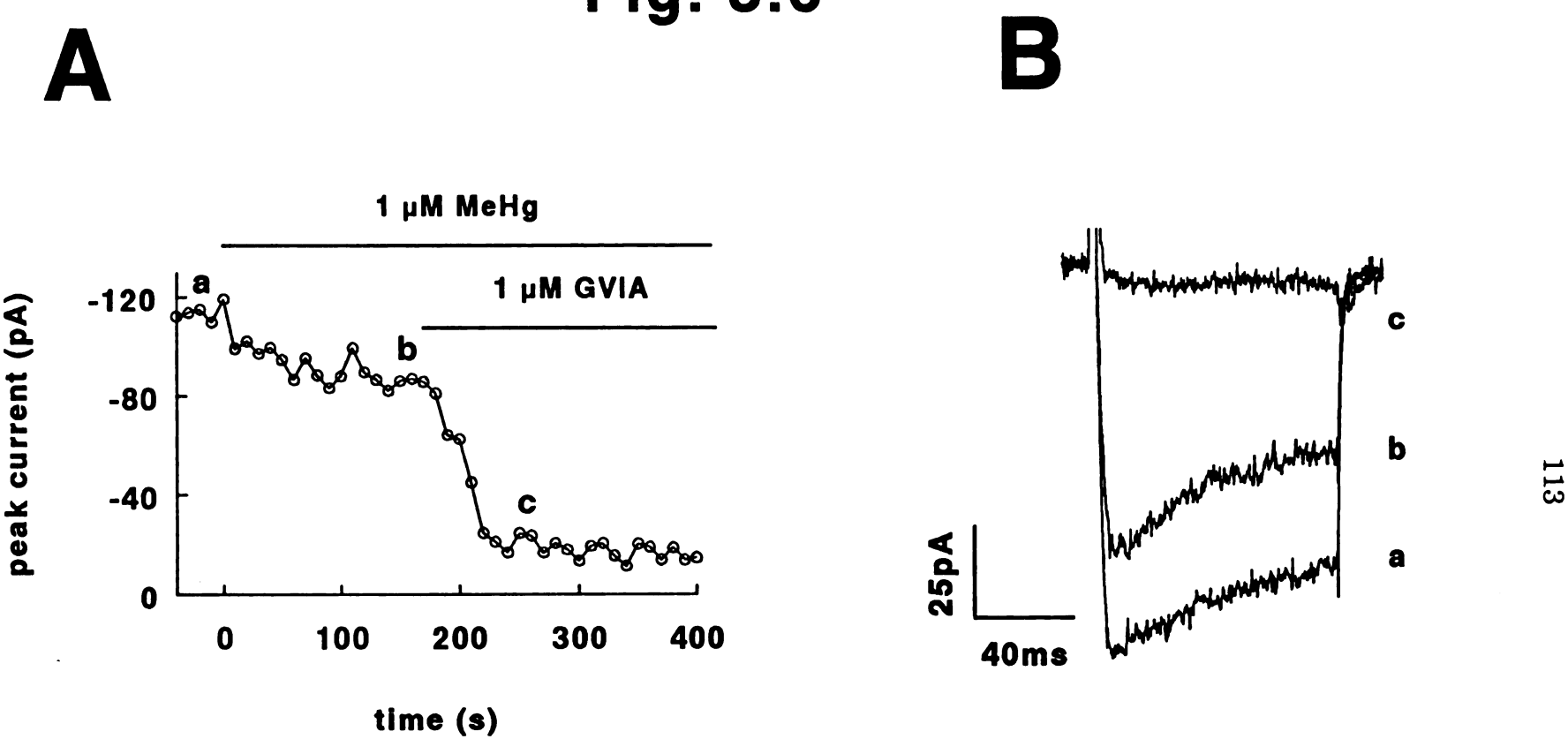
A
1 μM MeHg
1 μM GVIA
a
b
c
-120
-80
-40
0
peak current (pA)
0
100
200
300
400
time (s)
B
c
b
a
25pA
40ms

5%, respectively, prior to GVIA addition). Subsequent perfusion of GVIA resulted in a reduction of peak current which was similar to that observed with GVIA alone. Thus, MeHg does not prevent GVIA from eliciting a decrease in the current, suggesting that MeHg is not decreasing current carried through channels sensitive to the action of GVIA. Current traces from the experiment in **(A)** show that MeHg decreased a large amount of control Ba^{2+} current (compare **a** and **b**, Fig. 3.6B). Subsequent addition of GVIA also elicited a large reduction in the current. The extent and apparent rate of the reduction produced by the addition of GVIA in the presence of MeHg were similar to those observed with GVIA in the absence of MeHg (Fig. 3.7).

Reversing the order of addition of 1 μM MeHg and 1 μM GVIA did not affect the total amount of peak and end Ba^{2+} current blocked by the combination of these agents. When 1 μM MeHg was perfused on first, followed by GVIA, peak and end currents were decreased by 86 ± 3% and 80 ± 6%, respectively (n=4). In the reverse order, 92 ± 4% and 83 ± 5% (n=5) of peak and end currents were removed. In both cases, the time of exposure to MeHg was approximately 4-5 min.

Experiments which examined the effect of 1 μM MeHg and 1 μM GVIA perfused onto cells concurrently, revealed that the apparent rate of current decline produced by these two agents was nearly identical to that seen with GVIA alone (data not shown). Following exposure times which ranged from 2-5 min, MeHg and GVIA reduced peak and end currents by an

FIG. 3.7. Comparison of the apparent rate of peak Ba^{2+} current reduction by 1 μM ϖ-conotoxin GVIA alone (filled circles) and in the presence of 1 μM MeHg (open circles). In these experiments, MeHg had decreased an average of 50 ± 8% of the control peak current prior to GVIA addition (n=4). The apparent rate of current decline induced by perfusion of GVIA in the presence of 1 μM MeHg was similar to GVIA control experiments.

Fig. 3.7

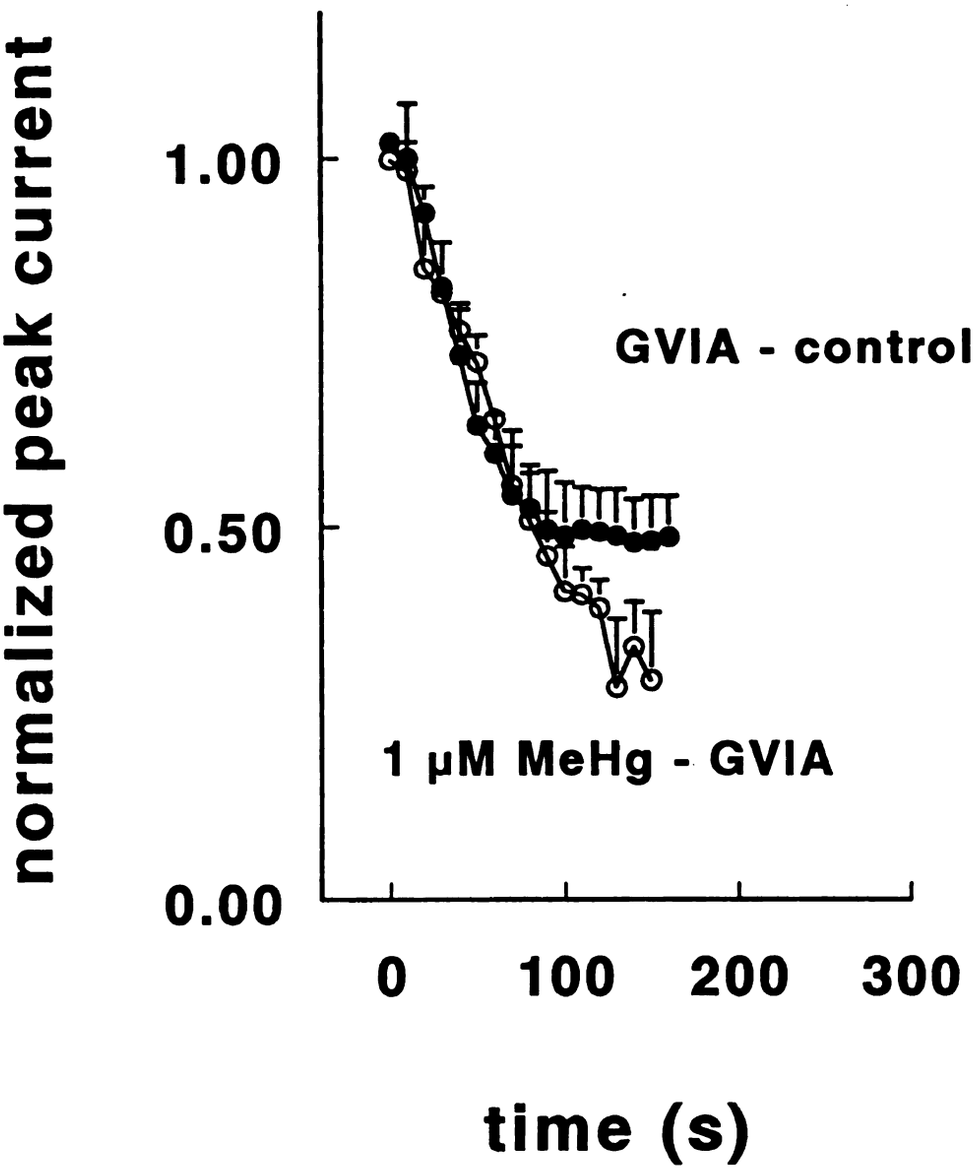
normalized peak current
1.00
0.50
0.00
GVIA - control
1 μM MeHg - GVIA
0
100
200
300
time (s)

average of 54 ± 9% and 63 ± 6%, respectively (n=5).

ϖ-Agatoxin-IVA experiments: ω-Agatoxin-IVA (Aga-IVA), a peptide toxin isolated from the Funnel Web spider *Agelenopsis aperta*, blocks preferentially current through P-type Ca^{2+} channels at low concentrations (Llinas *et al.*, 1989). Control peak and end currents were decreased only a small amount by 0.1 μM Aga-IVA (10 ± 3% and 8 ± 2%, respectively: n=7). Perfusion of MeHg onto cells following Aga-IVA resulted in a further reduction of peak and end Ba^{2+} currents (Fig. 3.8A). Current traces from the experiment in **A** show that Aga-IVA had a very modest effect on control current amplitude (compare **a** and **b**, Fig. 3.8B). Subsequent perfusion of MeHg removed a large fraction of current (Fig. 3.8B, **c**) which exhibited a predominantly non-inactivating pattern (Fig. 3.8C). A comparison of the apparent rate and extent of MeHg-induced decreases in peak current in the presence and absence of Aga-IVA shows that both are relatively similar over the course of a 5 min exposure (Fig. 3.9). Although the average reduction in current produced by a 5 min exposure to MeHg in the presence of Aga-IVA (50 ± 8% of peak current, 55 ± 10% of end current, n=6) was elevated over that observed with a 5 min exposure to MeHg alone, the effect was not statistically significant.

FIG. 3.8. Prior block of a portion of the peak Ba^{2+} current by 0.1 μM Aga-IVA does not prevent 1 μM MeHg-induced decreases in peak Ba^{2+} current. **(A)** Control peak current **(a)** was blocked only minimally by Aga-IVA **(b)**. Subsequent perfusion of 1 μM MeHg resulted in a further reduction of the peak current **(c)** which was similar to that observed in the absence of Aga-IVA. **(B)** Current traces from the experiment in **(A)** depicting control current **(a)**, current remaining in the presence of Aga-IVA **(b)** and current remaining following a 5 min exposure to 1 μM MeHg in the presence of Aga-IVA **(c)**. **(C)** Current sensitive to MeHg in the presence of Aga-IVA **(b-c)** exhibited a predominantly non-inactivating pattern.

Fig. 3.8

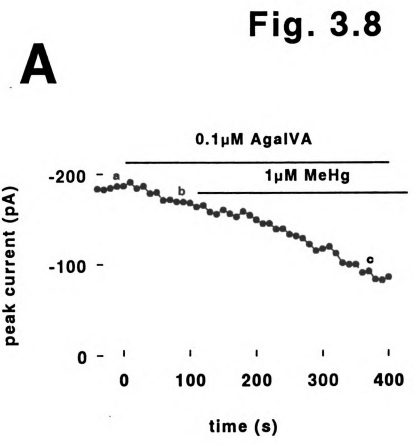
A
0.1μM AgaIVA
1μM MeHg
a
b
c
-200
-100
0
peak current (pA)
0
100
200
300
400
time (s)
B
c
b
a
50pA
40ms
C
b-c

FIG. 3.9. The extent and apparent rate of reduction of peak Ba^{2+} current by 1 μM MeHg is similar in the presence or absence of 0.1 μM Aga-IVA. Values represent the average (mean ± SEM) of normalized peak currents for MeHg alone (open circles) and addition of MeHg following block of the Aga-IVA-sensitive component (filled circles). Data in the presence of Aga-IVA and MeHg have been normalized to current remaining in the presence of Aga-IVA. Following stabilization of the Aga-IVA-induced block, perfusion of MeHg resulted in a further reduction of peak and end currents by 50 ± 8% and 55 ± 10%, respectively (n=6).

Fig. 3.9

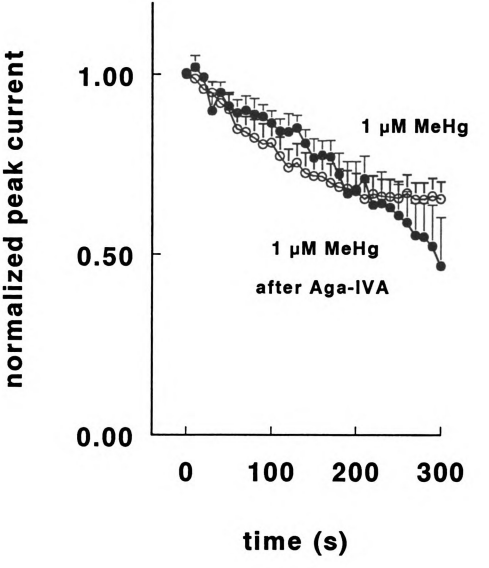
normalized peak current
1.00
0.50
0.00
1 µM MeHg
1 µM MeHg
after Aga-IVA
0
100
200
300
time (s)

ω-Conotoxin MVIIC experiments: ω-conotoxin MVIIC is a peptide toxin isolated from the marine snail *Conus magnus* (Hillyard *et al.*, 1992) which has been shown to block current carried through N- and P-type Ca^{2+} channels (Wheeler *et al.*, 1994). MVIIC is also capable of removing a fraction of current termed Q-type, which is resistant to block by GVIA, Aga-IVA and dihydropyridines (Sather *et al.*, 1993; Zhang *et al.*, 1993; Grantham *et al.*, 1994; Wheeler *et al.*, 1994). In my experiments, MVIIC rapidly blocked both peak (44 ± 6%) and end (43 ± 5%) currents. Following stabilization of MVIIC-induced block, 1 μM MeHg was able to cause an additional decrease in the current (Fig. 3.10A). Current traces from the experiment in **A**, show that MVIIC decreased a large amount of current (compare **a** and **b**, Fig. 3.10B). The subsequent addition of MeHg also blocked a large amount of current following a brief (~2 min) exposure (Fig. 3.10B, **c**). In 6 experiments where MeHg was applied after MVIIC, peak and end currents were decreased by an average of 26 ± 5% and 24 ± 4%, respectively. The time of exposure to MeHg in these experiments ranged from 2-5 min.

To test the ability of MeHg to alter MVIIC-induced block, MeHg was perfused onto the cell prior to MVIIC to allow a partial reduction of the whole cell Ba^{2+} current. MVIIC was then added in the presence of MeHg to determine if a rapid MVIIC-induced reduction in the current would still occur. In the experiment depicted in Figure 3.11A, 1 μM MeHg removed approximately 25% of the peak current following a 2.5 min

FIG. 3.10. Prior block of a portion of the peak Ba^{2+} current by 1 μM ϖ-conotoxin MVIIC does not prevent 1 μM MeHg-induced decreases in peak Ba^{2+} current. **(A)** Control peak current **(a)** was blocked approximately 40% by MVIIC **(b)**. Subsequent perfusion of 1 μM MeHg resulted in a further decrease of the current **(c)**. **(B)** Current traces from the experiment in **(A)** depicting control current **(a)**, current remaining following MVIIC-induced block **(b)** and current remaining following a 3 min exposure to 1 μM MeHg in the presence of MVIIC **(c)**.

Fig. 3.10

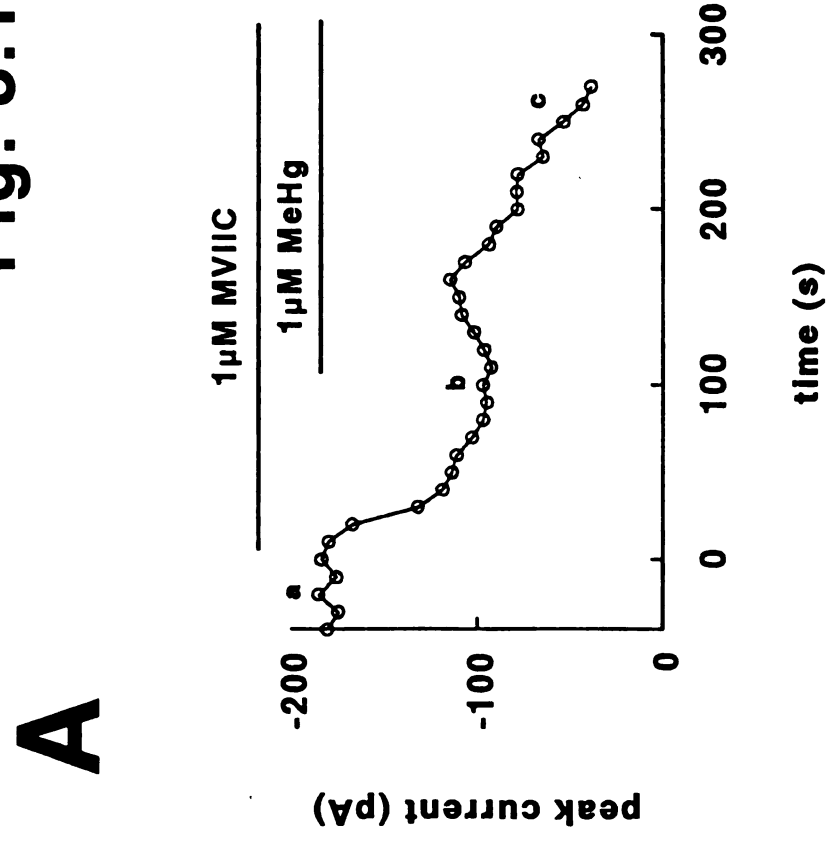
A
1μM MVIIC
1μM MeHg
a
b
c
-200
-100
0
0
100
200
300
time (s)
peak current (pA)
B
c
b
a
50pA
40ms

FIG. 3.11. Removal of a portion of the peak Ba^{2+} current by 1 μM MeHg apparently does not alter the block produced by 1 μM ω-conotoxin MVIIC. **(A)** The effect of 1 μM MVIIC on peak current following partial removal of the current by 1 μM MeHg. In this experiment, MeHg had decreased the control peak current **(a)** by approximately 25% **(b)** prior to MVIIC addition **(c,d)**. **(B)** Current traces from the experiment in **(A)** depicting control current **(a)**, current remaining following a 2 min exposure to MeHg **(b)** and current remaining after addition of MVIIC **(c)**. MeHg appeared to decrease all current components equally over the 2 min exposure (compare **a** and **b**). Following addition of MVIIC the remaining current was predominantly non-inactivating **(c,d)**.

Fig. 3.11

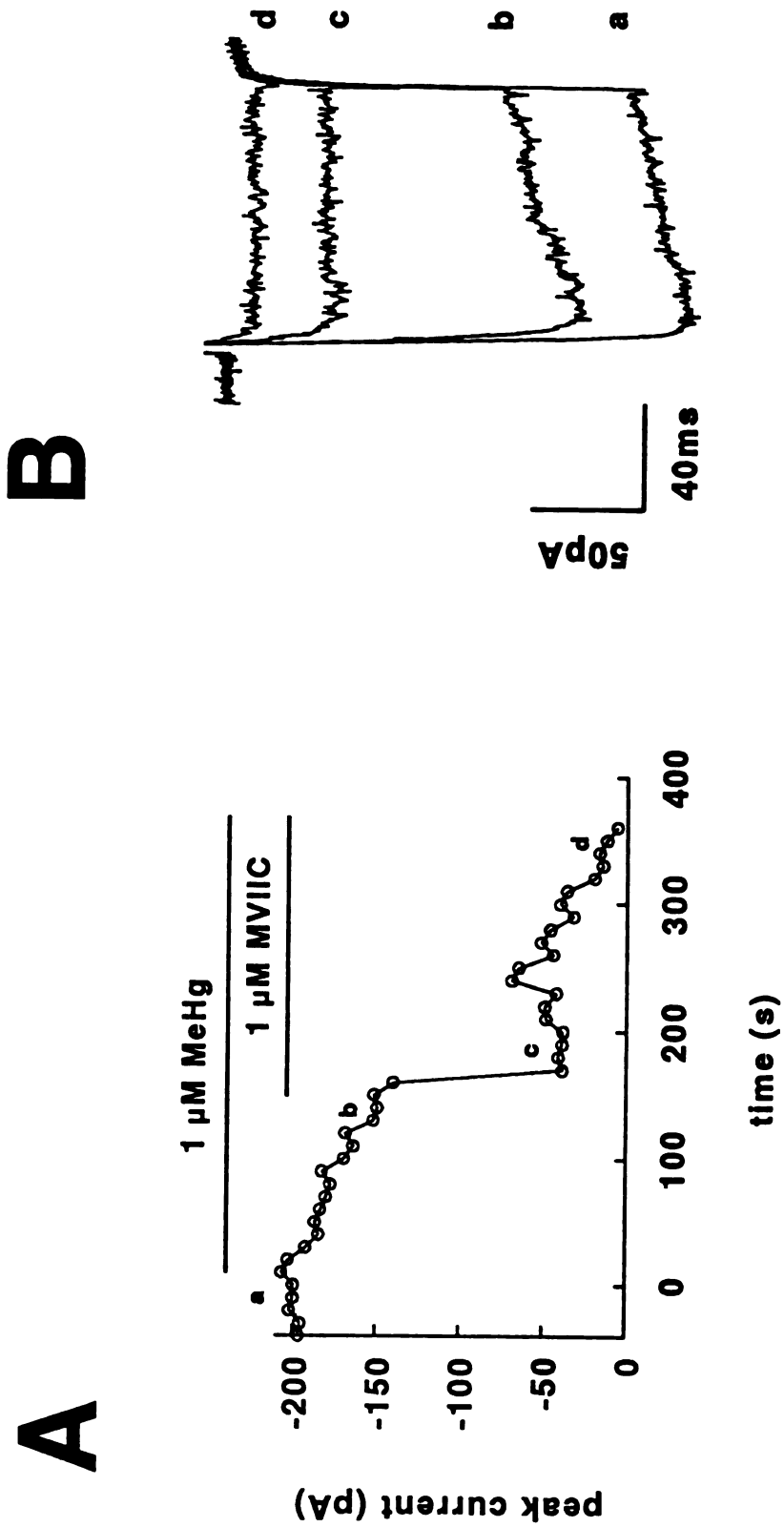
A
1 µM MeHg
1 µM MVIIC
a
b
c
d
-200
-150
-100
-50
0
0
100
200
300
400
time (s)
peak current (pA)
B
d
c
b
a
50pA
40ms

exposure (for pooled experiments the average MeHg-induced decrease prior to MVIIC addition was 30 ± 8% of the peak current, n=3). The subsequent perfusion of MVIIC resulted in a rapid reduction of the remaining current which was similar to that observed with MVIIC in the absence of MeHg. Current traces from the experiment in **A** show that MeHg decreased a sizable amount of current, and appeared to slightly alter current kinetics (compare **a** and **b**, Fig. 3.11B). The subsequent perfusion of MVIIC also blocked a large amount of current and appeared to decrease the inactivating portion of the current (Fig. 3.11B, **c**). The reduction in current progressed to near completion in the presence of these two agents (Fig. 3.11B, **d**).

A comparison of the reduction in normalized peak current by MVIIC alone and by MVIIC in the presence of 1 μM MeHg reveals that the two are apparently similar (Fig. 3.12). When MVIIC was added prior to MeHg, 71 ± 6% of peak and 68 ± 5% of end currents were blocked following exposure times from 2-5 min. In the reverse order, peak and end currents were decreased 99 ± 1% and 98 ± 2% (n=3), respectively. Time of exposure to MeHg in these experiments ranged from 4-6 min.

Calcicludine Experiments: Calcicludine, a 60 amino acid peptide isolated from the green mamba snake *Dendroapsis angusticeps*, has been shown to block L-, N- and P-type Ca^{2+} channels (Schweitz *et al.*, 1994). In cerebellar granule cells, this peptide blocks specifically L-type Ca^{2+} channel current (Schweitz *et al.*, 1994). In my experiments, granule cells exhibited

FIG. 3.12. Comparison of the apparent rate of peak Ba^{2+} current reduction induced by 1 μM ϖ-conotoxin MVIIC alone (filled circles) and in the presence of 1 μM MeHg (open circles). In these experiments, MeHg had removed an average of 30 ± 8% of the peak current (n=3). In the presence of MeHg, MVIIC was still able to elicit a rapid decrease in the remaining current, suggesting that MeHg does not interfere with the binding of MVIIC or its ability to elicit a decrease in the whole cell Ba^{2+} current. Data in the presence of MeHg and MVIIC have been normalized such that current elicited in the episode just prior to MVIIC addition is equal to 1.

Fig. 3.12

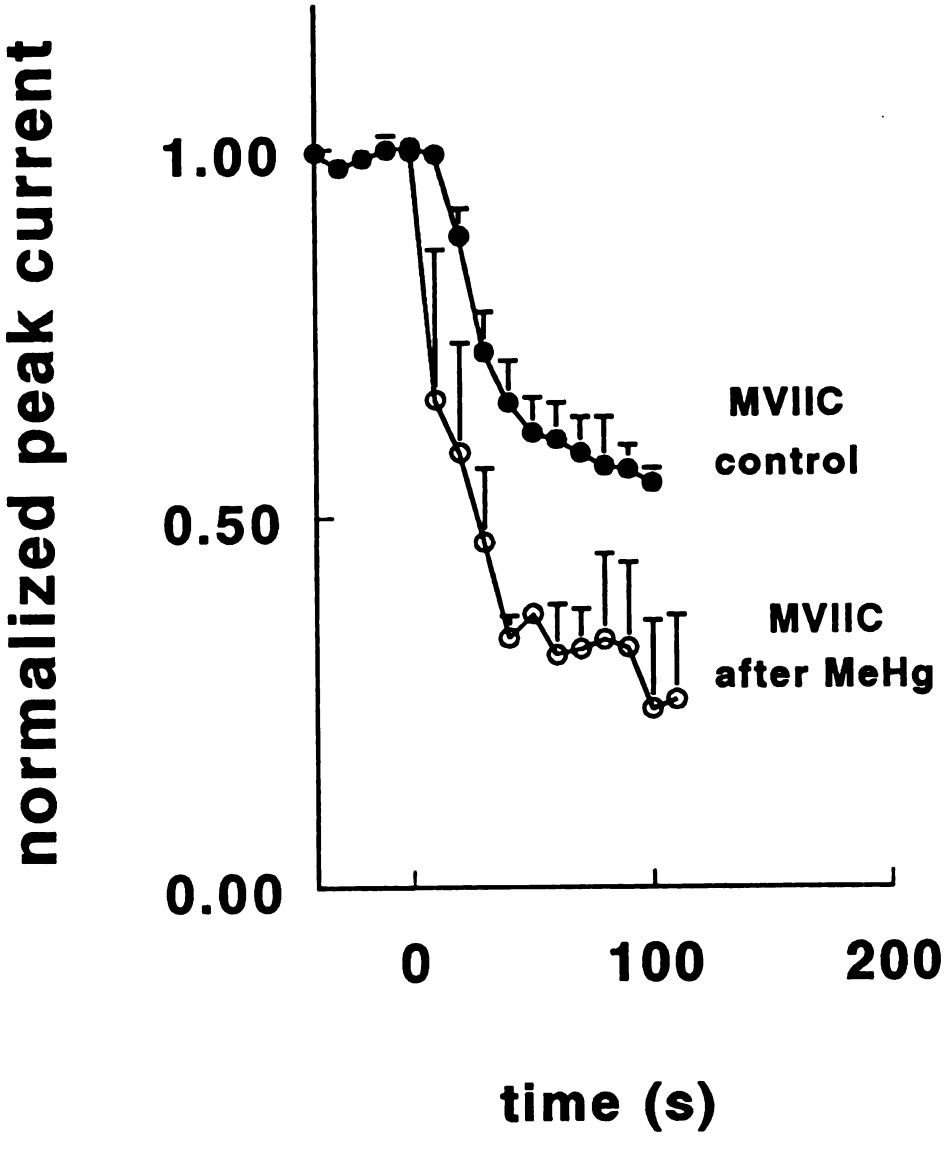
normalized peak current
1.00
0.50
0.00
0
100
200
time (s)
MVIIC
control
MVIIC
after MeHg

two different sensitivities to calcicludine. In 5 of 9 experiments calcicludine blocked only 11 ± 2% of peak and 14 ± 4% of end currents. In the other 4 experiments peak and end currents were blocked by 37 ± 3% and 41 ± 3%, respectively. When data from these nine experiments were combined, calcicludine blocked an average of 22 ± 5% of peak and 26 ± 5% of end current. Regardless of the amount of current blocked by calcicludine, the extent of current reduction produced by the subsequent perfusion of MeHg was always increased over that seen with MeHg alone. Figure 3.13A shows an experiment in which calcicludine blocked ~10% of peak and end currents. The subsequent reduction of current induced by 1 μM MeHg following a 5 min exposure was slightly enhanced over that observed with MeHg in the absence of calcicludine. The decrease in current induced by MeHg following calcicludine reached 57 ± 4% for peak and 53 ± 3 % for end currents (n=9). These values were significantly elevated over those observed following a 5 min exposure to MeHg in the absence of calcicludine.

Current traces from the experiment in **A** show that calcicludine did not appear to alter current inactivation (compare **a** and **b**, Fig. 3.13B). A 5 min exposure to MeHg resulted in a reduction of the peak current by ~50% (Fig. 3.13B, **c**). The waveform of the current sensitive to MeHg in the presence of calcicludine exhibited both inactivating and non-inactivating properties (Fig. 3.13C). A comparison of the apparent rate of peak current reduction by 1 μM MeHg alone and in the presence of 0.1 μM calcicludine reveals that initially, the two rates are similar (Fig.3.14). With continued

FIG. 3.13. Prior block of a portion of the peak Ba^{2+} current by 0.1 μM calcicludine does not prevent the 1 μM MeHg-induced reduction in peak Ba^{2+} current. **(A)** In this experiment, control current **(a)** was blocked approximately 10% by calcicludine **(b)**. In other experiments, calcicludine blocked approximately 40% of peak and end currents (data not shown). Regardless of the amount of block produced by calcicludine, 1 μM MeHg was still able to cause a further reduction in peak **(c)** and end currents. **(B)** Current traces from the experiment in **(A)** depicting control current **(a)**, current remaining in the presence of calcicludine **(b)** and current remaining following addition of 1 μM MeHg in the presence of calcicludine **(c)**. Current inactivation was not affected by calcicludine but appeared to be reduced following the addition of MeHg.

Fig. 3.13

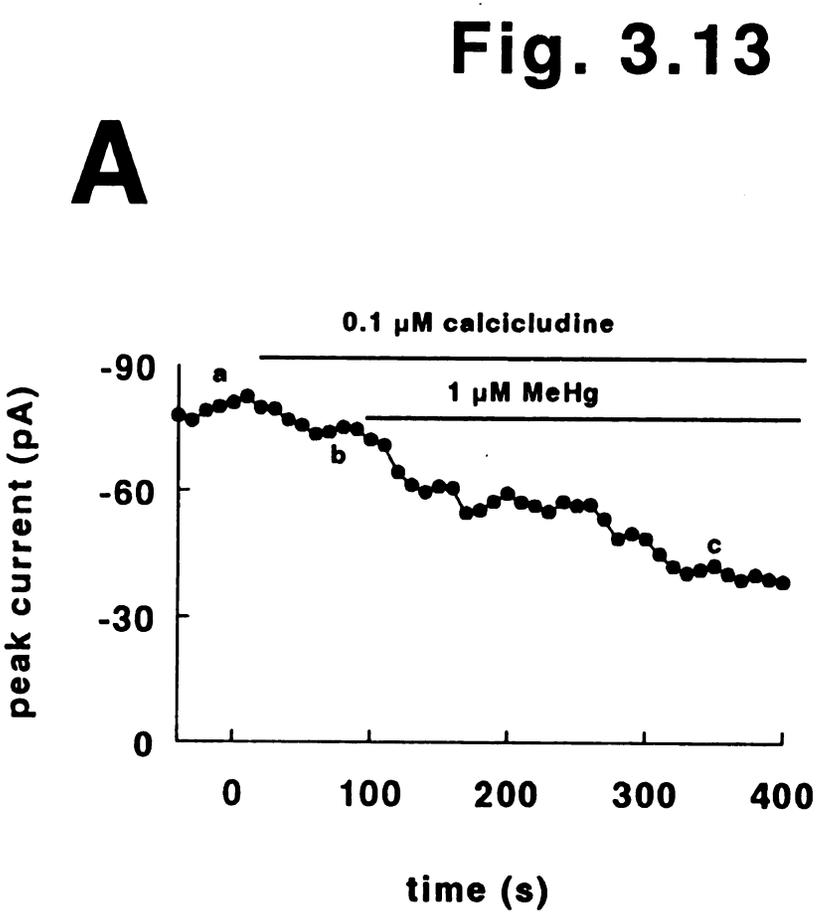
A
0.1 μM calcicludine
1 μM MeHg
peak current (pA)
-90
-60
-30
0
a
b
c
0
100
200
300
400
time (s)

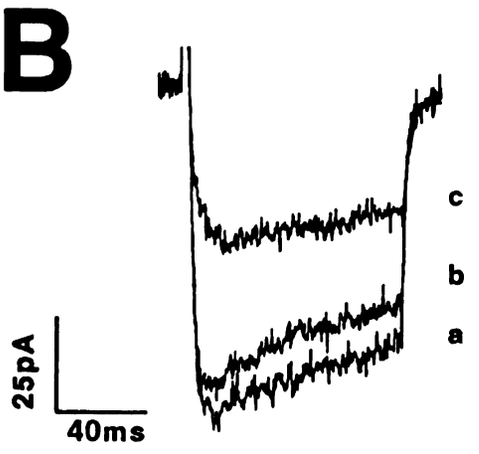
B
c
b
a
25pA
40ms

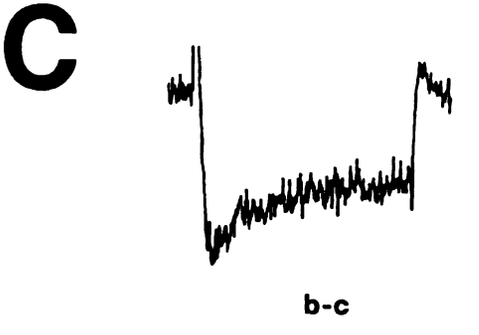
C
b-c

FIG. 3.14. The apparent rate of reduction of peak Ba^{2+} current by 1 μM MeHg is slightly enhanced in the presence of 0.1 μM calcicludine. Values represent the average (mean ± SEM) of normalized peak currents for MeHg alone (control, filled circles) and addition of MeHg following block of the calcicludine-sensitive component (open circles). Data in the presence of calcicludine and MeHg have been normalized to current remaining in the presence of calcicludine. Following stabilization of the calcicludine-induced block, perfusion of MeHg resulted in a further reduction of peak and end currents by 63 ± 4% and 57 ± 3%, respectively (n=6).

Fig. 3.14

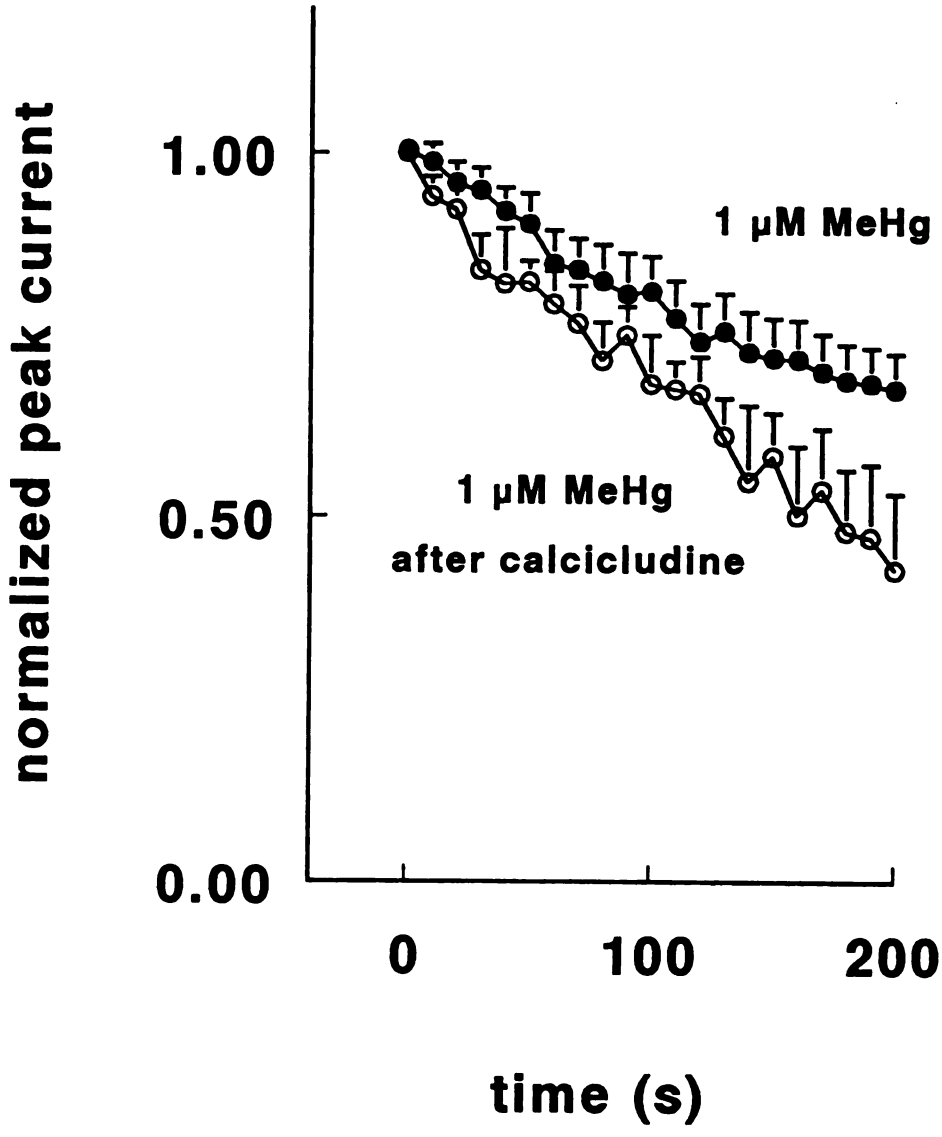
normalized peak current
1.00
0.50
0.00
1 μM MeHg
1 μM MeHg
after calcicludine
0
100
200
time (s)

exposure, the apparent rate of current decline in the presence of calcicludine steadily increases, leading eventually to an enhanced decrease in Ba^{2+} current following a 5 min exposure to MeHg.

Prior removal of a portion of the whole cell Ba^{2+} current by 1 μM MeHg also was not able to prevent the ability of 1 μM $CdCl_2$ to rapidly and completely abolish the remaining current (Fig. 3.15). Similar results were observed in 2 other experiments, suggesting that MeHg and Cd^{2+} do not utilize similar pathways to decrease Ca^{2+} channel current amplitude.

FIG. 3.15. 1 μM MeHg does not prevent 1 μM $CdCl_2$ from decreasing peak Ba^{2+} current. Following a MeHg-induced decrease the control peak current by approximately 50%, addition of 1 μM $CdCl_2$ rapidly and completely blocked the remaining fraction of the current, suggesting that MeHg and Cd^{2+} were not acting at the same site or that Cd^{2+} acts at multiple sites, of which one is not accesible to MeHg. Similar results were observed in two other experiments.

Fig. 3.15

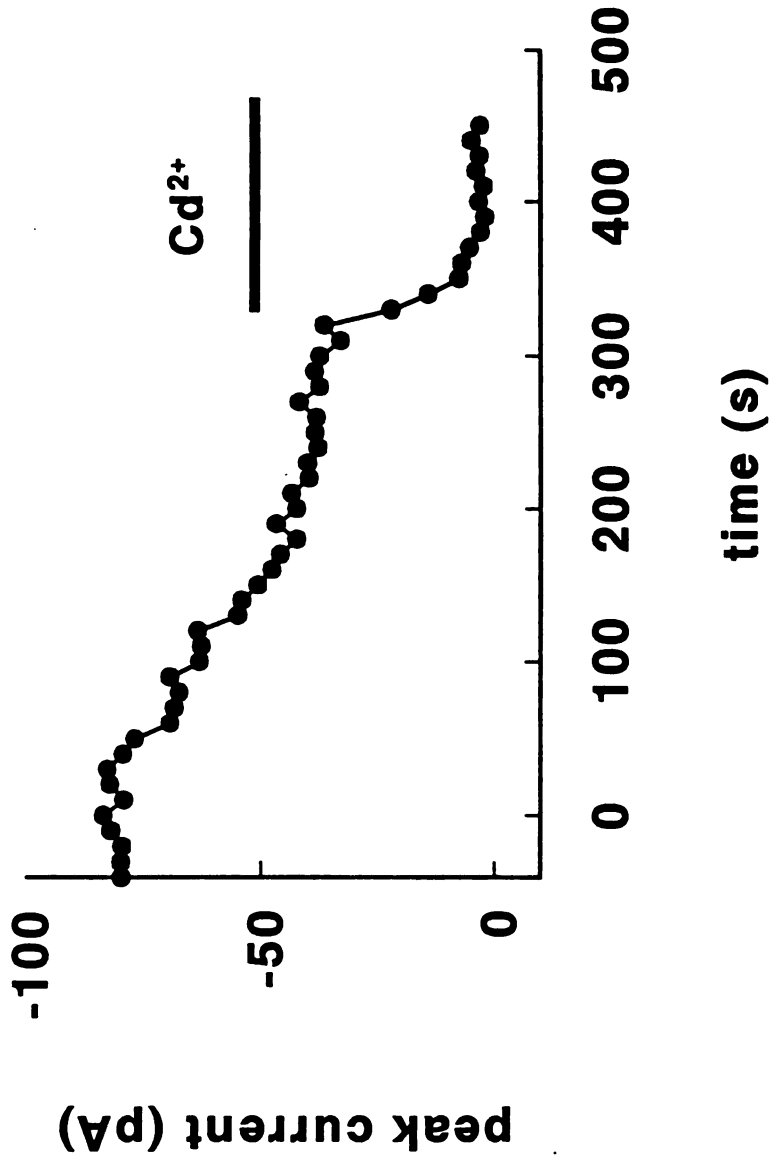
1 µM MeHg
Cd2+
-100
-50
0
0
100
200
300
400
500
peak current (pA)
time (s)

DISCUSSION

The ability of Ca^{2+} channel antagonists to delay or prevent the MeHg-induced decrease in whole cell Ba^{2+} currents was tested. None of the agents (nimodipine, ω-conotoxin GVIA, ω-agatoxin IVA, ω-conotoxin MVIIC or calcicludine) were able to decrease the magnitude of the MeHg-induced effect, demonstrating that MeHg does not act exclusively at sites sensitive to these antagonists. When calcicludine was perfused onto cells prior to, and in the presence of MeHg, the extent of reduction of peak and end currents following a 5 min exposure to MeHg was elevated over that observed with MeHg alone. A similar effect on peak Ba^{2+} current was observed when MeHg was added subsequent to nimodipine. When the order of addition was reversed and nimodipine was perfused onto cells after MeHg had caused a partial reduction of the whole cell Ba^{2+} current, the subsequent rate of current decline was apparently similar to that observed with MeHg alone. This suggests that the reduction in current produced by MeHg and nimodipine is not additive under these conditions. In control experiments, both GVIA and MVIIC induced a large, rapid decrease in Ba^{2+} current. In the presence of MeHg, application of either of these toxins resulted in large decreases in Ba^{2+} current which were similar to those observed in the absence of MeHg. Thus, MeHg apparently does not affect the ability of these toxins to bind and exert their effects. Taken together, these results suggest that the ability of MeHg to decrease Ba^{2+} current arises from an action(s) distinct from that utilized by Ca^{2+} channel

antagonists to reduce Ba^{2+} current. The facilitated effect of MeHg in the presence of nimodipine or calcicludine suggests that channels insensitive to these agents might be more susceptible to MeHg.

Cerebellar granule cells have been proposed to contain a diverse array of voltage-gated Ca^{2+} channel subtypes (Zhang *et al.*, 1993; Randall and Tsien, 1995). In addition to the commonly encountered L-, N- and P-type channels (Fox *et al.*, 1987), there are 2 distinct currents defined on the basis of their sensitivity to peptide toxins and dihydropyridine compounds. The so called "Q-type" current, which may correspond to currents elicited by expression of the cloned Ca^{2+} channel subunit α_{1A} in *Xenopus* oocytes (Sather *et al.*, 1993; Stea *et al.*, 1994), or a mammalian cell line (Niidome *et al.*, 1994), is insensitive to Aga-IVA, which blocks P-type current (Llinas *et al.*, 1989), but is sensitive to MVIIC (Hillyard *et al.*, 1994). In cerebellar granule cells, Q-type Ca^{2+} current constitutes the largest fraction (~35%) of the whole cell current (Randall and Tsien, 1995). In addition, a current which remains in the presence of GVIA, nimodipine, Aga-IVA and MVIIC has been termed R-type, or residual. This high voltage-activated channel is sensitive to Cd^{2+} and contributes about 20% of the whole cell current in granule cells (Randall and Tsien, 1995).

Numerous agents have been shown to prevent the flux of extracellular Ca^{2+} or Ba^{2+} into cells. Inorganic metals such as Cd^{2+} and Hg^{2+} as well as some of the toxins that were used (GVIA, MVIIC) block Ca^{2+} channels very rapidly and their effect typically reaches a peak within one

minute or less. Presumably, all of these agents act by physically occluding the pore subsequent to their binding at or near the channel proper (Miyamoto, 1983; Hess *et al.*, 1984; Hinkle *et al.*, 1987; Simons and Pocock, 1987; Olivera, 1991; 1994). The mechanism by which MeHg reduces Ca^{2+} channel current is apparently not as simple. The time course of the MeHg-induced reduction in Ba^{2+} current was not consistent with rapid entry of MeHg into the pore, similar to what is proposed to occur for inorganic metals. However, it is possible that MeHg may act via a similar pathway. If this were the case, either the rate at which MeHg binds within the channel or the production of the subsequent decrease in current, would have to be slowed relative to the inorganic metals. A further possibility is that MeHg causes an incomplete physical block of the channel, such that Ba^{2+} ions are still able to traverse the channel, albeit at a rate which is slower than that observed in the absence of MeHg.

The inability of any of the toxins or nimodipine to prevent or reduce MeHg-induced decreases in Ba^{2+} current does not rule out an action of MeHg at sites occupied by these agents. Evidence from a number of studies suggests that MeHg can interact with receptor binding sites to either inhibit (Komulainen *et al.*,1995; Von Burg *et al.*,1980) or enhance (Corda *et al.*, 1981) agonist binding. In PC12 cells and synaptosomes, MeHg disrupts the binding of GVIA and ^{3}H-nitrendipine, respectively (Shafer *et al.*, 1990). MeHg may also alter the affinity of agonist or antagonist for their respective binding sites via an action removed from the receptor site.

Voltage-gated Ca^{2+} channels are structurally complex and regulated in a strict fashion. Any number of MeHg-induced events, such as an alteration of enzyme function (Shamoo and MacLennan, 1975; Henderson, 1979; Tsuzuki, 1981; Kung *et al.*, 1989); elevation of $[Ca^{2+}]_i$ (Hare *et al.*, 1993; Hare and Atchison, 1994; Marty and Atchison, submitted); disruption of the plasma membrane or mitochondrial membrane potential (Hare and Atchison, 1992; Levesque *et al.*, 1991; Hare *et al.*, 1992); generation of second messengers (Sarafian, 1993); or altered protein phosphorylation states (Sarafian, 1993) could contribute to MeHg-induced reductions in Ba^{2+} current. Under the conditions used to record whole cell Ba^{2+} currents, it is unlikely that any of these processes would be operative. However, if these events occur following an *in vivo* exposure it is likely that they could contribute to the reduction in Ca^{2+} channel current, as well as to other MeHg-mediated events.

In an attempt to determine if MeHg decreased current through L-type channels, cells were exposed initially to MeHg. Following a partial reduction in the whole cell current by MeHg, nimodipine was added. If MeHg had spared L-type channels, the apparent rate of reduction of current induced by subsequent perfusion of nimodipine should have been enhanced relative to that observed with MeHg alone. Since the apparent rate of decline produced by MeHg and nimodipine was not different from that produced by MeHg alone, this suggests that MeHg may have altered the ability of nimodipine to elicit a decrease in current. This could occur *via*

initiation of an event which would inactivate L-type Ca^{2+} channels. MeHg does produce a number of effects which might be expected to drive Ca^{2+} channels into an inactivated state, including membrane depolarization (Hare and Atchison, 1991) and an increase in $[Ca^{2+}]_i$ (Hare *et al.*, 1993; Marty and Atchison, *submitted*), however these effects would not contribute in the paradigm utilized here. Alternatively, MeHg may inhibit either directly or indirectly, the nimodipine binding site, similar to what occurs in synaptosomes (Shafer *et al.*, 1990).

The binding site for dihydropyridines has been proposed to exist on or near the transmembrane domain of motif III between the 5th (S5) and 6th (S6) membrane spanning regions of the α_1 subunit (see Fig. 1.1), in a hydrophobic environment (Herbette *et al.*, 1989; Tang *et al.*, 1993). Since MeHg is a lipophilic compound it should be accessible to this site. Further, it has been proposed that the SS1/SS2 region which connects transmembrane segments S5 and S6 in each of the 4 motifs of the Ca^{2+} channel, contains the selectivity filter (Hille, 1992) a region responsible for controlling the flux of ions through the channel. In PC12 cells, MeHg has been shown to alter the permeation rate of Ca^{2+}, Sr^{2+} and Ba^{2+} suggesting some type of interaction between MeHg and the process which controls the selectivity of the channel (Shafer and Atchison, 1991). Thus, it is possible that MeHg could alter channel kinetics in a manner similar to dihydropyridines.

Following a nimodipine-induced reduction in the whole cell Ba^{2+}

current, addition of MeHg resulted in a further (MeHg-induced) reduction in peak current that was increased over that observed with MeHg alone. This contrasts with results obtained when the compounds are added in the reverse order, where MeHg appeared to prevent the ability of nimodipine to reduce the current. Previous studies utilizing the fluorescent Ca^{2+} indicator fura-2 have shown that nifedipine can delay the MeHg-induced elevation in $[Ca^{2+}]_i$ in both NG108-15 cells (Hare and Atchison, 1995) and cerebellar granule cells (Marty and Atchison, *submitted*). Since the effect only occurred at 1 μM nifedipine and above, a concentration range in which dihydropyridines supposedly have other non-specific effects (Zernig, 1990), the authors postulated that nifedipine prevented the interaction of MeHg with some other critical site(s) associated with MeHg entry into the cell. Perhaps in my experiments, nimodipine is preventing MeHg from reaching sites where it is sequestered in an inactive form. This may allow MeHg to bind at other sites which are critical for maintenance of Ca^{2+} channel function, resulting ultimately in a facilitation of the reduction in current.

Although the site at which peptide toxins has not been examined as exhaustively as that for the dihydropyridines, all ω-conotoxins and many of the spider toxins have been postulated to target a so-called macrosite (Olivera *et al.*, 1991; 1994). The specific binding of each of the toxins apparently results from variations in the macrosite, which form potential binding pockets for the peptide. The relative specificity of block for some of the peptide toxins could arise as a result of increased affinity for the

binding site, increased efficacy of block and also to the specificity of each Ca^{2+} channel subtype (Olivera *et al.*, 1994). It is generally thought that the α_1 subunit contains the binding site for the ϖ-conotoxins, although there is evidence to suggest that other Ca^{2+} channel subunits can participate in conotoxin binding (Olivera *et al.*, 1994).

GVIA apparently targets an extracellular site, from which it produces a physical block of the pore (Ellinor *et al.*, 1994). When added prior to MeHg, GVIA rapidly blocked a large fraction (~50%) of the whole cell Ba^{2+} current. In the continued presence of GVIA, MeHg decreased ~80% of the remaining current, which represents ~40% of the original control current. Although the actual amount of current reduced by MeHg in the presence and absence of GVIA is similar, the time required for MeHg to decrease that amount of current in the presence of GVIA was generally less than in its absence. Similarly large decreases in current (~40%) caused by MVIIC did not generally increase the extent of current reduction by MeHg to the extent observed with GVIA. However, this may have been due to the inability to hold the cell for longer periods following exposure to MVIIC and MeHg.

The only study to date which has examined the effect of calcicludine in granule cells (Schweitz *et al.*, 1994), suggested that this toxin targeted L-type Ca^{2+} channels. In my experiments, whole cell peak and end Ba^{2+} currents were blocked ~40% by calcicludine in some cases, an amount much greater than the 20% blocked by dihydropyridines in this study and in others (Randall and Tsien, 1995). Thus, channels other than L-type are

likely a target of calcicludine. In addition, the modest amount of block (~10%) observed in a subset of cells suggests that granule cells may posses complements of Ca^{2+} channels which are differentially susceptible to calcicludine. In other preparations, N- and P-type Ca^{2+} channels appear to be susceptible to calcicludine (Schweitz *et al.*, 1994), thus different culturing conditions or a differential expression of channel subtypes could be responsible for the differences in results. The MeHg-induced reduction of peak and end currents in the presence of calcicludine was increased over that observed with MeHg alone, further suggesting that MeHg does not act exclusively at a toxin sensitive site. This was true regardless of whether calcicludine had blocked 10% or 40% of the whole cell current. This also suggests that mechanisms other than an initial large antagonist-induced decrease in Ba^{2+} current are responsible for enhancing the MeHg-induced reduction in Ba^{2+} current.

It is difficult to determine why the reduction in current following a 5 min exposure to MeHg in the presence of either nimodipine or calcicludine is increased over that observed following a 5 min exposure to MeHg alone. One possibility is that MeHg may alter the block induced by these antagonists, which would confound interpretation of the results. Prior to MeHg addition, the block of Ba^{2+} current by all of the agents had levelled off. However, MeHg could remove the antagonist from its binding site. A situation could then be envisioned where either MeHg or the antagonist could cause subsequent re-block those channels which had previously been

blocked by the Ca^{2+} channel antagonist. This would result in the false assertion that MeHg-induced reduction of current insensitive to the antagonist is more efficacious than that of the control whole cell current in the absence of antagonist. For this to occur MeHg would likely have to interact with the antagonist binding site. Since MeHg did not prevent GVIA or MVIIC from rapidly decreasing a sizable amount of current, this argues against such an occurrence.

Thus, I have shown that the extent of MeHg-induced reduction of Ba^{2+} current can be enhanced by addition of agents which remove a portion of the whole cell Ba^{2+} current. In addition, prior removal of a portion of the whole cell Ba^{2+} current by MeHg does not disrupt the block produced by MVIIC or GVIA. The results are consistent with an ability of MeHg to disrupt Ca^{2+} channel function at a site or sites other than those utilized by the pharmacological antagonists to block Ba^{2+} current and also suggest that MeHg decreases whole cell Ba^{2+} current in a non-specific fashion.

CHAPTER FOUR

SUMMARY AND DISCUSSION

A. Summary of research.

Studies were performed on primary cultures of cerebellar granule cells, to determine if MeHg could decrease Ca^{2+} channel current. Ca^{2+} channels are important mediators of a number of events, including gene expression, neurite outgrowth and enzyme activation. Thus, MeHg-induced alterations in their function could contribute to the neurotoxic effects produced by *in vivo* exposure to MeHg. While the studies presented here have not determined the exact mechanism by which MeHg decreases Ca^{2+} channel current, several new findings have been presented: **1)** Low micromolar concentrations of MeHg decrease Ba^{2+} current in a concentration- and time dependent fashion at a stimulation frequency of 0.1 Hz. From V_h = -90 mV, all step potentials which elicited current were blocked to a similar extent. Only the highest concentration of MeHg appeared to slightly alter the voltage at which the current activated and the apparent reversal potential. **2)** An increase in the stimulation frequency to 0.2 Hz facilitates the reduction in Ba^{2+} current produced by 0.25 and 0.5 µM MeHg, but not 1 µM MeHg. **3)** When cells are exposed to MeHg in the absence of depolarizing stimuli, 0.25, and in some cases 0.5, µM MeHg decrease a greater amount of the end current relative to the peak current. In this situation, 1 µM MeHg decreases both peak and end Ba^{2+} currents equally. **4)** Addition of Ca^{2+} channel antagonists (nimodipine, ϖ-conotoxin GVIA, ϖ-conotoxin MVIIC, ϖ-agatoxin IVA, calcicludine) prior to MeHg does not prevent MeHg-induced reductions in Ba^{2+} current. **5)** Prior reductions

in Ba^{2+} current by MeHg do not prevent the rapid decrease in current produced by ϖ-conotoxin GVIA, ϖ-conotoxin MVIIC or the inorganic metal Cd^{2+}. **6)** Application of a prepulse more positive than the holding potential did not alter the extent of Ba^{2+} current reduction produced by any concentration of MeHg.

B. Possible mechanisms of the MeHg-induced decrease in granule cell Ca^{2+} channel current.

The failure of efforts to reduce or remove the MeHg-induced decrease of whole cell Ba^{2+} current lends support to the idea that more than one mechanism contributes to the observed decrease in Ba^{2+} current. The ability of MeHg to cause a reduction in Ba^{2+} current in the absence of stimulation demonstrates that channel activation is not required for the effect. Under these conditions, MeHg cannot enter the channel through the open pore. MeHg may diffuse within the membrane and interact with the channel to produce a reduction in current. Alternatively, MeHg may decrease Ba^{2+} current only following activation of the Ca^{2+} channel. This would require a relatively rapid association of MeHg with the channel, or some other modulatory site, that was not accessible during the quiescent period. If this were the case, a more rapid decline in current should have been observed with 1 μM MeHg at either 0.1 or 0.2 Hz. The fact that the decrease in Ba^{2+} current occurred in a gradual fashion makes it seem unlikely that MeHg rapidly associates with only activated (open) channels.

Experiments with Ca^{2+} channel antagonists support the idea that MeHg does not act exclusively at the Ca^{2+} channel pore to decrease the whole cell Ba^{2+} current. The toxins used in these experiments are all presumed to act by creating some type of physical block of the Ca^{2+} channel. If MeHg were to enter the pore in a manner similar to Ca^{2+} or Ba^{2+}, the presence of toxin should prevent the entry of MeHg, and presumably the reduction in Ba^{2+} current. Ba^{2+} current was reduced to a similar, and in some cases greater extent, in the presence of antagonist, suggesting that other mechanisms of action of MeHg are operative in causing a reduction in current.

Passive diffusion of MeHg within the membrane increases the possibility of interaction at a site critical to Ca^{2+} channel function. MeHg has been shown to penetrate lipid barriers (Lakowicz and Anderson, 1982), thus if that were the case in the present experiments, several sites of action could at least be inferred. The progressive decrease in Ca^{2+} channel current by MeHg is irreversible (Shafer and Atchison, 1991; Büsselberg, 1993; this report), as are effects at the neuromuscular junction (Atchison *et al.*, 1982). These findings suggest that the effect may be intracellular, where it would be less likely to be washed out. Alternatively, the binding of MeHg to certain critical functional groups may occur with such avidity that even protracted washings cannot remove the metal.

The ability of inorganic heavy metal ions such as Cd^{2+}, Hg^{2+}, Pb^{2+} and Co^{2+} to block Ca^{2+} channels arises due to the increased affinity of these ions

for the negatively charged binding sites within the pore (Hess and Tsien, 1984; Lansman *et al.*, 1986; Lansman, 1990). These ions are similar in ionic radius and possess the same divalent charge as Ca^{2+}. Once bound however, these ions are not removed as quickly as Ca^{2+}, thereby effectively creating a block of the channel. In essence then, the cell does not discriminate between ions which permeate the channel and those which block the channel (Lansman *et al.*, 1986; Lansman, 1990).

The ability of divalent cations to alter gating properties of voltage-gated ion channels are well described (Hille, 1992). Apparently, mechanisms responsible for controlling channel activation and inactivation are sensitive to changes in the surface potential near the membrane. Divalent cations can screen part of the negative charge associated with the membrane, resulting in a shift of the voltage-dependence of channel opening and closing. Monovalent cations, such as MeHg, should theoretically be able to induce a shift in the voltage-dependence of channel gating. Hg^{2+} is able to shift the activation and inactivation kinetics of K^+ channels in squid giant axons (Gilly and Armstrong, 1982). I found that 1 μM Hg^{2+} was able to cause a slight depolarizing shift in the potential at which the maximum peak current was reached, while both 0.5 and 1 μM MeHg produced a similarly small effect on the potential at which the maximum end current was elicited. Thus, some type of charge screening effect may have occurred with MeHg, but it appears to not have been significant.

MeHg also did not prevent the ability of Cd^{2+} to elicit a rapid block of

Ba^{2+} current. The effect of Cd^{2+} was always rapid in onset in contrast to the effect of MeHg which developed gradually over several minutes. As Cd^{2+} likely interacts with Ca^{2+} binding sites within the pore (Hess and Tsien, 1984; Lansman *et al.*, 1986; Hinkle *et al.*, 1987), the fact that prior exposure to MeHg cannot prevent the effect of Cd^{2+} suggests that MeHg does not act within the pore at a Cd^{2+}-sensitive site. It is also possible that Cd^{2+} has more than one site of action and that MeHg simply does not affect all of the potential sites. However, there is no evidence to suggest that Cd^{2+} causes complete removal of Ba^{2+} current by a means other than block of the pore.

MeHg-induced reductions in Ba^{2+} current did not prevent a rapid reduction in the remaining current following perfusion of either GVIA or MVIIC, even when up to 50% of the whole cell Ba^{2+} current had been removed by MeHg. In addition, a rapid decline of whole cell Ba^{2+} current, similar to that observed with GVIA alone, was noted when MeHg and GVIA were perfused on simultaneously. Apparently, GVIA reduces Ca^{2+} channel current by binding to the external face of the channel at an extracellular loop in the α_1 subunit on the third membrane spanning region (McCleskey *et al.*, 1987; Ellinor *et al.*, 1994). This interaction results in a direct block of the channel pore. Other evidence suggests that GVIA acts by altering the gating properties of N-type Ca^{2+} channels (Witcher *et al.*, 1993). Since MeHg is present during the GVIA (or MVIIC) addition, a certain amount must be somehow associated with the membrane. If this interaction does take place, apparently it does not prevent GVIA (or MVIIC) from reaching

their respective binding site(s). It was not possible to compare statistically the effect of GVIA or MVIIC in the control situation versus that in the presence of MeHg. This was because of the continual decline in current evidenced following addition of GVIA or MVIIC in the presence of MeHg. Because of this limitation, it is only possible to compare the **apparent** rate of current decline in the two situations.

The inability of MeHg to prevent a rapid reduction in current following addition of either GVIA or MVIIC be due structural characteristics of the toxin binding site(s). If this were the case, it seems more likely that a steric hinderance, rather than the actual location of the site, would prevent MeHg from associating with the binding site(s). As these toxins are relatively large, charged molecules, the site(s) at which they bind must be somewhat exposed. In synaptosomes, 100 μM MeHg did not affect the binding of GVIA either when the agents were applied together or when synaptosomes were pretreated with MeHg. A similar concentration of MeHg was able to elicit a decrease in the amount of bound GVIA in (Shafer *et al.*, 1990). These results may be explained by differences in GVIA affinity for binding in the two preparations. The possibility also exists that GVIA possesses more than one binding site (Werth *et al.*, 1991) in either synaptosomes or PC12 cells (or both) and that MeHg differentially effects GVIA binding at these sites.

In the absence of stimulation MeHg still decreases a measurable amount of current. Here again, the effect of the lower concentrations of

MeHg were different from 1 μM MeHg. End currents were consistently blocked to a greater extent at 0.25 μM MeHg and occasionally at 0.5 μM MeHg. Two possible scenarios could explain a facilitated reduction of the end current in the absence of stimulation. MeHg may preferentially remove one or more channel types which contribute a greater amount of current at the end of the depolarization step. This has been shown to occur with Cd^{2+} (Narahashi *et al.*, 1989). In contrast, fast inactivating Ca^{2+} channels in cerebellar granule cells are more effectively blocked by Ni^{2+}, relative to those which slowly inactivate (Rossi *et al.*, 1994). MeHg may also simultaneously decrease a portion of the whole cell current and increase the inactivation rate of the remaining current. Inactivation of Ca^{2+} channels occurs via both Ca^{2+}- (Tillotsen, 1979) and voltage-dependent means (Lux and Gutrick, 1986). Although MeHg can increase $[Ca^{2+}]_i$ and depolarize neuronal membranes (Kauppinen *et al.*, 1989), presumably, neither of these factors should contribute to the inactivation in granule cells as Ba^{2+} is substituted for Ca^{2+} and the cell membrane is held at -90 mV. Further, EGTA is in the pipette such that even if Ca^{2+} were present intracellularly it would be chelated. Interestingly, in one of the experiments where end current was blocked to a greater following exposure in the absence of stimulation, continued exposure to MeHg (for ~ 3 min) in the presence of 0.1 Hz stimulation caused the apparent rate of current inactivation to return to a level similar to that observed in the control situation. Thus, the interaction of MeHg with the Ca^{2+} channel and the subsequent pattern of

Ba^{2+} current reduction, appear to depend on the rate at which the cell is stimulated. Perhaps the act of activating the channel exposes MeHg-sensitive sites, which once bound by MeHg, contribute to the reduction in current.

The ability of MeHg to decrease Ba^{2+} current in a use-dependent manner could imply that MeHg has an increased affinity for the open or inactivated state of the channel. Alternatively, entry of MeHg into the cell through the Ca^{2+} channel may be facilitated due to the increased amount of time that the channel is open state. This could potentially lead to activation or inhibition of intracellular events, resulting ultimately in an enhanced reduction of Ba^{2+} currents. The lack of a facilitated effect in the presence of 0.2 Hz stimulation with 1 μM MeHg suggests that its mechanism of current reduction is different from that of the two lower concentrations. It is also possible that this concentration of MeHg may activate other pathways which modulate the ability of an increased stimulation frequency to facilitate the MeHg-induced block.

Since the effect of MeHg is not decreased by any of the antagonists that were tested, the question remains as to how MeHg exerts its blocking action. Whatever the case, some type of interaction with the plasma membrane must occur. Because MeHg is lipophilic, it could traverse this barrier to exert an intracellular effect. The slow onset of the MeHg effect compared to Cd^{2+} and some toxins, is consistent with this idea. Introduction of MeHg into the pipette perfusing the intracellular space might yield

additional information concerning the mechanism of action of MeHg, but these experiments would also be difficult to interpret as MeHg would likely cross the plasma membrane. This is supported by the ability of MeHg, but not Hg^{2+}, to elicit an increase in miniature end plate potential (MEPP) frequency at the neuromuscular junction in the presence of TTX and Co^{2+}. In the presence of these two agents, Na^{+} and Ca^{2+} channels would be blocked, thus preventing either compound from entering the cell via these routes. This suggests that the site of action was intracellular and that Hg^{2+} entered through Ca^{2+} and/or Na^{+} channels, while MeHg apparently has other means of gaining entrance to the cell (Miyamoto, 1983).

An explanation consistent with the results observed here is that MeHg decreases current through all Ca^{2+} channel types. Certainly, one must consider the potential interaction of MeHg with sulfur-containing proteins when trying to explain how reductions in current arise. The exact role which these proteins play in Ca^{2+} channel function has yet to be fully elucidated; however, it is likely that they at least contribute to processes such as channel activation and inactivation. Thus, many of the effects observed in the experiments presented here could be described by an interaction of MeHg at sulfur-containing proteins, or at any other potential complexation sites contained on proteins critical to channel function. Effects at these sites would be presumably less liable to be reversed by wash with MeHg-free bath solution.

C. Relationship to previous work.

In addition to disrupting ion flux through Ca^{2+} channels, MeHg can disrupt a number of other processes involving $[Ca^{2+}]_i$ regulation. Fura-2 studies in synaptosomes (Denny *et al.*, 1993; Denny and Atchison, 1994), NG108-15 cells (Hare *et al.*, 1993; Hare and Atchison, 1994) and cerebellar granule cells (Marty and Atchison, *submitted*), have shown that MeHg disrupts intracellular ion homeostasis in three temporally separate "phases". The first phase elevation in $[Ca^{2+}]_i$ results from MeHg-induced release of Ca^{2+} from an intracellular pool. This phase, which persists in the absence of $[Ca^{2+}]_e$, can be reduced by prior application of agents which generate inositol trisphosphate to release Ca^{2+} from the endoplasmic reticulum (Hare *et al.*, 1993). This is followed by an elevation in a non-Ca^{2+} cation, whose identity is presently unknown in granule cells, but which has been shown in synaptosomes to be Zn^{2+} (Denny and Atchison, 1994). The third phase consists of a massive influx of extracellular Ca^{2+} across the plasma membrane, leading eventually to the death of the cell. Conditions which delay the MeHg-induced alterations in fura-2 fluorescence include prior perfusion of the dihydropyridine antagonist nifedipine, the Na^+ channel blocker tetrodotoxin and also the purported P- and Q-type Ca^{2+} channel antagonist ϖ-conotoxin MVIIC. As the ability of MeHg to elicit the first phase increase in $[Ca^{2+}]_i$ persists in the absence of extracellular Ca^{2+}, this suggests nifedipine and MVIIC may prevent MeHg from entering the cell through Ca^{2+} channels. Nifedipine- and MVIIC-induced delays in the

second phase suggest that Ca^{2+} channels sensitive to these agents may contribute to the MeHg-induced elevation in $[Ca^{2+}]_i$ (Marty and Atchison, *submitted*).

A comparison of the time required for MeHg to elicit elevations in $[Ca^{2+}]_i$ versus the time required to observe a decrease in the whole cell Ba^{2+} current, reveals that the latter occurs following a much shorter latent period. At 1 µM MeHg, the average time required for the onset of the first phase elevation in $[Ca^{2+}]_i$ is about 5 min. Following a similar period of exposure at 1 µM, whole cell peak and end Ba^{2+} currents are decreased ~30-40%. The two events may be interrelated in some way, *vis a vis* MeHg entering the cell through voltage-dependent Ca^{2+} channels, an event which may block Ba^{2+} (or Ca^{2+}) flux through the channel. However, it is problematic to explain the ability of MeHg to cause a massive influx of $[Ca^{2+}]_e$ across the plasma membrane, when MeHg has been shown to irreversibly decrease Ca^{2+} channel current (Shafer and Atchison, 1991). Pathways sensitive to N-methyl *d*-aspartate (NMDA) antagonists do not contribute significantly to MeHg-induced elevations in $[Ca^{2+}]_i$ (Marty and Atchison, *submitted*). One possible contributor to the Ca^{2+}_e-mediated elevation in $[Ca^{2+}]_i$ is a MeHg-induced non-specific cation conductance. In dorsal root ganglion cells, MeHg elicits an inward current which is not blocked by La^{3+}, TTX or picrotoxin, suggesting that Ca^{2+}, Na^+ or Cl^- channels were not responsible for the current (Arakawa *et al.*, 1991). In other preparations, inorganic heavy metals such as Pb^{2+}, Cd^{2+} and Hg^{2+} have been

shown to activate an inward currents via non-specific cation channels (Weinreich and Wonderlin, 1987; Oortgiesen *et al.*, 1990). This conductance could occur through channels which do not discriminate well among the various cations. MeHg may also alter the selectivity of other voltage-gated channel types, resulting in Ca^{2+} entry through these channels.

At 1 µM and above, the dihydropyridine nifedipine causes a delay in the onset of the second phase increase in $[Ca^{2+}]_i$ as measured using fura-2 (Hare and Atchison, 1995; Marty and Atchison, *submitted*). Because 0.1 µM nifedipine was as effective as 1 µM nifedipine in blocking a K^+-stimulated increase in $[Ca^{2+}]_i$, it is possible that a mechanism not involving the Ca^{2+} channel is responsible for the delay. In my experiments, MeHg-induced reductions in peak Ba^{2+} current were actually facilitated by a similar dihydropyridine (nimodipine). The findings that dihydropyridine compounds both increase the time to onset of the MeHg-induced second phase elevation in $[Ca^{2+}]_i$ and facilitate the MeHg-induced reduction of Ba^{2+} current are consistent. In the fura-2 experiments, MeHg-induced reduction of ion flux through Ca^{2+} channels would in effect decrease the extent of the elevation in $[Ca^{2+}]_i$ which occurs as a result of influx of extracellular Ca^{2+}.

In cerebellar granule cells, ϖ-conotoxin MVIIC blocks about 40% of the whole cell peak current and a similar percentage of the K^+ depolarization-induced elevation in $[Ca^{2+}]_i$. This toxin also affords a delay in the onset of the second phase. At the concentration (1 µM) used in both studies, MVIIC can be presumed to be blocking P-, Q- and possibly N-type

Ca^{2+} channels. Thus, if these channel types contribute to the second phase elevation in $[Ca^{2+}]_i$, they either must not be affected by MeHg initially, or else the "block" is reversed following longer exposures, thereby allowing the influx of $[Ca^{2+}]_e$. In a small number of cells which were held for periods of up to 20 min, recovery from the MeHg-induced decrease of Ba^{2+} currents was never evident, suggesting that reversal of block was not likely. This dichotomous effect of MeHg - a reduction of Ca^{2+} channel current, coupled with an elevation in $[Ca^{2+}]_i$, mediated at least in part by Ca^{2+} channels, is difficult to explain, but may be the result of different experimental conditions.

MeHg-induced reductions in PC12 whole cell Ba^{2+} currents were voltage-dependent at a holding potential of -40 mV, but not at -70 or -90 mV (Shafer and Atchison, 1991). In synaptosomes, organic, but not inorganic, mercurials decrease $^{45}Ca^{2+}$ uptake in a voltage-dependent manner (Shafer *et al.*, 1990; Hewett and Atchison, 1992). In cerebellar granule cells, following prepulses ranging from -110 to 0 mV, the MeHg-induced reduction in current during a subsequent test pulse was not different from that observed in the absence of a test pulse. Thus, the mechanism by which MeHg reduces current in granule cells is not facilitated by changes in voltage. The differences between cerebellar granule cells, PC12 cells and synaptosomes in regards to voltage-dependence of the MeHg effect could be related to differences in their respective Ca^{2+} channel populations or to a differential interaction of MeHg at sites other than those which mediate Ca^{2+} channel

function.

Both MeHg and Hg^{2+} are able to decrease $^{45}Ca^{2+}$ uptake into synaptosomes in the absence of depolarization (Atchison *et al.*, 1986; Shafer and Atchison, 1989; Shafer *et al.*, 1990; Hewett and Atchison, 1992). MeHg was able to decrease the fraction of non-inactivating $^{45}Ca^{2+}$ influx and altered the rate constant of apparent inactivation in synaptosomes (Shafer *et al.*, 1990). In PC12 cells, exposure to MeHg in the absence of stimulation elicits a sizable decrease in peak and end Ba^{2+} currents and removes the inactivating component of the current (Shafer and Atchison, 1991). As MeHg is lipophilic, this action could be attributable to either a membrane effect or an intracellular event.

In cerebellar granule cells, DRG cells (Leonhardt *et al.*, 1996) and PC12 cells (Shafer and Atchison, 1991), 1 μM MeHg decreases a similar amount of whole cell Ca^{2+} channel current (~30-35%). Since the concentration of MeHg at which 50% of the Ba^{2+} current is reduced was not calculated for either PC12 cells or granule cells, it is difficult to effectively compare each of these three cell types. It would appear however, that Ca^{2+} channel currents in cerebellar granule cells are no more susceptible to MeHg-induced reduction than are other cell types. The complement of Ca^{2+} channels contained on each of the cell types differs, thus making it likely that MeHg does not target specific Ca^{2+} channel types.

D. Comparison of the MeHg-induced reduction of Ca^{2+} channel current in granule cells to MeHg-induced effects at other voltage-gated channels.

MeHg also disrupts both Na^+ and K^+ channel function as measured using patch clamp techniques. In N1E-115 mouse neuroblastoma cells, 20 to 60 µM MeHg blocked both Na^+ and K^+ currents (Quandt *et al.*, 1982). A steady increase in the threshold for action potential generation and eventual block of conduction was attributed to block of Na^+ and K^+ channels by MeHg (25-100 µM) in the squid giant axon (Shrivastav *et al.*, 1976). Na^+ channel function was also disrupted by MeHg (50-100 µM) in mouse *triangularis sterni* motor nerves (Shafer and Atchison, 1992).

Structurally, Na^+, Ca^{2+} and K^+ channels are somewhat different, but possess many of the same characteristics common to all voltage-dependent channels, such as multiple subunits, a voltage sensor and a selectivity filter (Hille, 1992). If reductions in current were occurring simply by physical occlusion of the pore, then MeHg should decrease current through all voltage-gated channels to a similar extent. Apparently this is not the case in cerebellar granule cells, as higher concentrations of MeHg (2-40 µM) produced only ~15-30% reduction in K^+ current following a 5 min exposure. It is not likely that differences in the size of the respective pores could explain the differences in the amplitude of a MeHg-induced reduction in current. Na^+, Ca^{2+} and K^+ channels have been shown to permit the passage of ions much larger than their respective ions (Hille, 1992). One possibility is that structural differences in functional groups within or surrounding the

Ca^{2+} channel may impart upon it a greater susceptibility to MeHg-induced reductions in Ba^{2+} current. Alternatively, actions of MeHg at sites removed from the channel protein may influence Ca^{2+} channel function to a greater extent than K^+ channel function.

MeHg can also alter functioning of receptor-gated channels, presumably by preventing access of the ligand to its receptor or impeding the flux of ions through the open channel subsequent to ligand binding. MeHg (10 μM) decreases the binding of [^{3}H]-nicotine and [^{3}H]-pilocarpine to nicotinic and muscarinic receptors, respectively (Eldefrawi *et al.*, 1977). $HgCl_2$ is more effective than MeHg at blocking binding of [^{3}H]-quinuclidinyl benzilate (QNB) to muscarinic cholinergic receptors from cortical membranes (Von Burg *et al.*, 1980; Abd-Elfattah and Shamoo 1981) and binding of ^{3}H-spiroperidol to striatal dopamine receptors (Bondy and Agrawal, 1980). Binding of other radiolabelled compounds such as spiroperidol to dopaminergic receptors and ^{3}H-diazepam to benzodiazepine receptors showed no consistent pattern of inhibition in the presence of MeHg (Bondy and Agrawal, 1980).

Other experimental evidence suggests that MeHg can interact with ligand-gated channels and disrupt their function. Nicotinic and muscarinic cholinergic receptor-mediated responses are decreased by MeHg in the N1E-115 mouse neuroblastoma cell line, while dopamine receptor-mediated responses are unaffected (Quandt *et al.*, 1982). Examination of muscle-type ACh receptor-activated ion channels from the G8 clonal myoblast cell line

using patch clamp techniques showed that MeHg did not affect the single channel conductance or the mean open and closed times following exposure to concentrations of 10 and 100 μM (Atchison, unpublished observations). Lack of effect on end-plate response to iontophoresis of ACh or on MEPP amplitude also implies little or no effect on muscle-type nicotinic receptors (Atchison and Narahashi, 1982).

Other mercurials such as $HgCl_2$, *p*-chloromercuribenzoate and *p*-chloromercuriphenylsulfonate increase markedly the binding of [^{3}H]α-amino-3-hydroxy-5-methylisoxazole-4-propionic acid (AMPA), a ligand for the AMPA subtype of glutamate receptors, to rat brain synaptic membranes (Terramani *et al.*, 1988). If sulfhydryl-groups and/or disulfide-linkages are important in either ligand-receptor interaction or the activation of the channel subsequent to this process, then mercurial interaction with these residues would be expected to alter channel properties. Mercurials may impede agonist interaction by binding at the receptor site and preventing its access, or alternatively may produce a redistribution of binding sites between high- and low- affinity states (Terramani *et al.*, 1988). This would explain the ability of mercurials both to enhance and inhibit the binding of different agonists.

In the hippocampal slice, MeHg (4-100 μM) blocked the response of CA1 neurons to iontophoresis of glutamate. This effect was not mediated solely by MeHg-induced depolarization of the membrane potential, suggesting that other mechanisms, such as block of glutamate receptors,

may be involved. Pretreatment of slices with bicucculine, a $GABA_A$ antagonist, removed the ability of MeHg (100 μM) to initially increase neuronal excitability prior to block. Pretreatment of the slice with strychnine, an antagonist of the glycine receptor, did not prevent the MeHg-induced increase in excitability (Yuan and Atchison, 1996). This suggests that MeHg may act at $GABA_A$ receptors to decrease inhibitory neurotransmission, thereby unmasking an excitatory effect. Both MeHg and Hg^{2+} have been shown to block more potently inhibitory postsynaptic potentials compared to excitatory postsynaptic potentials (Yuan and Atchison, 1995), suggesting a complex mechanism of action of these mercurials. Thus, mercurials may interact with receptors in a distinctive manner that is apparently dependent on charge and lipophilicity.

The ability of MeHg to alter flux through ion channels, as well as the binding of radiolabelled agonist to their receptors, has thus been shown in several different experimental paradigms. These experiments provide useful information about the behavior of specific channel types, and the interaction of agonists with receptor in the presence of mercurial. Differential results observed with Hg^{2+} and MeHg support the idea that these metals act *via* different mechanisms. The end result of mercurial binding is also likely to depend on a number of factors inherent to the mercurial or the site at which they act.

E. Possible consequences of a MeHg-induced reduction of Ca^{2+} channel current.

As previously described, Ca^{2+} channels are responsible for mediating a wide array of cellular events. Spatially distinct, temporally controlled elevations in $[Ca^{2+}]_i$ serve as a transducer which convert extracellular signals into intracellular events such as transmitter release or enzyme activation. Because of their location on the plasma membrane, their complex regulation by a number of factors and the large number of events which they mediate, Ca^{2+} channels are inherently sensitive to many neurotoxic agents. The studies presented here have shown that MeHg can decrease Ca^{2+} channel current in numerous ways. This action may occur in parallel or prior to such events as elevations in $[Ca^{2+}]_i$ or unregulated activation of enzymes, events considered to be an initial step in Ca^{2+}-mediated cell death.

APPENDIX

APPENDIX

A. Effect of dithiothreitol on 1μM MeHg-induced decrease in whole cell Ba^{2+} current

All mercurials possess a high affinity for cysteine-containing proteins (Hughes, 1957). Disulfide linkages, present in a number of proteins, are comprised of two linked cysteine residues. Modification of disulfide linkages, which contribute to both protein structure and function, has been shown to affect the activity of a number of channel types including Na^+ channels (Backx *et al.*, 1992), K^+ channels (Ruppersberg *et al.*, 1991), Ca^{2+}-activated non-selective cation channels (Koivisto *et al.*, 1993), and L-type Ca^{2+} channels (Chiamvimonvat *et al.*, 1995). Thus, these sites represent a potential target of MeHg and, depending on the role that they play in shaping current amplitude and/or kinetics, may play a significant role in the ability of MeHg to decrease current carried through Ca^{2+} channels.

Dithiothreitol (DTT), an agent which reduces intramolecular disulfide bonds to yield free sulfhydryl groups, was tested for its ability to alter the MeHg-induced decrease in whole cell Ba^{2+} current. DTT (50 μM) caused only marginal increases in peak (12 ± 13%) and end (8 ± 13%) currents (n=5). Interestingly, channel rundown in the presence of DTT appeared to be much slower than that observed in the control situation. This suggests that modification of sulfhydryl residues may play a role in Ca^{2+} channel rundown. In 3 of the 5 experiments DTT increased peak current amplitude

(24-70%), an effect which remained stable over 2 min. Subsequent application of MeHg resulted in a decrease of peak and end currents by 35 ± 11% and 39 ± 11%, respectively, after 5 min of exposure to MeHg. When DTT elicited either a decrease or caused no change in the current amplitude, 1 μM MeHg caused further reduction of the peak and end currents by 84 ± 6% and 83 ± 1%, respectively (Fig. A.1). When results from all experiments were pooled, the mean amount of current reduction produced by MeHg in the presence of DTT (55 ± 13%, 57 ± 12% reduction of peak and end currents, respectively; n=5) was slightly more than that produced by MeHg alone. In only one of 5 experiments was 50 μM DTT protective against the effect of 1 μM MeHg with DTT enhanced peak and end currents being blocked only 13% and 18 %, respectively, following a 5 min exposure to MeHg. Thus, either MeHg is not acting at sulfhydryl groups or prior reduction of these entities does not alter the action of MeHg.

Experiments were also performed which examined the ability of DTT to reverse the MeHg-induced reduction of granule cell Ba^{2+} current. Perfusion of 1 μM MeHg prior to DTT resulted in a reduction of peak and end currents by 32 ± 9% and 31 ± 10% (n=4), respectively, following 2-5 min of exposure. Addition of DTT did elicit a slight recovery from the MeHg-induced reduction in current in some cases (Fig. A.2). In other experiments a leveling off of the MeHg-induced decrease in Ba^{2+} current was observed in the presence of DTT.

FIG. A.1. Dithiothreitol (DTT, 50 μM) does not prevent the 1 μM MeHg-induced decrease in peak Ba^{2+} current. **(A)** Addition of DTT did not appreciably alter the control peak or end (not shown) current **(a,b)**. In 6 experiments DTT increased peak and end currents by 12 ± 13% and 8 ± 13%, respectively. Subsequent perfusion of MeHg resulted in a large decrease in peak and end currents **(c,d)** which averaged 55 ± 13% and 57 ± 12%, respectively (n=5). **(B)** Current traces from the experiment in **A** showing control current **(a)**, current immediately after addition of DTT **(b)** and the current remaining following addition of MeHg in the presence of DTT **(c,d)**.

Fig. A.1

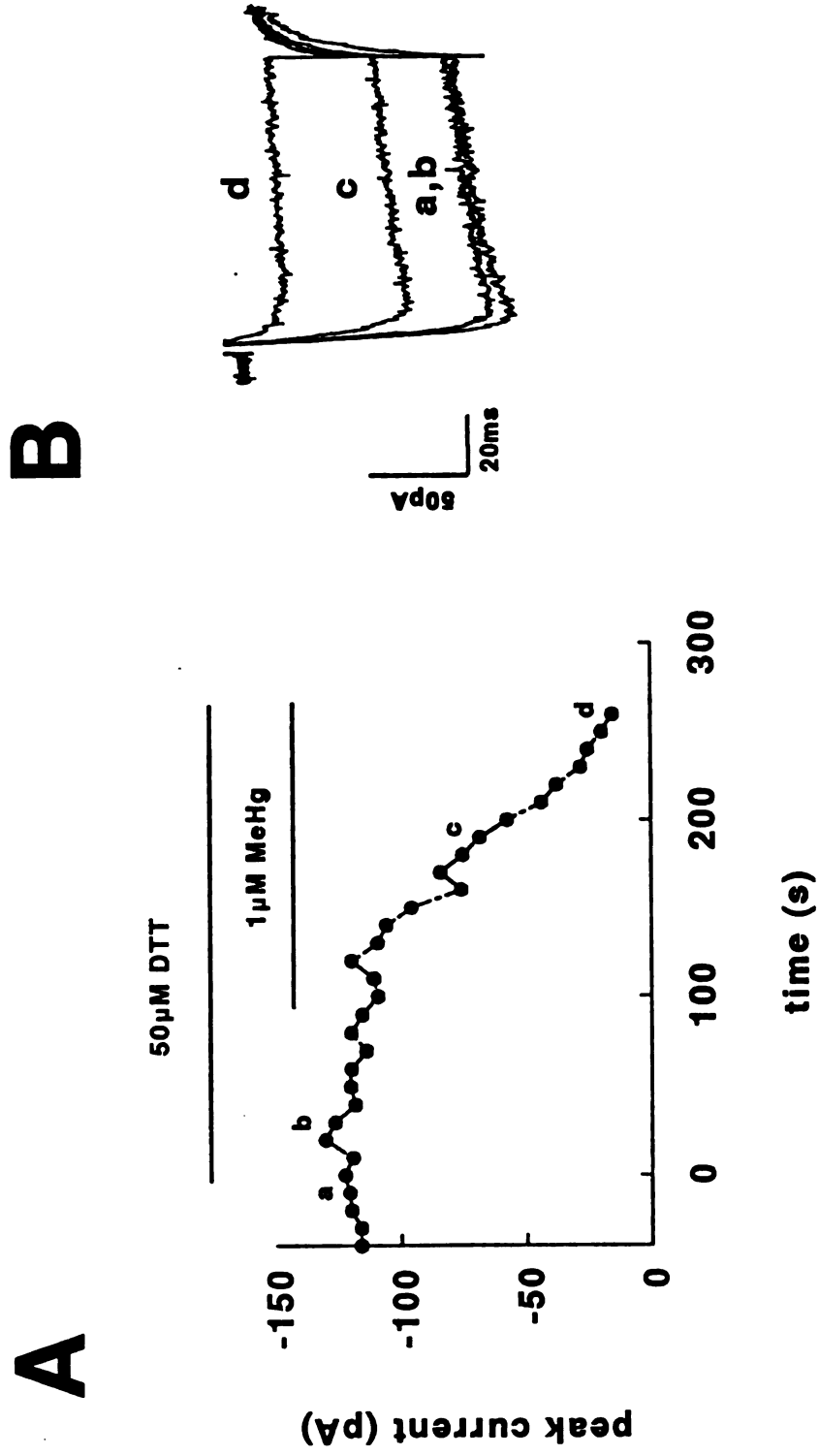
A
50μM DTT
1μM MeHg
a
b
c
d
-150
-100
-50
0
0
100
200
300
time (s)
peak current (pA)
B
d
c
a,b
50pA
20ms

FIG. A.2. Dithiothreitol can partially reverse a 1 μM MeHg-induced decrease in peak Ba^{2+} current. **(A)** 1 μM MeHg caused a large decrease in peak current over a 3 min exposure. Subsequent addition of DTT (50 μM) caused a slight reversal of the effect that remained stable over a 2 min period. When MeHg was re-perfused onto the cell, current was again decreased at a rate similar to that observed during the initial MeHg exposure. In 2 of 4 experiments, DTT induced ~20% recovery. **(B)** Current traces from the experiment in **A** depicting control **(a)**, MeHg-induced decrease **(b)**, reversal by DTT **(c)** and the subsequent MeHg-induced decrease **(d)**.

Fig. A.2

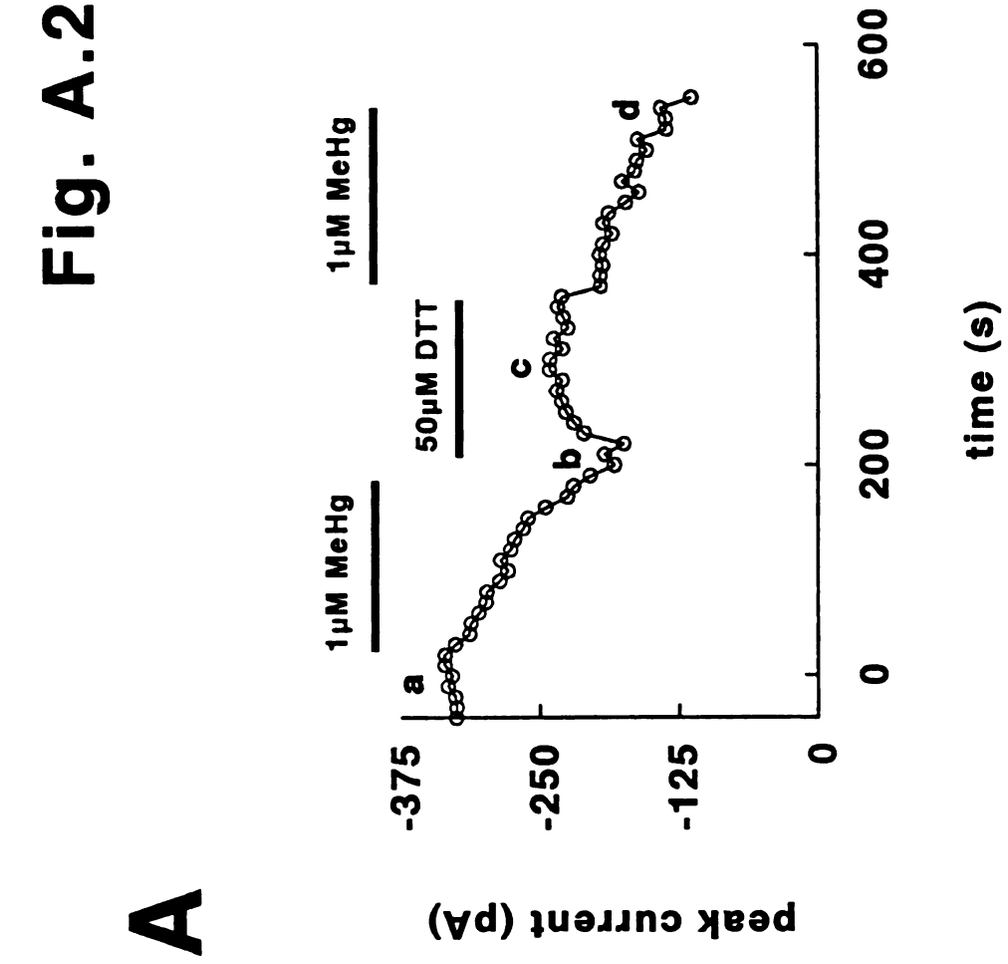
A
peak current (pA)
-375
-250
-125
0
0
200
400
600
time (s)
1μM MeHg
50μM DTT
1μM MeHg
a
b
c
d
B
100 pA
30 ms
a
c
b
d

B. 20 mM Ba^{2+} experiments

Experiments were performed in 20 mM Ba^{2+} to determine if the effect of MeHg was similar to that observed when 5 mM Ba^{2+} was the charge carrier. Currents elicited in 20 mM Ba^{2+} were larger than those seen in 5 mM Ba^{2+} (mean control peak current was -160 ± 13 pA, n=42). Current kinetics appeared to be similar to those observed in 5 mM Ba^{2+}. At a stimulation frequency of 0.1 Hz, 1μM MeHg blocked 54 ± 7% of peak and 52 ± 6% of end currents (Fig. A.3; n=5). These values were greater than those observed with 1 μM MeHg using 5 mM Ba^{2+} as the charge carrier. An increase in the stimulation frequency to 0.2 Hz resulted in similar percentages of peak and end current decline (56 ± 8% and 55 ± 10%). It is difficult to compare these two sets of experiments to the 5 mM Ba^{2+} experiments however, as the length of the depolarization step was more than twice as long in experiments utilizing 20 mM Ba^{2+} (250 msec versus 105 msec in 5 mM Ba^{2+}). Although it is purely speculative to assume that the larger extent of current reduction is caused by the longer depolarization step, this finding is consistent with the elevated reduction in current caused by 1 μM MeHg during I-V relationship experiments.

Higher concentrations of MeHg were also used when 20 mM Ba^{2+} was the charge carrier. Figure A.4 shows the effect of 5 μM MeHg at 3 different stimulation frequencies in 20 mM Ba^{2+}. At 0.1 Hz, 5 μM MeHg caused a rapid, incomplete reduction of the current. At higher concentrations such as this, cells were typically lost prior to complete removal of the Ba^{2+} current.

FIG. A.3. An increase in charge carrier concentration does not prevent the 1 μM MeHg-induced decrease in peak and end Ba^{2+} current. **(A)** Control peak and end currents, which were 2-3 times larger in 20 mM Ba^{2+} (vs 5 mM), were blocked 49 ± 8% and 42 ± 7%, respectively (n=5). In the experiment depicted, a longer exposure (~10 min) to MeHg resulted in nearly complete removal of both peak and end currents. **(B)** Current traces from the experiment in **A**, depicting control **(a)** and the decrease elicited following approximately 4 **(b)** and 10 **(c)** min of exposure. **(C)** Current sensitive to MeHg obtained by subtracting trace c from trace a. Depolarizing steps were 250 ms in duration.

Fig. A.3

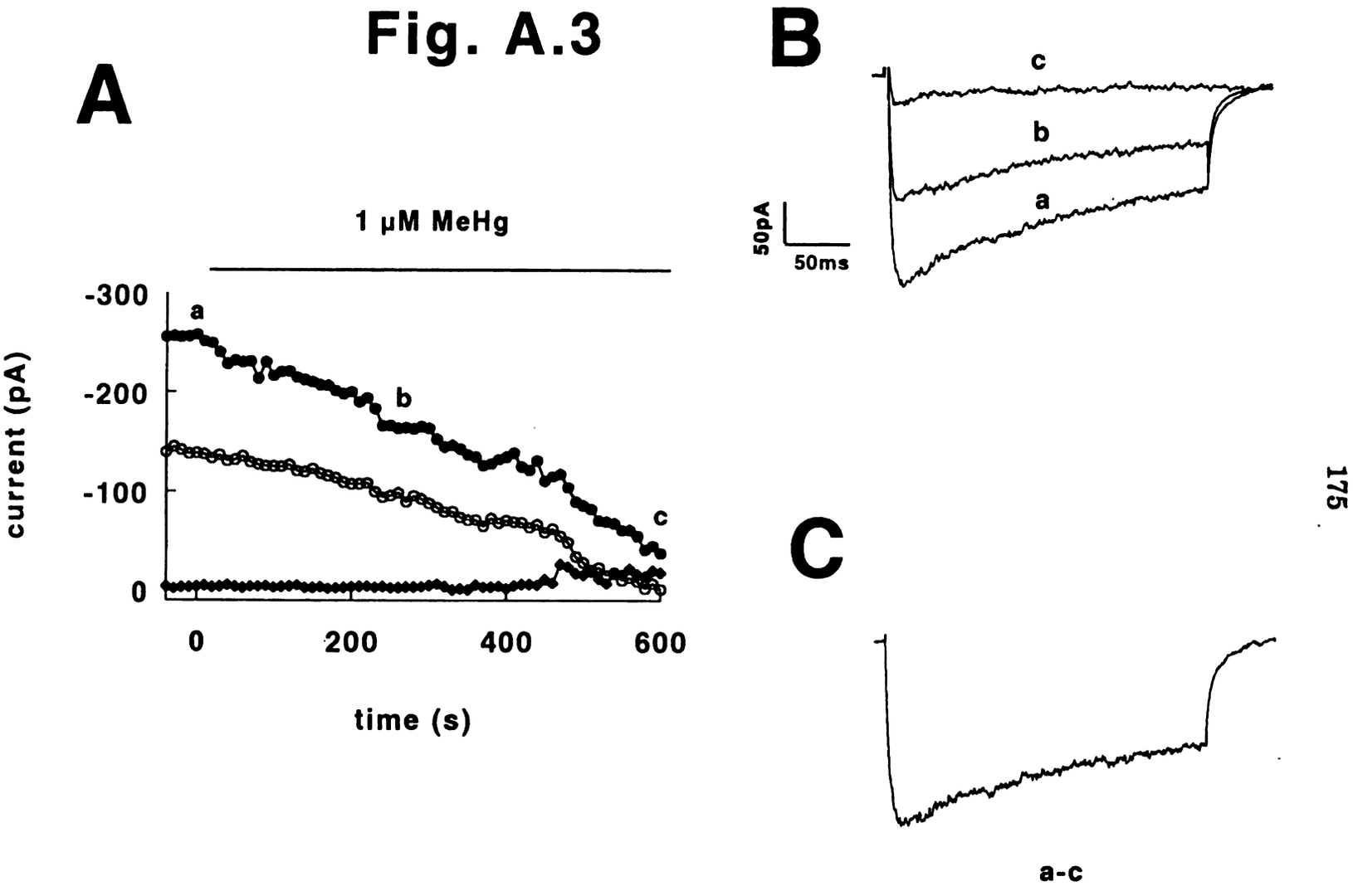
A
1 μM MeHg
-300
-200
-100
0
current (pA)
a
b
c
0
200
400
600
time (s)
B
c
b
a
50pA
50ms
C
a-c

Thus it is difficult to say whether the reduction in current would have progressed to completion. Pooled experiments showed that at a stimulation frequency of 0.1 Hz, 5 μM MeHg decreased 69 ± 4% and 72 ± 4% of peak and end currents (n=8) respectively. Exposure times ranged from 30 sec to 3 min. When the stimulation frequency was increased to 0.2 Hz no further facilitation of the effect was noted (74 ± 6% and 77 ± 1% reduction of peak and end currents). Increasing the stimulation frequency to 0.4 Hz resulted in peak and end current decreases of 94 ± 2% and 93 ± 4%, respectively.

At 10 μM, MeHg removed 74 ± 11 and 81 ± 7% of peak and end currents following brief exposures (1 min to 2.5 min). Increasing the stimulation frequency to 0.2 Hz in the presence of 10 μM MeHg hastened the loss of a seal between the cell and the pipette. As such, exposure times were shortened and 10 μM MeHg blocked only 56 ± 15% of peak and 60 ± 15% of end currents. It is likely that further reductions in current would have taken place had the cells been maintained for longer periods of time. Increases in the stimulation frequency to 0.4 Hz resulted in nearly complete removal of the Ba^{2+} current (peak and end currents were decreased 92 ± 3% and 94 ± 3%).

FIG. A.4. 5 μM MeHg-induced reduction of peak Ba^{2+} current at 0.1, 0.2 and 0.4 Hz. **(A,C,E)** Representative traces depicting the rapid effect of 5 μM MeHg. **(B,D,E)** Current traces from the representative experiments. Removal of the Ba^{2+} current was nearly complete in all cases, often with little or no apparent change in the inactivation profile of the current.

Fig. A.4

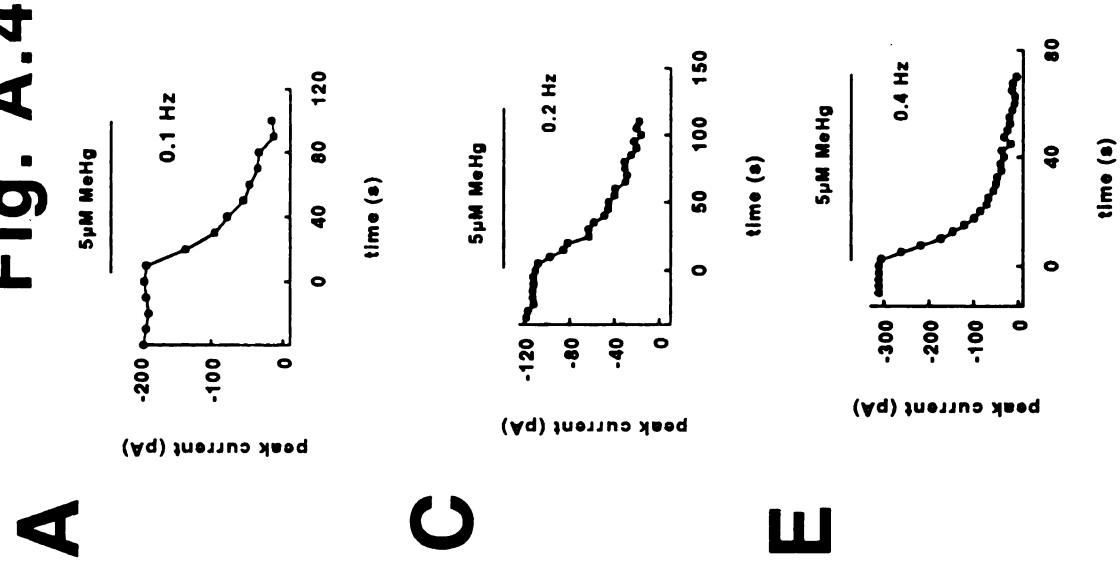
A
5μM MeHg
0.1 Hz
-200
-100
0
0
40
80
120
time (s)
peak current (pA)
B
80pA
50ms
C
5μM MeHg
0.2 Hz
-120
-80
-40
0
0
50
100
150
time (s)
peak current (pA)
D
30pA
50ms
E
5μM MeHg
0.4 Hz
-300
-200
-100
0
0
40
80
time (s)
peak current (pA)
F
75pA
50ms

C. Effect of 1 μM nimodipine on the 1 μM MeHg-induced reduction of whole cell Ba^{2+} current.

In NG108-15 cells (Hare and Atchison, 1985) as well as cerebellar granule cells (Marty and Atchison, *submitted*), the dihydropyridine L-type Ca^{2+} channel antagonist nifedipine is able to delay the onset of MeHg-induced alterations in fura-2 fluorescence. In both cases however, nifedipine only does this at concentrations of 1 μM or above. Dihydropyridines can cause effects at sites other than the Ca^{2+} channel (Zernig, 1990), especially at higher concentrations. Thus, the delay in the onset of the MeHg-induced effects may arise from some type of non-specific action of the dihydropyridine compound.

When perfused on in the control situation, 1 μM nimodipine elicited a similar amount of block of peak current (19 ± 4%, n=4) as 0.1 μM nimodipine (18 ± 2%). End current was actually blocked less in the higher concentration of nimodipine (20 ± 2% with 1 μM versus 31 ± 4 with 0.1 μM). Thus, if non-specific events were occurring, they apparently did not facilitate the decline in Ba^{2+} current. When 1 μM MeHg and 1 μM nimodipine were perfused onto cells concurrently, the apparent rate of peak and end current reduction was slower than that for either MeHg or nimodipine perfused alone. With continued exposure, the reduction in peak current approached that of MeHg alone, while the effect on the end current in the presence of the two agents was slightly less compared to MeHg alone.

The slow rate of current reduction in the presence of MeHg and

nimodipine suggests that each of these agents may modify the ability of the other to bind and elicit a decrease in current. MeHg (100 μM) disrupts the pattern of ^{3}H-nitrendipine binding in synaptosomes (Shafer *et al.*, 1990). Thus, it is possible that these two agents either compete for a similar site or that their respective actions have opposite effects on Ba^{2+} current amplitude. With longer exposures, the effect is apparently overcome, but it is not known which of the agents is eliciting the decrease in current as both have approximately the same rate of initial decrease of the whole cell Ba^{2+} current.

D. Effect of BayK 8644 on control Ba^{2+} current and the 1 μM MeHg-induced decrease in Ba^{2+} current.

The dihydropyridine agonist BayK 8644 was tested to determine its ability to facilitate L-type Ca^{2+} channel current. Experiments were performed with two different concentrations of BayK 8644 (10 and 100 nM). At either concentration, BayK 8644 had very little effect on the whole cell current. Any increase that did occur was usually very small and transient. In only 1 of 12 experiments did BayK (100 nM) cause a large, sustained enhancement (~70%) of the current (Fig. A.5). A 4 min exposure to MeHg following this effect produced a nearly complete removal of peak and end currents. In general however, the effect of MeHg following addition of BayK 8644 was similar to that observed in the absence of BayK 8644.

FIG. A.5. The effect of the dihydropyridine agonist BayK 8644 on control peak Ba^{2+} current and 1 μM MeHg-induced reduction of peak Ba^{2+} current. **(A)** In this experiment, a slight enhancement of peak current was observed. In 5 experiments with 100 nM BayK 8644, average increases of peak and end currents were 11 ± 5% and 9 ± 2%, respectively). Typically, BayK 8644-induced increases in peak and end Ba^{2+} current were not sustained. Following BayK 8644, 1 μM MeHg decreased peak and end currents 63 ± 13% and 68 ± 12%, respectively (exposure times were 1.5 min to 4 min).

Fig. A.5

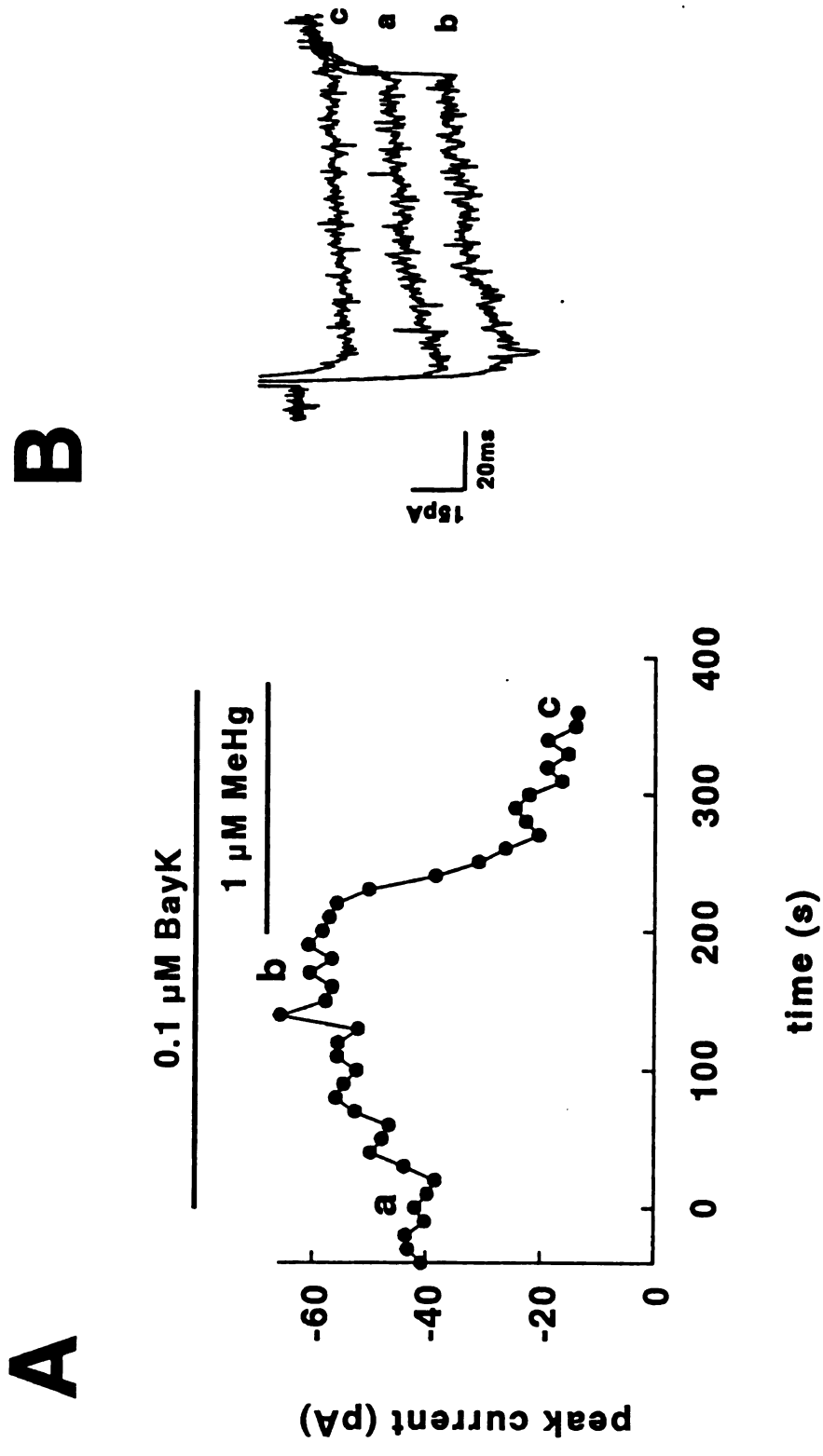
A
0.1 μM BayK
1 μM MeHg
a
b
c
-60
-40
-20
0
peak current (pA)
0
100
200
300
400
time (s)
B
a
b
c
15pA
20ms

BIBLIOGRAPHY

BIBLIOGRAPHY

Abd-Elfattah, A.A., and Shamoo, A.E. (1981) Regeneration of a functionally active rat brain muscarinic receptor by *d*-penicillamine after inhibition with methylmercury and mercuric chloride. Evidence for essential sulfhydryl groups in muscarinic receptor binding sites. *Mol. Pharmacol.* **20**, 492-497.

Arakawa, O., Nakahiro, M., and Narahashi, T. (1991) Mercury modulation of GABA-activated chloride channels and non-specific cation channels in rat dorsal root ganglion neurons. *Brain Res.* **551**, 58-63.

Armstrong, C.M., and Bezanilla, F. (1977) Inactivation of the sodium channel. II. Gating current experiments. *J. Gen. Physiol.* **70**, 567-590.

Atchison, W.D., Clark, A.W., and Narahashi, T. (1984) Presynaptic effects of methylmercury at the mammalian neuromuscular junction, In: *Cellular and Molecular Neurotoxicology*, Narahashi T, ed, New York, Raven Press, pp 23-43.

Atchison, W.D. (1986) Extracellular calcium-dependent and -independent effects of methylmercury on spontaneous and potassium-evoked release of acetylcholine at the neuromuscular junction. *J. Pharmacol. Exp. Ther.* **237**, 672-680.

Atchison, W.D. (1987) Effects of activation of sodium and calcium entry on spontaneous release of acetylcholine induced by methylmercury. *J. Pharmacol. Exp. Ther.* **241**, 131-139.

Atchison, W.D. (1988) Effects of neurotoxicants on synaptic transmission: Lessons learned from electrophysiological studies. *Neurotoxicol. Teratol.* **10**, 393-416.

Atchison, W.D., Joshi, U., and Thornburg, J.E. (1986) Irreversible suppression of calcium entry into nerve terminals by methylmercury. *J. Pharmacol. Exp. Ther.* **283**, 618-624.

Bakir, F., Damluji, S.F., Amin-Zaki, A., Murtadha, M., Khalidi, A., Al-Rawi, N.Y., Tikriti, S., Dhahir, H.I., Clarkson, T.W., Smith, J.C., and Doherty, R.A. (1973) Methylmercury poisoning in Iraq. *Science* **181**, 230-241.

Backx, P.H., Yue, D.T., Lawrance, J.H., Marban, E., and Tomaselli, G.F. (1992) Molecular localization of an ion-binding site within the pore of mammalian sodium channels. *Science* **257**, 248-251.

Bean, B.P. (1984) Nitrendipine block of cardiac calcium channels: high affinity binding to the inactivated state. *Proc. Natl. Acad. Sci. USA* **81**, 6388-6392.

Beiswanger, C.M., Mandella, R.D., Graessle, T.R., Reuhl, K.R., and Lowndes, H.E. (1993) Synergistic neurotoxic effects of styrene oxide and acrylamide: glutathione-independent necrosis of cerebellar granule cells. *Toxicol. Appl. Pharmacol.* **118**, 233-244.

Bondy, S.C., and Agrawal, A.K. (1980) The inhibition of cerebral high affinity receptor sites by lead and mercury compounds. *Arch. Toxicol.* **46**, 249-256.

Bossu, J.-L., and Feltz, A. (1986) Inactivation of the low-threshold transient calcium current in rat sensory neurones: evidence for a dual process. *J. Physiol. (Lond.)* **376**, 341-357.

Brehm, P., and Eckert, R. (1978) Calcium entry leads to inactivation of calcium channels in *Paramecium*. *Science* **202**, 1203-1206.

Brown, A.M., Morimoto, K., Tsuda, Y., and Wilson, D.L. (1981) Calcium current-dependent and voltage-dependent inactivation of calcium channels in *Helix aspera*. *J. Physiol. (Lond.)* **320**, 193-218.

Büsselberg, D., Pekel, M., Michael, D., and Platt, B. (1994) Mercury (Hg^{2+}) and zinc (Zn^{2+}): two divalent cations with different actions on voltage-activated calcium channel currents. *Cell. Mol. Neurobiol.* **14**, 675-687.

Büsselberg, D. (1995) Calcium channels as target sites of heavy metals. *Toxicol. Lett.* **82/83**, 255-261.

Carbone, E., and Lux, H.D. (1984) A low voltage-activated, fully inactivating Ca channel in vertebrate sensory neurones. *Nature (Lond.)* **310**, 501-502.

Catterall, W.A. (1986) Molecular properties of voltage-sensitive sodium channels. *Annu. Rev. Biochem.* **55**, 953-985.

Catterall, W.A. (1993) Structure and function of voltage-gated ion channels. *Trends Neurosci.* **16**, 500-506.

Catterall, W.A. (1995) Structure and function of voltage-gated ion channels. *Annu. Rev. Biochem.* **64**, 493-531.

Chad, J.E., and Eckert, R. (1986) An enzymatic mechanism for calcium current inactivation in dialysed *Helix* neurons. *J. Physiol. (Lond.)* **378**, 31-51.

Chang, L.W. (1977) Neurotoxic effects of mercury. A review. *Environ. Res.* **14**, 329-373.

Chiamvimonvat, N., O'Rourke, B., Kamp, T.J., Kallen, R.G., Hoffman, F., Flockerzi, V., and Marban, E. (1995) Functional consequences of sulfhydryl modification in the pore-forming subunits of cardiovascular Ca^{2+} and Na^{+} channels. *Circ. Res.* **76**, 325-334.

Cohen, C.J., and MaCarthy, R.T. (1987) Nimodipine block of calcium channels in rat anterior pituitary cells. *J. Physiol. (Lond.)* **387**, 195-225.

Cooper, G.P., and Manalis, R.S. (1983) Influence of heavy metals on synaptic transmission: A Review. *NeuroToxicology* **4**, 69-84.

Corda, M.G., Concas, A., Rossetti, Z., Guarneri, P., Corongiu, F.P., and Biggio, G. (1981) Methyl mercury enhances [^{3}H]diazepam binding in different areas of the rat brain. *Brain Res.* **229**, 264-269.

Dales, L.G. (1972) The neurotoxicity of alkyl mercury compounds. *Amer. J. Med.* **53**, 219-232.

Denny, M.F., Hare, M.F., and Atchison, W.D. (1993) Methylmercury alters intrasynaptosomal concentrations of endogenous polyvalent cations. *Toxicol. Appl. Pharmacol.* **122**, 222-232.

Denny, M.F., and Atchison, W.D. (1994) Methylmercury-induced elevations in intrasynaptosomal zinc concentrations: An ^{19}F-NMR study. *J. Neurochem.* **63**, 383-386.

Eccles, J.C., Ito, M., and Szentagothai, J. (1967) *The Cerebellum as a Neuronal Machine.* New York, Springer-Verlag.

Eckert, R., and Tillotsen, D.L. (1981) Calcium-mediated inactivation of the calcium conductance in caesium-loaded giant neurones of *Aplysia californica. J. Physiol. (Lond.)* **314**, 265-280.

Eldefrawi, M.E., Mansour, N.A., and Eldefrawi, A.T. (1977) Interactions of acetylcholine receptors with organic mercury compounds. In, *Membrane Toxicity*, Miller, M.W. and Shamoo, A.E., *eds.*, New York, Plenum Press, pp 439-462.

Ellinor, P.T., Zhang, J.-F., Horne, W.A., and Tsien, R.W. (1994) Structural determinants of the blockade of N-type calcium channels by a peptide neurotoxin. *Nature (Lond.)* **372**, 273-275.

Fehling, C., Abdulla, M., Brun, A., Dictor, M., Schutz, A., and Skerfving, S. (1975) Methylmercury poisoning in the rat: A combined neurological, chemical, and histopathological study. *Toxicol. Appl. Pharmacol.* **33**, 27-37.

Fox, A.P., Nowycky, M.C., and Tsien, R.W. (1987) Kinetic and pharmacological properties distinguishing three types of calcium channels in chick sensory neurones. *J. Physiol. (Lond.)* **394**, 149-172.

Gilly, W.F., and Armstrong, C.M. (1982) Divalent cations and the activation kinetics of potassium channels in squid giant axons. *J. Gen. Physiol.* **79**, 965-996.

Grantham, C.J., Bowman, D., Bath, C.P., Bell, D.C., and Bleakman, D. (1994) ϖ-Conotoxin MVIIC reversibly inhibits a human N-type calcium channel and calcium influx into chick synaptosomes. *Neuropharmacology* **33**, 255-258.

Gutnick, M.J., Lux, H.D., Swandulla, D. and Zucker, H. (1989) Voltage-dependent inactivation of calcium channel current in identified snail neurones. *J. Physiol. (Lond.)* **412**, 197-220.

Hamill, O.P., Marty, A., Neher, E., Sakmann, B., and Sigworth, F.J. (1981) Improved patch-clamp techniques for high-resolution current recording from cells and cell-free membrane patches. *Pflügers Arch.* **391**, 85-100.

Hare, M.F., McGinnis, K.M. and Atchison, W.D. (1993) Methylmercury increases intracellular concentrations of Ca^{2+} and heavy metals in NG108-15 cells. *J. Pharmacol. Exp. Ther.* **266**, 1626-1635.

Hare, M.F., and Atchison, W.D. (1995) Methylmercury mobilizes Ca^{++} from intracellular stores sensitive to inositol 1,4,5-trisphosphate in NG108-15 cells. *J. Pharmacol. Exp. Ther.* **272**, 1016-1023.

Hare, M.F., and Atchison, W.D. (1995) Nifedipine and tetrodotoxin delay the onset of methylmercury-induced increase in $[Ca^{2+}]_i$ in NG108-15 cells. *Toxicol. Appl. Pharmacol.* **135**, 299-307.

Heintze, U., Edwardsson, S., Dérand, T., and Birkhed, D. (1983) Methylation of mercury from dental amalgam and mercuric chloride by oral streptococci *in vitro*. *Scand. J. Dent. Res.* **91**, 150-152.

Helting, T.B., and Zwisler, O. (1977) Structure of tetanus toxin. I. Breakdown of the toxin molecule and discrimination between polypeptide fragments. *J. Biol. Chem.* **252**, 187-193.

Henderson, G.R., Huang, W.-H., and Askari, A. (1979) Transport ATPase-the different modes of inhibition of the enzyme by various mercury compounds. *Biochem. Pharmacol.* **28**, 429-433.

Herbette, L.G., Vant-Erve, Y.M., and Rhodes, D.G. (1989) Interaction of 1,4-dihydropyridine calcium channel antagonists with biological membranes: lipid bilayer partitioning could occur before drug binding to receptors. *J. Mol. Cell. Cardiol.* **21**, 187-201.

Hess, P., and Tsien, R.W. (1984) Mechanism of ion permeation through Ca^{2+} channels. *Nature (Lond.)* **309**, 453-456.

Hess, P., Lansman, J.B., and Tsien, R.W. (1984) Different modes of Ca channel gating behaviour favoured by dihydropyridines and Ca agonists and antagonist. *Nature (Lond.)* **311**, 538-544.

Hewett, S.J., and Atchison, W.D. (1992) Effects of charge and lipophilicity on mercurial-induced reduction of $^{45}Ca^{2+}$ uptake in isolated nerve terminals of the rat. *Toxicol. Appl. Pharmacol.* **113**, 267-273.

Hille, B. (1977) Local anesthetics: Hydrophilic and hydrophobic pathways for the drug-receptor reaction. *J. Gen. Physiol.* **69**, 497-515.

Hille, B. (1992) *Ionic Channels of Excitable Membranes*, Sinauer Associates Inc., Sunderland, MA.

Hillyard, D.R., Monje, V.D., Mintz, I.M., Bean, B.P., Nadasdi, L., Ramachandran, J., Miljanich, G., Azimi-Zoonooz, A., McIntosh, J.M., Cruz, L.J., Imperial, J.S., and Olivera, B.M. (1992) A new *Conus* peptide ligand for mammalian presynaptic Ca^{2+} channels. *Neuron.* **9**, 69-77.

Hinkle, P.M., Kinsella, P.A., and Osterhoudt, K.C. (1987) Cadmium uptake and toxicity via voltage-sensitive calcium channels. *J. Biol. Chem.* **262**, 16333-16337.

Hoffman, F., Biel, M., and Flockerzi, V. (1994) Molecular basis of Ca^{2+} channel diversity. *Annu. Rev. Neurosci.* **17**, 399-418.

Huang, L.M. (1989) Calcium channels in isolated rat dorsal horn neurones, including labelled spinothalamic and trigeminothalamic cells. *J. Physiol. (Lond.)* **411**, 161-177.

Hughes, W.L. (1957) A physiochemical rationale for the biological activity of mercury and its compounds. *Ann. NY Acad. Sci.* **65**, 454-460.

Hunter, D., Bomford, R.R., and Russell, D.S. (1940) Poisoning by methylmercury compounds. *Quart. J. Med.* **9**, 193-220.

Hunter, D. and Russell, D.S. (1954) Focal cerebral and cerebellar atrophy in a human subject due to organic mercury compounds. *Neurol. Neurosurg. Psychiat.* **17**, 235-241.

Jahn, R., and Südhof, T.C. (1994) Synaptic vesicles and exocytosis. *Annu. Rev. Neurosci.* **17**, 219-246.

Juang, M.S. (1976) Depression of frog muscle contraction by methylmercuric chloride and mercuric chloride. *Toxicol. Appl. Pharmacol.* **35**, 183-185.

Kauppinen, R.A., Komulainen, H., and Taipale, H. (1989) Cellular mechanisms underlying the increase in cytosolic free calcium concentration induced by methylmercury in cerebrocortical synaptosomes from guinea pig. *J. Pharmacol. Exp. Ther.* **248**, 1248-1254.

Kennedy, M.B. (1989) Regulation of neuronal function by calcium. *TINS* **12**, 417-419.

Koivisto, A., Siemen, D., and Nedergaard, J. (1993) Reversible blockade of the calcium-activated nonselective cation channel in brown fat cells by the sulfhydryl reagents mercury and thimerosal. *Pflügers Arch.* **425**, 549-551.

Komulainen, H., and Bondy, S.C. (1987) Increased free intrasynaptosomal Ca^{2+} by neurotoxic organometals: distinctive mechanisms. *Toxicol. Appl. Pharmacol.* **88**, 77-86.

Komulainen, H., Keränen, A., and Saano, V. (1995) Methylmercury modulates $GABA_A$ receptor complex differentially in rat cortical and cerebellar membranes in vitro. *Neurochem. Res.* **20**, 659-662.

Kung, M.-P., Kostyniak, P.J., Olson, J.R., Sansone, F.M., Nickerson, P.A., Malone, M.A., Ziembiec, N., and Roth, J.A. (1989) Cell specific enzyme markers as indicators of neurotoxicity: Effects of acute exposure to methylmercury. *NeuroToxicology* **10**, 41-52.

Lakowicz, J.R., and Anderson, C.J. (1980) Permeability of lipid bilayers to methylmercuric chloride: quantification by fluorescence quenching of a carbazole-labeled phospholipid. *Chem. Biol. Inter.* **30**, 309-323.

Lansman, J.B. (1990) Blockade of current through single calcium channels by trivalent lanthanide cations. Effect of ionic radius on the rates of ion entry and exit. *J. Gen. Physiol.* **95**, 679-696.

Lansman, J.B., Hess, P., and Tsien, R.W. (1986) Blockade of current through single calcium channels by Cd^{2+}, Mg^{2+} and Ca^{2+}. *J. Gen. Physiol.* **88**, 321-347.

Leonhardt, R., Pekel, M., Platt, B., Haas, H.L., Büsselberg, D. (1996) Voltage-activated calcium channel currents of rat DRG neurons are reduced by mercuric chloride ($HgCl_2$) and methylmercury (CH_3HgCl). *NeuroToxicology* **17**, 85-92.

Levi, G., Gordon, R.D., Gallo, V., Wilkin, G.P., Balazs, R. (1982) Putative acidic amino acid transmitters in the cerebellum. I. Depolarization-induced release. *Brain Res.* **239**, 425-445.

Leyshon-Sorland, K., Jasani, B., and Morgan, A.J. (1994) The localization of mercury and metallothionein in the cerebellum of rats experimentally exposed to methylmercury. *Histochem. J.* **26**, 161-169.

Llinás, R. and Yarom, Y. (1981) Properties and distribution of ionic conductances generating electroresponsivenesss of mammalian inferior olivary neurones in vitro. *J. Physiol. (Lond.)* **315**, 569-584.

Llinás, R. (1988) The intrinsic electrophysiological properties of mammalian neurons: insights into central nervous system function. *Science* **242**, 1654-1664.

Llinás, R., Sugimori, M., Lin, J-W., and Cherksey, N. (1989) Blocking and isolation of a calcium channel from neurons in mammals and cephalopods utilizing a toxin fraction (FTX) from funnel-web spider poison. *Proc. Natl. Acad. Sci. USA* **86**, 1689-1693.

Lux, H.D., and Brown, A.M. (1984) Single channel studies on inactivation of calcium currents. *Science* **225**, 432-434.

Lux, H.D., and Gutrick, M.J. (1986) Voltage-dependent repriming of inactivated calcium current in identified *Helix* neurons. *Exp. Brain Res.* **S14**, 51-60.

Manalis, R.S., and Cooper, G.P. (1975) Evoked transmitter release increased by inorganic mercury at frog neuromuscular junction. *Nature (Lond.)* **257**, 690-691.

Marchetti, C., Carignani, C., and Robello, M. (1991) Voltage-dependent calcium currents in dissociated granule cells from rat cerebellum. *Neuroscience* **43**, 121-133.

Marty, M.S., and Atchison, W.D. Pathways mediating Ca^{2+} entry in rat cerebellar granule cells following *in vitro* exposure to methylmercury, *submitted.*

McCleskey, E.W., Fox, A.P., Feldman, D.H., Cruz, L.J., Olivera, B.M., Tsien, R.W., and Yoshikami, D. (1987) ϖ-conotoxin: Direct and persistent blockade of specific types of calcium channels in neurons but not muscle. *Proc. Natl. Acad. Sci.* **84**, 4327-4331.

Miyamoto, M.D. (1983) Hg^{2+} causes neurotoxicity at an intracellular site following entry through Na and Ca channels. *Brain Res.* **267**, 375-379.

Moran, O., Lin, F., Zegarra-Moran, O., and Sciancalepore, M. (1991) Voltage dependent calcium channels in cerebellar granule cell primary cultures. *Eur. Biophys. J.* **20**, 157-164.

Morgan, K.T., Senberg, J.A., Hamm, T.E., Wolkowski-Tyl, R., and Phelps, M. (1982) Histopathology of acute toxic response in rats and mice exposed to methyl chloride by inhalation. *Fundam. Appl. Toxicol.* **2**, 293-399.

Nachshen, D.A. (1984) Selectivity of the Ca binding site in synaptosome Ca channels: Inhibition of Ca influx by multivalent metal cations. *J. Gen. Physiol.* **83**, 941-967.

Narahashi, T., Tsunoo, A., and Yoshii, M. (1987) Characterization of two types of calcium channels in mouse neuroblastoma cells. *J. Physiol. (Lond.)* **383**, 231-249.

Niidome, T., Teramoto, T., Murata, Y., Tanaka, I., Seto, T., Sawada, K., Mori, Y., and Katayama, K. (1994) Stable expression of the neuronal BI (Class A) calcium channel in baby hamster kidney cells. *Biochem. Biophys. Res. Commun.* **203**, 1821-1827.

Ogura, A., Myojo, Y.and Higashida, H. (1990) Bradykinin-evoked acetylcholine release via inositol trisphosphate-dependent elevation in free calcium in neuroblastoma X glioma hybrid NG108-15 cells. *J. Biol. Chem.* **265**, 3577-3584.

Olivera, B.M., Rivier, J., Scott, J.K., Hillyard, D.R., and Cruz, L.J. (1991) *J. Biol. Chem.* **266**, 22067-22070.

Olivera, B.M., Miljanich, G.P., Ramachandran, J., and Adams, M.E. (1994) Calcium channel diversity and neurotransmitter release: The ϖ-conotoxins and ϖ-agatoxins. *Annu. Rev. Biochem.* **63**, 823-867.

Oortgiesen, M., van Kleef, R.G.D.M., and Vijverberg, H.P.M. (1990) Novel type of ion channel activated by Pb^{2+}, Cd^{2+}, and Al^{3+} in cultured mouse neuroblastoma cells. *J. Membr. Biol.* **113**, 261-268.

Palay, S.L., and Chan-Palay, V. (1974) *Cerebellar Cortex Cytology and Organisation*, Springer, Berlin.

Pearson, H.A., Sutton, K.G., Scott, R.H., and Dolphin, A.C. (1993) Ca^{2+} currents in cerebellar granule neurones: role of internal Mg^{2+} in altering characteristics and antagonist effects. *Neuropharmacology* **32**, 1171-1183.

Pearson, H.A., Sutton, K.G., Scott, R.H., and Dolphin, A.C. (1995) Characterization of Ca^{2+} channel currents in cultured rat cerebellar granule neurones. *J. Physiol. (Lond.)* **482**, 493-509.

Pekel, M., Platt, B., and Büsselberg, D. (1993) Mercury (Hg^{2+}) decreases voltage-gated calcium channel currents in rat DRG and *Aplysia* neurons. *Brain Res.* **632**, 121-126.

Quandt, F.N., Kato, E., and Narahashi, T. (1982) Effects of methylmercury on electrical responses of neuroblastoma cells. *NeuroToxicology* **3**, 205-220.

Randall, A., and Tsien, R.W. (1995) Pharmacological dissection of multiple types of Ca^{2+} channel currents in rat cerebellar granule neurons. *J. Neurosci.* **15**, 2995-3012.

Redman, R.S., and Silinsky, E.M. (1994) Decrease in calcium currents induced by aminoglycoside antibiotics in frog motor nerve endings. *Br. J. Pharmacol.* **113**, 375-378.

Robitaille, R., and Charlton, M.P. (1990) Strategic location of calcium channels at transmitter release sites of frog neuromuscular synapses. *Neuron* **5**, 773-779.

Rossi, A.D., Larsson, O., Manzo, L., Orrenius, S., Vahter, M., Berggren, P.O., and Nicotera, P. (1993) Modifications of Ca^{2+} signaling by inorganic mercury in PC12 cells. *FASEB J* **7**, 1507-1514.

Ruppersberg, J.P., Stocker, M., Pongs, O., Heinemann, S.H., Frank, R., and Koenen, M. (1991) Regulation of fast inactivation of cloned mammalian $I_K(A)$ channels by cysteine oxidation. *Nature (Lond.)* **352**, 711-714.

Rustam, H., Von Burg, R., Amin-Zaki, L., and El Hassani, S. (1975) Evidence for a neuromuscular disorder in methylmercury poisoning. Clinical and electrophysiological findings in moderate to severe cases. *Arch. Environ. Hlth.* **30**, 190-195.

Sarafian, T.A. (1993) Methylmercury increases intracellular Ca^{2+} and inositol phosphate levels in cultured cerebellar granule neurons. *J. Neurochem.* **61**, 648-657.

Sather, W.A., Tanabe, T., Zhang, J.-F., Mori, Y., Adams, M.E., and Tsien, R.W. (1993) Distinctive biophysical and pharmacological properties of class A (BI) calcium channel α_1 subunits. *Neuron* **11**, 291-303.

Schweitz, H., Heurteaux, C., Bois, P., Moinier, D., Romey, G., and Lazdunski, M. (1994) Calcicludine, a venom peptide of the Kunitz-type protease inhibitor family, is a potent blocker of high-threshold Ca^{2+} channels with a high affinity for L-type channels in cerebellar granule neurons. *Proc. Natl. Acad. Sci. USA* **91**, 878-882.

Scott, R.H., Pearson, H.A., and Dolphin, A.C. (1991) Aspects of vertebrate neuronal voltage-activated calcium currents and their regulation. *Prog. Neurobiol.* **36**, 485-520.

Shafer, T.J., and Atchison, W.D. (1989) Block of $^{45}Ca^{2+}$ uptake into synaptosomes by methylmercury: Ca^{2+} and Na^{+}-dependence. *J. Pharmacol. Exp. Ther.* **248**. 696-702.

Shafer, T.J., and Atchison, W.D. (1991) Methylmercury blocks N- and L-type Ca^{2+} channels in nerve growth factor-differentiated pheochromocytoma (PC12) cells. *J. Pharmacol. Exp. Ther.* **258**, 149-157.

Shafer, T.J., and Atchison, W.D. (1992) Effects of methylmercury on perineural Na^{+} and Ca^{2+}-dependent potentials at neuromuscular junctions of the mouse. *Brain Res.* **595**, 215-219.

Shafer, T.J., Contreras, M.L., and Atchison, W.D. (1990) Characterization of interactions of methylmercury with Ca^{2+} channels in synaptosomes and pheochromocytoma cells: Radiotracer flux and binding studies. *Mol. Pharmacol.* **38**, 102-113.

Shamoo, A.E., and MacLennan, D.H. (1975) Separate effects of mercurial compounds on the ionophoric and hydrolytic functions of the (Ca^{++} + Mg^{++})-ATPase of sarcoplasmic reticulum. *J. Memb. Biol.* **25**, 65-74.

Shrager, P. (1977) Slow sodium inactivation in nerve after exposure to sulfhydryl blocking reagents. *J. Gen. Physiol.* **69**, 183-202.

Shrivastav, B.B., Brodwick, M.S., and Narahashi, T. (1976) Methylmercury: Effects on electrical properties of squid axon membranes. *Life Sci.* **18**, 1077-1082.

Sigworth, F.J. (1993) Voltage gating of ion channels. *Quart. Rev. Biophys.* **27**, 1-40.

Simons, T.J.B., and Pocock, G. (1987) Lead enters bovine adrenal medullary cells through calcium channels. *J. Neurochem.* **48**, 383-389.

Sirois, J.E., and Atchison, W.D. (1995) Methylmercury-induced inhibition of whole cell potassium current in rat cerebellar granule cells. *Soc. Neurosci. Abstr.* **21(3)**, 1985.

Sirois, J.E., and Atchison, W.D. (1996) Methylmercury decreases whole cell barium current in cerebellar granule neurons. *The Toxicologist* **30(2)**, 26 (abstract).

Skerfving, S., Hansson, A., and Lindsten, J. (1970) Chromosome breakage in human subjects exposed to methylmercury through fish consumption. *Arch. Environ. Health.* **21**, 133-139.

Slatin, S.L., Qiu, X.Q., Jakes, K.S., and Finkelstein, A. (1994) Identification of a translocated protein segment in a voltage-dependent channel. *Nature (Lond.)* **371**, 158-161.

Somjen, G.G., Herman, S.P., and Klein, R. (1973) Electrophysiology of methyl mercury poisoning. *J. Pharmacol. Exp. Ther.* **186**, 579-591.

Soong, T.W., Stea, A., Hodson, C.D., Dubel, S.J., Vincent, S.R., Snutch, T.P. (1993) Structure and functional expression of a member of the low-voltage-activated calcium channel family. *Science* **260**, 1133-1136.

Standen, N.B. (1981) Ca channel inactivation by intracellular Ca injection into helix neurones. *Nature (Lond.)* **293**, 158-159.

Stea, A., Tomlinson, W.J., Soong, T.W., Bourinet, E., Dubel, S.J., Vincent, S.R., and Snutch, T.P. (1994) The localization and functional properties of a rat brain α_{1A} calcium channel reflect similarities to neuronal Q- and P-type channels. *Proc. Natl. Acad. Sci. USA* **91**, 10576-10580.

Streit, J., and Lux, H.D. (1987) Voltage-dependent calcium currents in PC12 growth cones and cells during NGF-induced cell growth. *Pflügers Arch.* **408**, 634-641.

Streit, J., and Lux, H.D. (1989) Distribution of calcium currents in sprouting PC12 cells. *J. Neurosci.* **9**, 4190-4199.

Südhof, T.C., and Jahn, R. (1991) Proteins of synaptic vesicles involved in exocytosis and membrane recycling. *Neuron* **6**, 665-677.

Suzuki, K., Ikebuchi, H., and Terao, T. (1985) Mercuric and cadmium ions stimulate phosphorylation of band 4.2 protein on human erythrocyte membranes. *J. Biol. Chem.* **260**, 4526-4530.

Swartz, K.J., Mintz, I.M., Boland, L.M. and Bean, B.P. (1993) Block of calcium channels in central and peripheral rat neurons by ϖ-CTx-MVIIC. *Soc. Neurosci. Abstr.* **19**, 1478.

Takeuchi, T., Matsumoto, H., Sashi, M., Kambara, T., Shiraishi, Y., Hirata, Y., Nobukiro, M., and Ito, H. (1968) Pathology of Minamata Disease. *Kumamato Med. J.* **34**, 521-524.

Tang, C.M., Presser, F., and Morad, M. (1988) Amiloride selectively blocks the low threshold (T) calcium channel. *Science* **240**, 213-215.

Tang, S., Mikala, G., Bahinski, A., Yatani, A., Varadi, G., and Schwartz, A. (1993) Molecular localization of ion selectivity sites within the pore of a human L-type cardiac calcium channel. *J. Biol. Chem.* **268**, 13026-13029.

Terramani, T., Kessler, M., Lynch, G., and Baudry, M. (1988) Effects of thiol-reagents on [^{3}H]α-amino-3-hydroxy-5-methylisoxazole-4-propionic acid binding to rat telencephalic membranes. *Mol. Pharm.* **34**, 117-123.

Tillotsen, D. (1979) Inactivation of Ca conductance dependent on entry of Ca ions in molluscan neurons. *Proc. Natl. Acad. Sci. USA* **76**, 1497-1500.

Traxinger, D.L., and Atchison, W.D. (1987) Reversal of methylmercury-induced block of nerve-evoked release of acetylcholine at the neuromuscular junction. *Toxicol. Appl. Pharmacol.* **90**, 23-33.

Tsuzuki, Y. (1981) Effect of chronic methylmercury exposure on activities of neurotransmitter enzymes in rat cerebellum. *Toxicol. Appl. Pharmacol.* **60**, 379-381.

Umbach, J.A., and Gundersen, C.B. (1989) Mercuric ions are potent noncompetitive antagonists of human brain kainate receptors expressed in *Xenopus* oocytes. *Mol. Pharmacol.* 582-588.

Verity, M.A., Sarafian, T., Pacifici, E.H.K., and Sevanian, A. (1994) Phospholipase A_2 stimulation by methyl mercury in neuron culture. *J. Neurochem.* **62**, 705-714.

Von Burg, R., and Landry, T. (1976) Methylmercury and the skeletal muscle receptor. *J. Pharm. Pharmacol.* **28**, 548-551.

Von Burg, R., Northington, F.K., and Shamoo, A. (1980) Methylmercury inhibition of rat brain muscarinic receptors. *Toxicol. Appl. Pharmacol.* **53**, 285-292.

Weinreich, D., and Wonderlin, W.F. (1987) Copper activates a unique inward current in molluscan neurones. *J. Physiol. (Lond.)* **394**, 429-443.

Weinsberg, F., Bickmeyer, U., and Wiegand, H. (1995) Effects of inorganic mercury (Hg^{2+}) on calcium channel currents and catecholamine release from bovine chromaffin cells. *Arch. Toxicol.* **69**, 191-196.

Werth, J.L., Hirning, L.D., and Thayer, S.A. (1991) Omega-conotoxin exerts functionally distinct low and high affinity effects in the neuronal cell line NG108-15. *Mol. Pharmacol.* **40**, 742-749.

Wheeler, D.B., Randall, A., and Tsien, R.W. (1994) Roles of N-type and Q-type Ca^{2+} channels in supporting hippocampal synaptic transmission. *Science* **264**, 107-111.

Witcher, D.R., DeWaard, M., Sakamoto, J., Franzini-Armstrong, C., Pragnell, M., Kahl, S.D., and Campbell, K.P. (1993) Subunit identification and reconstitution of the N-type Ca^{2+} channel complex purified from brain. *Science* **261**, 486-489.

Yan, C.H., and Atchison, W.D. (1996) Characterization of interaction of methylmercury (MeHg) with Ca^{2+} channels of rat cerebellar synaptosomes. *The Toxicologist* **30(2)**, 187 (abstract).

Yang, N., George, A.L., and Horn, R. (1996) Molecular basis of charge movement in voltage-gated sodium channels. *Neuron* **16**, 113-122.

Yuan, Y., and Atchison, W.D. (1993) Disruption by methylmercury of membrane excitability and synaptic transmission of CA1 neurons in hippocampal slices of the rat. *Toxicol. Appl. Pharmacol.* **120**, 203-215.

Yuan, Y., and Atchison, W.D. (1994) Comparative effects of inorganic divalent mercury, methylmercury and phenylmercury on membrane excitability and synaptic transmission of CA1 neurons in hippocampal slices of the rat. *NeuroToxicology* **15(2)**, 403-412.

Yuan, Y., and Atchison, W.D. (1995) Methylmercury (MeHg) acts on multiple sites to block hippocampal synaptic transmission. *J. Pharmacol. Exp. Ther.* **275**, 1304-1316.

Zernig, G. (1990) Widening potential for Ca^{2+} antagonists: Non L-type Ca^{2+} channel interaction. *Trends Pharmacol. Sci.* **11**, 38-44.

Zhang, J.F., Randall, A.D., Ellinor, P.T., Horne, W.A., Sather, W.A., Tanabe, T., Schwarz, T.L., and Tsien, R.W. (1993) Distinctive pharmacology and kinetics of cloned neuronal Ca^{2+} channels and their possible counterparts in mammalian CNS neurons. *Neuropharmacology* **32**, 1075-1088.